

อิทธิพลของน้ำหนักโมเลกุลของสารช่วยกระจายพีดีดีเอต่อสมบัติเชิงกลและสมบัติทางความร้อน
ของยางธรรมชาติ/นาโนซิลิกาคอมพอสิต

นางสาวกิตติวรรณ ทองยิ้ม

วิทยานิพนธ์นี้เป็นส่วนหนึ่งของการศึกษาตามหลักสูตรปริญญาวิทยาศาสตรมหาบัณฑิต
สาขาวิชาวิทยาศาสตร์พอลิเมอร์ประยุกต์และเทคโนโลยีสิ่งทอ ภาควิชาวัสดุศาสตร์
คณะวิทยาศาสตร์ จุฬาลงกรณ์มหาวิทยาลัย
ปีการศึกษา 2554

บทคัดย่อและแฟ้มข้อมูลฉบับเต็มของวิทยานิพนธ์นี้ยังได้ถูกจัดเก็บไว้ในบริการในคลังปัญญาจุฬาฯ (CUIR)
เป็นแฟ้มข้อมูลของนิสิตเจ้าของวิทยานิพนธ์ที่ส่งผ่านทางบัณฑิตวิทยาลัย

The abstract and full text of theses from the academic year 2011 in Chulalongkorn University Intellectual Repository (CUIR)
are the thesis authors' files submitted through the Graduate School.

INFLUENCES OF MOLECULAR WEIGHT OF PDDA DISPERSING AGENT ON
MECHANICAL AND THERMAL PROPERTIES OF NATURAL RUBBER/NANOSILICA
COMPOSITES

Miss Kittiwat Thongyim

A Thesis Submitted in Partial Fulfillment of the Requirements
for the Degree of Master of Science Program in Applied Polymer Science and Textile Technology

Department of Materials Science

Faculty of Science

Chulalongkorn University

Academic Year 2011

Copyright of Chulalongkorn University

Thesis Title INFLUENCES OF MOLECULAR WEIGHT OF PDDA DISPERSING
AGENT ON MECHANICAL AND THERMAL PROPERTIES OF
NATURAL RUBBER/NANOSILICA COMPOSITES

By Miss Kittiwat Thongyim

Field of Study Applied Polymer Science and Textile Technology

Thesis Advisor Kanoktip Boonkerd, Ph.D.

Thesis Co-advisor Assistant Professor Nisanart Traiphol, Ph.D.

Accepted by the Faculty of Science, Chulalongkorn University in Partial
Fulfillment of the Requirements for the Master's Degree

..... Dean of the Faculty of Science
(Professor Supot Hannongbua, Dr.rer.nat.)

THESIS COMMITTEE

..... Chairman
(Assistant Professor Usa Sangwatanaroj, Ph.D.)

..... Thesis Advisor
(Kanoktip Boonkerd, Ph.D.)

..... Thesis Co-advisor
(Assistant Professor Nisanart Traiphol, Ph.D.)

..... Examiner
(Assistant Professor Mantana Opaprakasit, Ph.D.)

..... External Examiner
(Piyaporn Kampeerapappun, Ph.D.)

กิตติวรรณ ทองยิ้ม : อิทธิพลของน้ำหนักโมเลกุลของสารช่วยกระจายพีดีดีเอต่อสมบัติเชิงกลและสมบัติทางความร้อนของยางธรรมชาติ/นาโนซิลิกาคอมพอสิต. (INFLUENCES OF MOLECULAR WEIGHT OF PDDA DISPERSING AGENT ON MECHANICAL AND THERMAL PROPERTIES OF NATURAL RUBBER/NANOSILICA COMPOSITES) อ. ที่ปรึกษาวิทยานิพนธ์หลัก : อ.ดร.กนกทิพย์ บุญเกิด, อ.ที่ปรึกษาวิทยานิพนธ์ร่วม : ผศ.ดร.นิศานาถ ไตรผล, 120 หน้า.

วัตถุประสงค์ของงานวิจัยนี้คือการศึกษอิทธิพลของสารช่วยกระจายพีดีดีเอต่อสมบัติของยางธรรมชาติ/นาโนซิลิกาคอมพอสิต ปัจจัยที่ทำการศึกษาคือ น้ำหนักโมเลกุล โครงสร้างทางเคมี และปริมาณการเติมสารช่วยกระจาย สารช่วยกระจายที่ใช้มีอยู่สองประเภทประกอบไปด้วย สารช่วยกระจายพีดีดีเอเอกพันธ์ (homo-PDDA) และสารช่วยกระจายพีดีดีเอร่วม (co-PDDA) สำหรับสารช่วยกระจายพีดีดีเอเอกพันธ์ที่ใช้มีน้ำหนักโมเลกุลแตกต่างกันอยู่สามประเภทประกอบไปด้วย สารช่วยกระจายพีดีดีเอน้ำหนักโมเลกุลต่ำ (l-PDDA) (น้ำหนักโมเลกุล = 100,000-200,000) สารช่วยกระจายพีดีดีเอน้ำหนักโมเลกุลปานกลาง (m-PDDA) (น้ำหนักโมเลกุล = 200,000-350,000) และสารช่วยกระจายพีดีดีเอน้ำหนักโมเลกุลสูง (h-PDDA) (น้ำหนักโมเลกุล = 400,000-500,000) อัตราส่วนปริมาณซิลิกาที่ใช้ ได้แก่ ร้อยละ 1 2 3 และ 4 โดยน้ำหนัก ในขณะที่ความเข้มข้นของสารช่วยกระจายที่ใช้ อยู่ที่ ร้อยละ 1 และ 3 โดยน้ำหนักของซิลิกา ในขั้นแรกของการเตรียมพื้นผิวของนาโนซิลิกาถูกดัดแปรด้วยสารช่วยกระจายในรูปของสารแขวนลอย โครงสร้างของซิลิกา-พีดีดีเอเกิดขึ้นได้โดยใช้หลักการเซลฟอสเซมบลีแบบอาศัยการเกิดอันตรกิริยาทางไฟฟ้าสถิต หลังจากนั้นนำไปผสมกับยางธรรมชาติเพื่อให้อยู่ในรูปของแผ่นยางธรรมชาติ/นาโนซิลิกาคอมพอสิต ผลของสารช่วยกระจายประเภทต่างๆที่มีต่อการตกตะกอน แสดงให้เห็นว่าสารช่วยกระจายพีดีดีเอเอกพันธ์และสารช่วยกระจายพีดีดีเอร่วมช่วยลดการตกตะกอนและปรับปรุงเสถียรภาพของสารแขวนลอยซิลิกาอย่างไรก็ตาม น้ำหนักโมเลกุลทั้งสามประเภทของสารช่วยกระจายพีดีดีเอเอกพันธ์ให้ค่ากลางของขนาดอนุภาคที่ใกล้เคียงกันและมีขนาดอนุภาคที่เล็กกว่าขนาดอนุภาคที่ใช้สารช่วยกระจายพีดีดีเอร่วม เมื่อเปรียบเทียบกับยางธรรมชาติที่ไม่ได้เติมซิลิกา ผลที่ได้แสดงให้เห็นว่าการเติมสารช่วยกระจายสามารถเพิ่มสมบัติเชิงกลและสมบัติทางความร้อนอย่างสังเกตเห็นได้ชัด เมื่อเปรียบเทียบสารช่วยกระจายที่ใช้ทั้งหมด โดยเรียงลำดับตามการเพิ่มขึ้นจากมากไปน้อยของการทนแรงดึงและการทนแรงฉีกขาด เป็นต้น สารช่วยกระจายพีดีดีเอน้ำหนักโมเลกุลต่ำ, สารช่วยกระจายพีดีดีเอน้ำหนักโมเลกุลปานกลาง, สารช่วยกระจายพีดีดีเอน้ำหนักโมเลกุลสูง, สารช่วยกระจายพีดีดีเอร่วม เหตุผลคือ สารช่วยกระจายไม่เพียงแต่ลดการเกิดแอกไกลเมอเรต เพิ่มอันตรกิริยาระหว่างสารตัวเติมและยางธรรมชาติ ยังเพิ่มการเชื่อมขวางของยางธรรมชาติ/นาโนซิลิกาคอมพอสิต อย่างไรก็ตาม การใช้สารช่วยกระจายไม่มีผลต่อเสถียรภาพทางความร้อนของนาโนคอมพอสิต นอกเหนือจากนั้น อุณหภูมิเริ่มต้นในการสลายตัวของความร้อนไม่ขึ้นอยู่กับปริมาณการเติมซิลิกา ในขณะที่อุณหภูมิสุดท้ายในการสลายตัวของความร้อนเพิ่มขึ้นเล็กน้อยเมื่อเพิ่มปริมาณซิลิกา การเพิ่มปริมาณของสารช่วยกระจายจากร้อยละ 1 ไป 3 โดยน้ำหนักซิลิกา สมบัติต่างๆไม่เพิ่มขึ้นตามที่คาด ตามความเป็นจริง ดูเหมือนว่าสมบัติของยางธรรมชาติ/นาโนซิลิกาคอมพอสิตจะลดน้อยลง เนื่องมาจากกลุ่มก้อนซิลิกามีขนาดใหญ่ขึ้นซึ่งดูได้จากค่ากลางของขนาดอนุภาคที่มีขนาดใหญ่ขึ้น

ภาควิชา.....วัสดุศาสตร์.....ลายมือชื่อนิสิต.....
 สาขาวิชา.....วิทยาศาสตร์พอลิเมอร์ประยุกต์และเทคโนโลยีสิ่งทอ.....ลายมือชื่อ อ.ที่ปรึกษาวิทยานิพนธ์หลัก.....
 ปีการศึกษา.....2554.....ลายมือชื่อ อ.ที่ปรึกษาวิทยานิพนธ์ร่วม.....

5272226023 : MAJOR APPLIED POLYMER SCIENCE AND TEXTILE TECHNOLOGY

KEYWORDS : SELF-ASSEMBLY/NATURAL RUBBER LATEX/SILICA/ELECTROSTATIC INTERACTION

KITTIWAN THONGYIM: INFLUENCES OF MOLECULAR WEIGHT OF PDDA DISPERSING
AGENT ON MECHANICAL AND THERMAL PROPERTIES OF NATURAL RUBBER/NANOSILICA
COMPOSITES. ADVISOR : KANOKTIP BOONKERD, Ph.D., CO-ADVISOR : ASST.PROF.
NISANART TRAIIPHOL, Ph.D., 120 pp.

The aim of this thesis is to study the influence of dispersing agent on the properties of the NR/silica nanocomposite. The factor focused here were the molecular weight, chemical structure and loading of dispersing agent. There were two different types of dispersing agent including homo-PDDA and co-PDDA. For homo-PDDA, there were three different MW PDDAs: l-PDDA (MW =100,000-200,000), m-PDDA (MW = 200,000-350,000) and h-PDDA (MW = 400,000-500,000). The silica loadings were varied from 1 to 2, 3 and 4 wt% while the concentrations of dispersing agent were fixed at 1 and 3 wt% of silica. In the beginning preparation, nanosilica surface was modified by dispersing agent in aqueous suspension form. The silica-PDDA structure was generated via self-assembly electrostatic adsorption, and then blended with the NR in order to form NR/silica nanocomposite sheet. The effects of the dispersing agent types on precipitation were investigated here. The results revealed that both homo- and co-PDDA reduced the precipitation and improved the stabilization of the silica/dispersing agent colloid. However, homo-PDDA with all three molecular weights gave nearly the same median particle size and much smaller than that of co-PDDA. Compared with the pure NR, the result showed that the addition of dispersing agent clearly enhance the mechanical properties of the NR/silica nanocomposite. Comparing amongst the dispersing agent, the level of enhancement tensile and tear strength was in the order of l-PDDA > m-PDDA > h-PDDA > co-PDDA. The reason for this was not just only the reduction of silica agglomeration and increment of filler-rubber interaction but also the increase of crosslink density of the NR/silica nanocomposites. However, the onset and endset decomposition temperature of the nanocomposites was not affected by the presence of the dispersing agent. Moreover, the onset decomposition temperature was independent of the silica loading while the endset one slightly increased with increasing silica loading. The increasing amount of dispersing agent from 1 wt% to 3 wt% of silica did not enhance any properties significantly as expected. In fact, this seemed to deteriorate the properties of NR/silica nanocomposites. This was due to the formation of larger silica cluster indicated by the larger median particle size.

Department : Materials Science..... Student's Signature

Field of Study : Applied Polymer Science..... Advisor's Signature

: and Textile Technology..... Co-advisor's Signature

Academic Year : 2011.....

ACKNOWLEDGEMENTS

This thesis would not have been possible without the kindness of my advisor, Dr. Kanoktip Boonkerd, who was abundantly helpful, support and offered invaluable assistance. And my co-advisor Assistant Professor Dr. Nisanart Traiphol, who gave useful advice and suggestion throughout this thesis.

I would like to truthfully appreciate to Assistant Professor Dr. Usa Sangwatanaroj, Assistant Professor Dr. Mantana Opaprakasit and Dr. Piyaporn Kampeerapappun for their valuables suggestions and comments for thesis fulfillment.

I would like to appreciatively acknowledge Center of Excellence on Petrochemical and Materials Technology, Chulalongkorn University, Thai Rubber Latex PLC., Thailand and Rubber Research Institute of Thailand for financial, material and equipment support. And many thank must be given to all of my teachers and staffs of Department of Materials Science, for their knowledge, suggestion and helpful in providing facilities for my thesis experiment. Also, I would like to special thanks to my friends for their sincerely relationship, kindness and helpfulness.

Finally, my graduation would not be achieved without greatest love from my family, who always understand and support me for everything through the duration of my graduate study.

CONTENTS

| | Page |
|---|------|
| ABSTRACT (THAI)..... | iv |
| ABSTRACT (ENGLISHI)..... | v |
| ACKNOWLEDGEMENTS..... | vi |
| CONTENTS..... | vii |
| LIST OF TABLES..... | xi |
| LIST OF FIGURES..... | xii |
| | |
| CHAPTER I INTRODUCTION..... | 1 |
| CHAPTER II THEORETICAL AND LITERATURE REVIEW..... | 3 |
| 2.1 Natural Rubber..... | 3 |
| 2.1.1 Natural Rubber Latex..... | 3 |
| 2.1.2 Latex Composition..... | 4 |
| 2.1.2.1 Rubber Phase..... | 5 |
| 2.1.2.2 Serum Phase..... | 5 |
| 2.1.2.3 Bottom Phase..... | 6 |
| 2.2 Production of Natural Rubber Latex..... | 6 |
| 2.2.1 Preserved Field Latex..... | 6 |
| 2.2.2 Concentrated Latex..... | 7 |
| 2.2.2.1 Creaming..... | 7 |
| 2.2.2.2 Centrifugation..... | 7 |
| 2.2.3 Prevulcanized Latex..... | 8 |
| 2.2.3.1 Stabilizer..... | 8 |
| 2.2.3.2 Vulcanising Agent..... | 9 |
| 2.2.3.3 Activator..... | 9 |
| 2.2.3.4 Accelerator..... | 9 |
| 2.2.3.5 Antioxidants..... | 11 |

| | Page |
|---|------|
| 2.2.3.6 Filler and Pigment..... | 11 |
| 2.2.3.7 Special Additives..... | 11 |
| 2.3 Dispersion and Emulsion of Filler in Latex..... | 11 |
| 2.3.1 Dispersion of Dry Power Additives in Latex..... | 12 |
| 2.3.2 Emulsion of Liquid Additives in Latex..... | 12 |
| 2.4 Compounding Latex..... | 12 |
| 2.5 Maturation of Latex..... | 12 |
| 2.6 Dipping Technique..... | 13 |
| 2.7 Filler for Elastomers..... | 14 |
| 2.7.1 Particle Size of Filler..... | 14 |
| 2.7.2 Particle Surface Area..... | 15 |
| 2.7.3 Structure of Filler..... | 15 |
| 2.7.4 Surface Activity..... | 16 |
| 2.8 Silica..... | 16 |
| 2.8.1 Fumed Silica or Pyrogenic Silica..... | 16 |
| 2.8.2 Precipitated Silica..... | 17 |
| 2.9 Characteristics of Synthetic Silica..... | 17 |
| 2.9.1 Surface of Silica..... | 17 |
| 2.9.2 Silica Structure and Surface Area..... | 18 |
| 2.9.3 Chemical Modification Method..... | 19 |
| 2.9.4 Physical Modification Method..... | 20 |
| 2.10 Colloidal Composite Method..... | 20 |
| 2.10.1 Self-assembly Technique..... | 21 |
| 2.11 Particle Size Analysis..... | 25 |
| 2.11.1 Sample Dispersion Technique..... | 25 |
| 2.11.2 Laser Diffraction Particle Analysis..... | 26 |
| 2.11.3 Interpretation of Particle Size Distribution Data..... | 26 |

| | Page |
|--|------|
| 2.11.3.1 Mean..... | 27 |
| 2.11.3.2 Median..... | 27 |
| 2.11.3.3 Mode..... | 28 |
| 2.12 Polyelectrolyte..... | 28 |
| CHAPTER III EXPERIMENTAL..... | 31 |
| 3.1 Materials and Chemical Agents..... | 31 |
| 3.2 Equipment..... | 32 |
| 3.3 Characterization and Testing..... | 33 |
| 3.4 Experiment Procedure..... | 33 |
| 3.4.1 Preparation of the Silica/Dispersing Agent Aqueous Suspension..... | 34 |
| 3.4.2 Preparation of NR/Silica Nanocomposite..... | 35 |
| 3.5 Characterization and Testing..... | 38 |
| 3.5.1 Particle Size Distribution of Dispersing Agent Aqueous Suspension..... | 38 |
| 3.5.2 Morphology of NR/Silica Nanocomposite..... | 38 |
| 3.5.3 Thermal Properties of NR/Silica Nanocomposite..... | 39 |
| 3.5.4 Tensile Strength..... | 39 |
| 3.5.5 Tear Strength..... | 40 |
| 3.5.6 Crosslink Density..... | 41 |
| CHAPTER IV RESULTS AND DISCUSSION..... | 43 |
| 4.1 Optimal Preparing Condition for Silica/Dispersing Agent Aqueous Suspension..... | 43 |
| 4.1.1 Effect of Ultrasonic Time for Preparing Silica Aqueous Suspension..... | 43 |
| 4.1.2 Effect of pH Value for Preparing Silica Aqueous Suspension..... | 45 |

| | Page |
|--|------|
| 4.2 Characterization of Silica/Dispersing Agent Aqueous Suspension... | 47 |
| 4.2.1 The Stability of Silica/Dispersing Agent Aqueous Suspension..... | 47 |
| 4.2.2 Particle Size Distribution of Silica/Dispersing Agent Aqueous Suspension..... | 49 |
| 4.3 Crosslink Density, Mechanical and Thermal Properties and Morphology of the Pure NR and NR/Silica Nanocomposite..... | 57 |
| 4.3.1 Crosslink Density..... | 57 |
| 4.3.2 Mechanical Properties..... | 59 |
| 4.3.2.1 Tensile Strength..... | 59 |
| 4.3.2.2 Tensile Modulus..... | 64 |
| 4.3.2.3 Elongation at Break..... | 70 |
| 4.3.2.4 Tear Strength..... | 74 |
| 4.3.3 Thermal Properties..... | 76 |
| 4.3.4 Morphology..... | 82 |
| 4.3.4.1 Physical Appearance..... | 82 |
| 4.3.4.2 SEM Pictures..... | 83 |
| CHAPTER V CONCLUSIONS | 86 |
| REFERENCES..... | 90 |
| APENDICES..... | 94 |
| Appendix A..... | 96 |
| Appendix B..... | 102 |
| BIOGRAPHY..... | 120 |

LIST OF TABLES

| Table | | Page |
|-------|---|------|
| 2.1 | Typical composition of field latex..... | 4 |
| 2.2 | General properties of fumed silica..... | 17 |
| 2.3 | Mechanical properties of NR/silica nanocomposite..... | 24 |
| 2.4 | Commercial polyelectrolyte..... | 30 |
| 3.1 | Materials and Chemical Agents..... | 31 |
| 3.2 | The list of equipment..... | 32 |
| 3.3 | The list of instruments..... | 33 |
| 3.4 | Formation of prevulcanized natural rubber latex..... | 36 |
| 4.1 | The onset degradation temperatures of pure NR and NR/silica nanocomposites with various silica contents..... | 80 |
| 4.2 | The endset degradation temperatures of pure NR and NR/silica nanocomposites with various silica content..... | 81 |

LIST OF FIGURES

| Figure | Page |
|--|------|
| 2.1 Cis-1, 4-polyisoprene of natural rubber..... | 3 |
| 2.2 Illustration of centrifuged NR latex..... | 4 |
| 2.3 Composition of the rubber particle..... | 5 |
| 2.4 The outline of low-ammonia latex and high-ammonia concentrated latex..... | 10 |
| 2.5 Classification of fillers based on their particle size..... | 15 |
| 2.6 Illustration of three types of surface silanol..... | 18 |
| 2.7 Illustration of silica morphology..... | 18 |
| 2.8 Chemical structure of silane coupling agent..... | 19 |
| 2.9 Illustration of morphologies of colloidal polymer/silica composite..... | 21 |
| 2.10 The schematic of PS core-mesoporous silica nanoparticle shell nanocomposites process..... | 22 |
| 2.11 The schematic of PVA/silica nanocomposites process..... | 23 |
| 2.12 The schematic of self-assembly NR/silica nanocomposite process..... | 24 |
| 2.13 Equivalent sphere representation for an irregularly shaped particle..... | 26 |
| 2.14 Symmetric distribution when mean, median and mode lie in the same position..... | 27 |
| 2.15 Symmetric distribution: D10, D50 and D90..... | 28 |
| 3.1 VCX-130, Sonic & Materials high intensity ultrasonic processor | 35 |
| 3.2 H.J.UNKEL, (Tech), Mechanical stirrer | 35 |
| 3.3 The outline of the experiment..... | 37 |
| 3.4 Mastersizer 2000, Malvern particle size distribution analyzer | 38 |
| 3.5 JSM-6400, JEOL Scanning electron microscope..... | 38 |
| 3.6 TGA/SDTA 851 ^o , Mettler Toledo Thermogravimetric instrument..... | 39 |
| 3.7 Tensile specimen type II according to ISO 37..... | 39 |
| 3.8 Tear specimen type C according to ISO 34..... | 41 |

| Figure | Page |
|---|------|
| 4.1 Physical appearance of 1 wt% silica aqueous suspension at different ultrasonicate times..... | 44 |
| 4.2 Effect of ultrasonicate time on the particle size distribution of 1 wt% silica aqueous suspension..... | 44 |
| 4.3 Zeta potential vs. pH of a very fine 10 % wt silica system..... | 46 |
| 4.4 Particle size distribution of 1 wt% silica suspensions when varying pH values..... | 46 |
| 4.5 The schematic of colloidal stability..... | 48 |
| 4.6 Illustration of electrosteric stabilization of polyelectrolyte attached to the particles..... | 49 |
| 4.7 Particle size distribution of 1 wt% silica aqueous suspensions with dispersing agent at (a) 1 wt% and (b) 3 wt% of silica..... | 50 |
| 4.8 Median particle sizes of 1 wt% silica suspension at dispersing agent 1 and 3 wt% of silica..... | 51 |
| 4.9 Particle size distributions of 2 wt% silica aqueous suspensions with dispersing agent at (a) 1wt% and (b) 3 wt% of silica..... | 52 |
| 4.10 Median particle sizes of 2 wt% silica suspension at dispersing agent 1 and 3 wt% of silica | 53 |
| 4.11 Particle size distributions of 3 wt% silica aqueous suspensions with dispersing agent at (a) 1wt% and (b) 3 wt% of silica..... | 54 |
| 4.12 Median particle sizes of 3 wt% of silica suspension at dispersing agent 1 and 3 wt% of silica..... | 54 |
| 4.13 Particle size distributions of 4 wt% silica aqueous suspensions with dispersing agent at (a) 1wt% and (b) 3 wt% of silica..... | 55 |
| 4.14 Median particle sizes of 4 wt% of silica suspension at dispersing agent 1 and 3 wt% of silica..... | 55 |
| 4.15 Median particle sizes of the silica aqueous suspension at various silica loadings with dispersing agent (a) 1 and (b) 3 wt% of silica..... | 56 |

| Figure | Page |
|--------|--|
| 4.16 | Crosslink densities of the pure NR and the NR/1 wt % silica with different dispersing agents at 1 and 3 wt% of silica..... 57 |
| 4.17 | Crosslink densities of the pure NR and the NR/2 wt% silica with different dispersing agents at 1 and 3 wt% of silica 57 |
| 4.18 | Crosslink densities of the pure NR and the NR/3 wt% silica with different dispersing agents at 1 and 3 wt% of silica 58 |
| 4.19 | Crosslink densities of the pure NR and the NR/4 wt% silica with different dispersing agents at 1 and 3 wt% of silica..... 58 |
| 4.20 | Tensile strengths of the pure NR and the NR/1 wt% silica with different dispersing agents at 1 and 3 wt% of silica 60 |
| 4.21 | Tensile strengths of the pure NR and the NR/2 wt% silica with different dispersing agents at 1 and 3 wt% of silica..... 60 |
| 4.22 | Tensile strengths of the pure NR and the NR/3 wt% silica with different dispersing agents at 1 and 3 wt% of silica..... 61 |
| 4.23 | Tensile strengths of the pure NR and the NR/4 wt% silica with different dispersing agents at 1 and 3 wt% of silica..... 61 |
| 4.24 | Tensile modulus at (a) 100% strain and (b) 300% strain of the pure NR and the NR/1 wt% silica with different dispersing agents at 1 and 3 wt% of silica 65 |
| 4.25 | Tensile modulus at (a) 100% strain and (b) 300% strain of the pure NR and the NR/2 wt% silica with different dispersing agents at 1 and 3 wt% of silica..... 66 |
| 4.26 | Tensile modulus at (a) 100% strain and (b) 300% strain of the pure NR and the NR/3 wt% silica with different dispersing agents at 1 and 3 wt% of silica..... 67 |
| 4.27 | Tensile modulus at (a) 100% strain and (b) 300% strain of the pure NR and the NR/4 wt% silica with different dispersing agents at 1 and 3 wt% of silica..... 68 |

| Figure | Page |
|---|------|
| 4.28 Elongations at break of the pure NR and the NR/1 wt% silica with different dispersing agents at 1 and 3 wt% of silica..... | 70 |
| 4.29 Elongations at break of the pure NR and the NR/2 wt% silica with different dispersing agents at 1 and 3 wt% of silica..... | 71 |
| 4.30 Elongations at break of the pure NR and the NR/3 wt% silica with different dispersing agents at 1 and 3 wt% of silica..... | 71 |
| 4.31 Elongations at break of the pure NR and the NR/4 wt% silica with different dispersing agents at 1 and 3 wt% of silica..... | 72 |
| 4.32 Tear strengths of the pure NR and the NR/1 wt% silica with different dispersing agents at 1 and 3 wt% of silica..... | 74 |
| 4.33 Tear strengths of the pure NR and the NR/2 wt% silica with different dispersing agents at 1 and 3 wt% of silica..... | 74 |
| 4.34 Tear strengths of the pure NR and the NR/3 wt% silica with different dispersing agents at 1 and 3 wt% of silica..... | 75 |
| 4.35 Tear strengths of the pure NR and the NR/4 wt% silica with different dispersing agents at 1 and 3 wt% of silica..... | 75 |
| 4.36 TG curves of the NR/1 wt% silica nanocomposite with different dispersing agents at (a) 1 and (b) 3 wt% of silica..... | 77 |
| 4.37 TG curves of the NR/2 wt% silica nanocomposite with different dispersing agents at (a) 1 and (b) 3 wt% of silica..... | 77 |
| 4.38 TG curves of the NR/3 wt% silica nanocomposite with different dispersing agents at (a) 1 and (b) 3 wt% of silica..... | 78 |
| 4.39 TG curves of the NR/4 wt% silica nanocomposite with different dispersing agents at (a) 1 and (b) 3 wt% of silica..... | 78 |
| 4.40 Physical appearance of the NR/silica nanocomposite sheet..... | 82 |
| 4.41 Images of the NR/silica nanocomposite surface (a) without PDDA (b) with PDDA | 82 |

| Figure | | Page |
|--------|---|------|
| 4.42 | SEM image of silica nanopowder..... | 83 |
| 4.43 | SEM micrograph of NR/silica nanocomposites: (a) 1%silica_PDDA, (b) 2%silica_PDDA, (c) 3%silica_PDDA, (d)4%silica_PDDA..... | 84 |

CHAPTER I

INTRODUCTION

Polymer/inorganic nanocomposite has gained more attention recently due to properly combining of the advantage properties of polymer such as flexibility, ductility and easy process ability with those of inorganic material such as rigidity and thermal stability. The nano-inorganic material has small particle size and high surface area, thus leading to substantially enhance thermal and mechanical properties of nanocomposite when comparing with traditional composite [1, 2]. Inorganic nanoscale has several filler forms, including calcium carbonate [3], montmorillonite [4], carbon black [5] and so forth. Among of these, nanosilica is principally used as filler in the field of polymer/inorganic nanocomposite.

The nanosilica has been used as reinforcing filler in natural rubber (NR) matrix to improve some drawbacks of NR product such as low thermal resistance, poor tensile and tear strength which always occur in the thin film product prepared from the latex. Although, the nanosilica has many benefit characteristics when used as reinforcing filler in the nanocomposite, it tends to form self aggregation via hydrogen bond due to its surface consisting of a lot of hydroxyl groups. Moreover, it is difficult to disperse the nanosilica in the rubber matrix. The ability to disperse inorganic nanoparticles in the polymer matrix has a most critical factor affecting on the properties of the nanocomposites [6]. To improve the silica distribution, various methods have been studied such as sol-gel, blending and in situ method. Self-assembly technique is one of the choices to prepare the polymer/silica nanocomposites. This technique is based on electrostatic attractive interaction of oppositely charged polyelectrolyte [1, 7]. The polyelectrolyte usually used as dispersing agent can reduce the formation of silica agglomerate and enhance silica-polymer interaction. The preparation of the polymer/silica nanocomposite through self-assembly technique is widely occurred in core shell formation.

There were few reports about the preparation of the NR/silica nanocomposite using self-assembly technique. Compared with the pure NR, the mechanical and thermal properties of the obtained natural rubber/silica nanocomposites are markedly enhanced. However, there is one important limitation of this technique which is the optimal silica loading. Regardless of type of dispersing agent and polymer matrix, the nanosilica loading was ranged between 1-4 wt% [8-9]. Above this loading, the formation of silica agglomerate will be observed according with the poorer properties. However, there is no report about how molecular weight, chemical structure (homo- or copolymer), amount of dispersing agent effect on the properties of the obtained NR/silica nanocomposites. Mostly, only silica loading was concerned.

Thus, this present work was aimed to study the influence of molecular weight, chemical structure (homo- or copolymer) and concentration of Poly (diallyldimethyl ammonium chloride), dispersing agent, on the mechanical and thermal properties of NR/silica nanocomposites prepared through the self-assembly and latex compounding technique. The study was also carried out at different silica loadings, 1, 2, 3 and 4 wt%. It was expected that the insight on how these factors effect on the properties will lead to the formation of the NR/silica nanocomposite with the better properties.

CHAPTER II

THEORETICAL AND LITERATURE REVIEW

2.1 Natural Rubber [10-12]

Natural rubber (NR) is a naturally occurring substance acquired from latex that is excreted by tapping from mainly rubber tree *Hevea Brasiliensis*. The natural rubber composes of the repeating units of isoprene which is in the cis configuration, with the empirical formula of C_5H_8 . The chemical structure of natural rubber is shown in Figure 2.1.

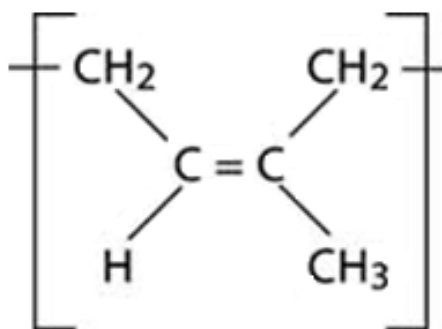


Figure 2.1 Cis-1, 4-polyisoprene of natural rubber

2.1.1 Natural Rubber Latex [10, 12-13]

Natural rubber latex is a polydispersed colloidal system of rubber particle in aqueous. The latex excreted by tapping is normally called field latex that features as milky. Field latex has dry rubber content between 25-40% and non-rubber substances between 5-10% by weight. The non-rubber substances consist of proteins, carbohydrates, lipid, and inorganic salts. The variation is due to many factors such as the type of trees, the tapping method, the soil conditions, and the season. The composition of typical field latex is shown in Table 2.1.

Table 2.1 Typical composition of field latex [14-17]

| | % Composition |
|-----------------------------|---------------|
| Rubber hydrocarbon | 36 |
| Proteins | 1.4 |
| Carbohydrates | 1.6 |
| Neutral lipid | 1.0 |
| Glycolipids + Phospholipids | 0.6 |
| Inorganic constituents | 0.5 |
| Others | 0.4 |
| Water | 58.5 |

2.1.2 Latex Composition [14-17]

When the field latex is centrifuged, phase separation in latex is generated. It can be divided into three principal phases as follows. And the component of each phase is revealed in Figure 2.2.

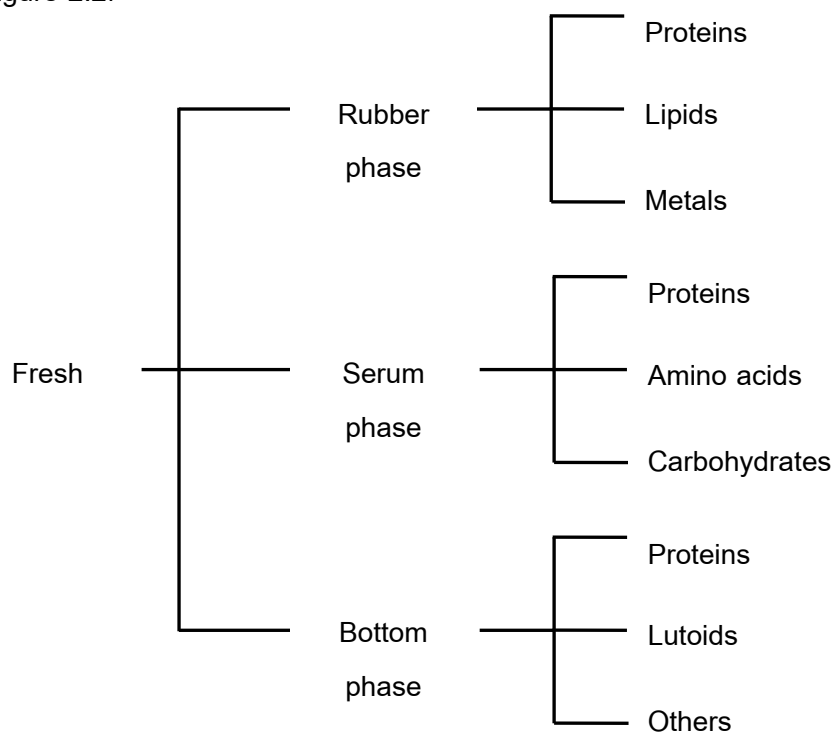


Figure 2.2 Illustration of centrifuged NR latex

2.1.2.1 Rubber Phase

The rubber phase, white layer latex, is on the top. This layer is about 30-36% of the latex. The main component in this layer is rubber particle. Most of rubber particle is in a spherical shape. The average particle size is usually considered to be between 0.25-0.8 μm , depending on the method used to calculate the average. The surface of the rubber particle in field latex is covered with a protective bilayer of phospholipids and protein. The principal component of the protein layer is probably appeared as α -globulin that can be dissolved in the aqueous phase. The outer layer proteins have a negative charge (carboxylate, ROO^-), causing rubber particle to stabilize in colloidal form. **Figure 2.3** represents the composition of rubber particle as compose of three main components: hydrocarbon, phospholipid and protein.

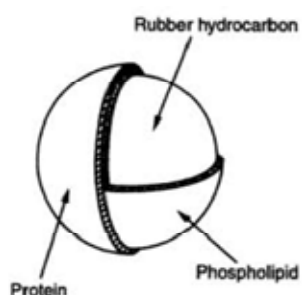


Figure 2.3 Composition of the rubber particle [17]

2.1.2.2 Serum Phase

Serum phase, locating at the middle, is a liquid phase of latex. The major composition is soluble substance. The portion of this layer is about 44-55% of the latex. The serum phase comprises in variety of chemical species such as carbohydrates, protein and amino acid.

Carbohydrate is a substance known as l-methyl inositol or quebrachitol. This is most intensively occurred on the liquid phase. The other carbohydrates are present in a few amounts in latex. There are galactose, sucrose, glucose, fructose and various other inositols.

Proteins contain several types that have differing isoelectric points. As mentioned above, the dominant protein type is α -globulin. Another protein is presented in serum phase besides α -globulin that is known as hevein. Solubility of α -globulin is insoluble in water, but can be soluble in neutral salt, acid and alkaline solutions. It has an isoelectric point at 4.8. Hevein consists of 5% of sulphur as cystine-type linkages. The isoelectric point is at pH 4.5. It is soluble in water at all pH. Hevein insignificantly affects the colloidal properties of natural rubber latex.

2.1.2.3 Bottom Phase

It is a sediment phase with the content of about 15-20% of the latex. The principal constituent is luteoid particle. Luteoid particle is in spherical shape with the diameter in the range of 0.3-5 μm . Luteoid particle is rather larger than the rubber particle. The luteoid particle is enveloped with a membrane layer that sensitively produces an osmotic membrane. This causes luteoid particles to lose their stability easily. Therefore, the freshly tapped latex should be separated from luteoid particles by centrifuging in order to avoid spontaneous coagulation in the latex.

2.2 Production of Natural Rubber Latex

2.2.1 Preserved Field Latex [18-21]

In the Hevea rubber tree, the latex can generate colloidal stability due to the negative charge of the protein layer. When latex is excreted from the Hevea rubber tree, the natural protein can be attacked by bacteria in the atmosphere. The degradation of protein causes the coagulation of latex that can occur within a period of 6-12 hours after tapping. This process is known as spontaneous coagulation. Thus, the field latex must be preserved and fortified against bacterial attack by immediately adding preservatives. There are many types of preservative that can be used in the latex such as ammonia, caustic soda, formaldehyde, sodium bisulphate, borate, phosphate and oxalate. In commercial practice, the most widely used is ammonia with a minimum of 1% of the latex. The advantage of ammonia lies in the possibility of removing it by an accretion process.

2.2.2 Concentrated Latex [19-21]

As mentioned in the previous part, the latex directly acquired from Hevea tree consists of rubber only 30% of the latex. The main component (about 65%) of the latex is water. To make the latex suitable for the production line and to reduce transportation cost, the certain amount of water must be removed. The latex with low water content is called as concentrated latex. Basically, the process to make the concentrated latex involves the removal of a substantial quantity of serum from field latex and making latex richer in rubber content.

The important processes to produce the concentrated latex can be separated are creaming, centrifugation, evaporation and electrodecantation. Commercially, the creaming and centrifugation are commonly used to prepare the concentrate latex. The detail of these two methods is described as follows.

2.2.2.1 Creaming

This is the earliest and simplest process to produce the concentrated latex. The processing of latex into creamed concentrate involves the mixing of a creaming agent such as ammonia alginate, sodium alginate and tamarind seed powder with properly reserved field latex and then allowing the latex to separate into two layers for a period of at least two days until a concentrate of the desired dry rubber content is obtained. The density of the rubber particles is less than that of the dispersion medium. So, the rubber particle tends to rise upon the surface of the dispersion medium. The layer rubber of serum is removed, leaving the latex concentrate having about 50-55% dry rubber content (DRC).

2.2.2.2 Centrifugation

Concentration by centrifugation was first used in 1898 by Biffin. Most of commercial concentrated latex is mainly prepared by centrifugation because the obtained product can be suitably used in various rubber applications. The processing of latex into concentrated latex by centrifugation involves the separation of preserved field latex into two fractions, one containing the concentrated latex more than 60% of dry

rubber and the other containing 4-8% of dry rubber (skim latex). Skim latex is generally coagulated with sulphuric acid, made into crepe, dried and marketed as skim rubber. There are two types of concentrated latex made on a large scale by this method.

- HA (high-ammonia) latex, preserved with 0.7% ammonium

- LA (low-ammonia) latex, preserved with 0.25% ammonia and other chemical agents such as 0.025% tetramethylthiuram disulfide, zinc oxide, 0.04-0.05% lauric acid as ammonialaurate.

The outline of low-ammonium and high-ammonium in concentrated latex is illustrated in **Figure 2.4**.

2.2.3 Prevulcanized Latex [16, 19, 20, 22]

The prevulcanized latex can be referred to pre-compounded latex either with slightly crosslink or without crosslink. The crosslinking of rubber in latex can be affected by reaction with sulphur, sulphur-donors and peroxide. In general most prevulcanized latex requires different types of additive. The additives usually used in prevulcanized latex are:

2.2.3.1 Stabilizer

2.2.3.2 Vulcanizing agents

2.2.3.3 Activators

2.2.3.4 Accelerators

2.2.3.5 Antioxidants

2.2.3.6 Fillers and Pigments

2.2.3.7 Special Additives

2.2.3.1 Stabilizer

Stabilizer is a substance that is added to latex to increase or modify rubber stability. It is a very important substance. The chemicals that are used as stabilizers can be classified as anionic, cationic, amphoteric and non-ionogenic types. Anionic stabilizers are predominant in the latex industry. When an anionic stabilizer is dissolved in water, the negatively charged anions are of greater magnitude than the

positively charged cations, and surround the rubber droplets so they repel each other. Cationically stabilized latex would be just the opposite, but is no longer common. Commercially, there are various stabilizers for latex such as potassium hydroxide (KOH) and Teric 16 A16. (Surfactant with c16-c18 alcohol ethoxylate) that is used about 0.2-0.5 phr. For fatty acid soap such as potassium laurate and potassium oleate, the required amount is about 0.2-0.4 phr.

2.2.3.2 Vulcanising Agents

Vulcanising agents are the chemicals that connect the molecular rubber chains together. Since the chains are linked, a force is required to pull them apart. The strength of this force is a measure of the efficiency and number of connectors or crosslinks. The force required to stretch a crosslinked polymer to a specified elongation is called modulus. The force required to completely separate a crosslinked polymer is called tensile strength. The normal vulcanizing agent of the natural rubber latex is sulfur. Sulfur is used approximately as 0.5-2 phr.

2.2.3.3 Activator

Activators are chemicals increasing the effectiveness of sulfur. That is to say, sulfur alone will vulcanize (cure or crosslink) rubber latexes. However, at higher temperatures, the process will theoretically take days, during which time oxidation would destroy the polymer before sufficient crosslinking could take place. Zinc oxide activates the crosslinking action of the sulfur. A sulfur/zinc oxide cure of the rubber latex now can take place in a matter of hours at higher temperatures. The optimal amount is 0.05-5 phr.

2.2.3.4 Accelerator

These are chemicals added to latex to reduce the vulcanization time and vulcanization temperature. Accelerators also increase the properties of vulcanized product. Most accelerators for sulfur cures are nitrogen-bearing. They fall into classes such as: zinc diethyl dithiocarbamates or ZDEC with the required amount of 0.5-1.6 phr, Zinc-2 mercaptobenzthiazole or ZMBT with the required amount of 0.25-0.5. Tetramethylthiuram disulfide or TMTD is also used but rarely.

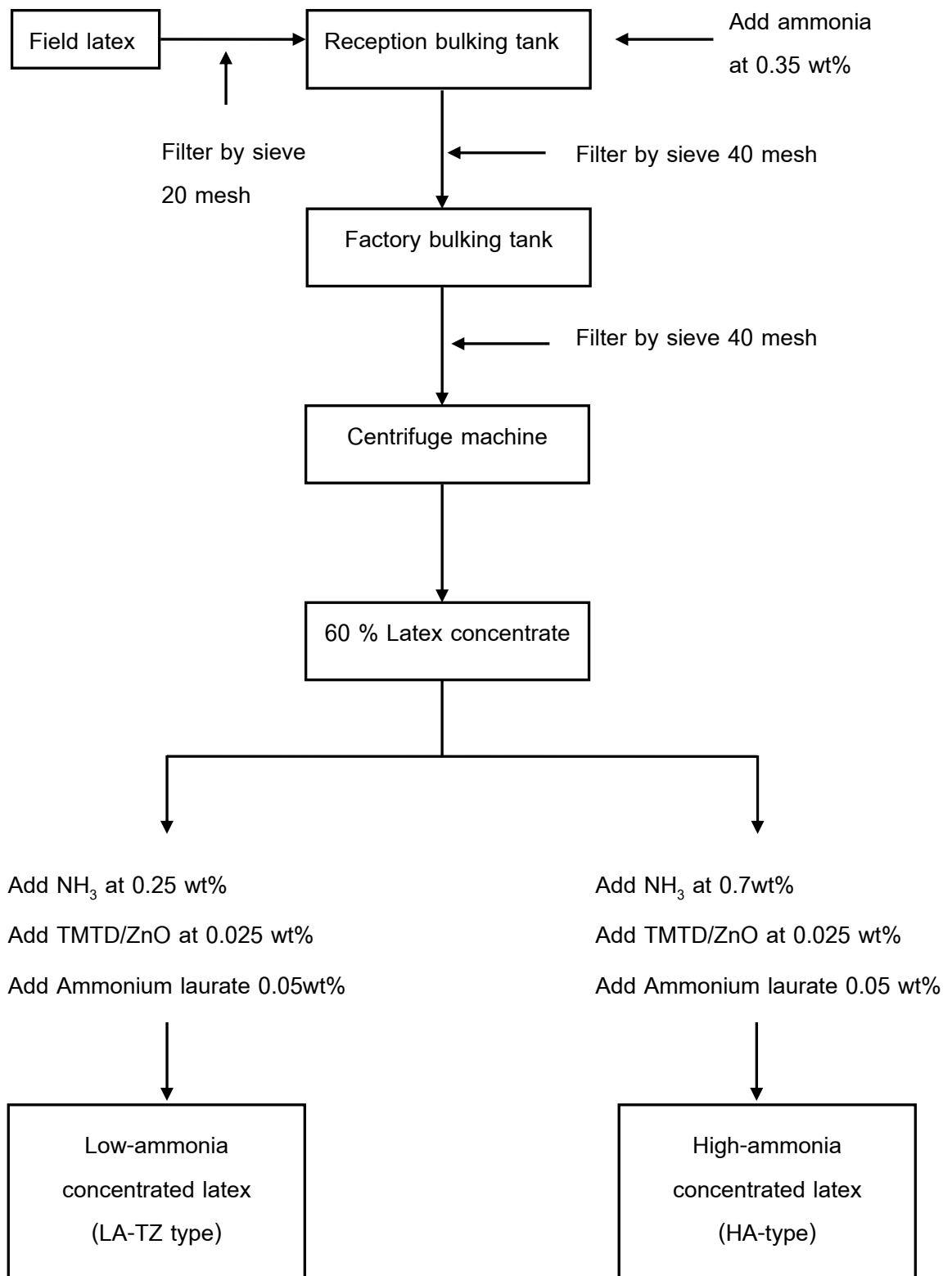


Figure 2.4 The outline of low-ammonia latex and high-ammonia concentrated latex [21]

2.2.3.5 Antioxidants

Oxygen attacks and degrades latex rubber films in the same manner that it degrades dry rubber products. The common antioxidants used in latex product fall into two classes including amine derivative and phenolic derivative. Amine derivatives are powerful antioxidants but they are limited to products where staining and discoloration are of no consequence, such as some adhesives and saturants for paper. Phenolic derivatives which are generally less effective antioxidant but they have an advantage in minimal staining or discoloration products such as gloves, condoms, balloons, thread, foam and carpet backing.

2.2.3.6 Filler and Pigments

The main reasons to use fillers in latex are to reduce cost and improve its properties. The fillers with discoloration generally used in latex are silica and calcium carbonate. The loading is in the range of 20-40 phr. Titanium dioxide is used as a white pigment in the latex. The quantity of titanium dioxide required is about 10-15 phr.

2.2.3.7 Special Additives

The special additives are also added into latex depending on the nature of the process, or the end use. Examples of special additives are foaming agents, potassium oleate or coagulant, etc.

2.3 Dispersion and Emulsion of Filler in Latex [20]

The most of chemical ingredients used in latex compounding are mainly in the forms of dry powder and water-insoluble liquid like oil. When adding in the latex, they may agglomerate or coagulate. Therefore, both must be processed into a form that will be miscible with the latex, as dispersion and emulsion, respectively. The commonality is to decrease the size of the particles or droplets and to protect them so that they:

1. will be compatible with the latex colloidal system,
2. can be dispersed uniformly throughout the latex, and
3. will not agglomerate or coalesce.

2.3.1 Dispersion of Dry Power Additives in Latex

Grinding the powder in a ball mill is a method to prepare a dispersion. The ingredients are water, dispersing agent and suspending agent (thickener or viscosity modifier). A wetting agent can be used to reduce the surface tension of the water to allow the solid particles to wet out. While ball mill grinding, a solid particle trapped between “stones” that collide is crushed, thus reducing its size. With continual grinding, all the ingredients become homogeneous and can be added to the latex.

2.3.2 Emulsion of Liquid Additives in Latex

Emulsion of liquid additives is prepared by reducing oil droplets to microscopic size in a medium. The oil becomes part of soap. It is usually made by blending a water phase and an oil phase under high shear.

2.4 Compounding Latex [23]

Latex and ingredients are become homogeneous by mixing compounding techniques. Water-insoluble ingredients are added as dispersion or emulsion as mentioned in the previous part. The colloidal stability of the latex must be maintained during and after adding the ingredients. The ingredients are added to the latex slowly in order to generate a base compound. The ingredients should be added to the latex in the accurate order of priority. The general arrangement of ingredients is as follows: stabilizers > vulcanizing agents > accelerators > antioxidant > activators > fillers and pigments.

Each ingredient when added in the latex should be stirred slowly for about 5-10 minutes. To ensure uniformly distribute of ingredients, the compound are gradually stirred further for about 30-60 minutes.

2.5 Maturation of Latex [23]

After mixing, the latex compounding is stored. Normally a storage time of 12-16 hours at temperature with 25-30 °C is adequate to confirm dispersion of the compounding ingredients. The maturation allows time for any air-bubbles in latex

compounding to rise to the surface. The time for removal depends on their size and viscosity of the compound. The compound should be gently stirred during maturation to avoid creaming and skin formation. Then, the compound is filtrated by nylon sieves.

2.6 Dipping Technique [20, 22-23]

The largest application in the natural rubber latex is the dipped products. Latex dipping is the simplest technique involved the formation of a polymer deposit around the entire outside of the former, which thin-walled of polymer is produced. Natural rubber latex is the most used in the dipping technique. Among the dipped products rubber gloves, condoms and balloons are always manufactured.

The latex dipping techniques are classified as straight dipping and coagulant dipping. The different of two methods depend on manufacture of them. The straight dipping is manufactured without the use of coagulant; while coagulant is used in coagulant dipping. The coagulant is an electrolyte solution to increase fixation of natural rubber when deposit on a former. Either calcium nitrate or calcium chloride is commonly used as coagulant. The principals of the dipping technique are followed:

- A suitably shaped former is immersed in a latex compound for a suitable time and subsequently slowly withdrawn from it. The latex compound uniformly deposits on it.
- The latex depositing on the former is dried and vulcanized.
- The finished product is stripped from the former.

In this place, only gloves production was focused. Gloves are prepared by the coagulant dipping process. Firstly, the ceramic former is slowly dipped into bath, which filled with coagulant solution, and upon drying. The dry former is slowly immersed into a second bath of natural latex, left for an appropriate time and then slowly withdrawn. The uniform coating with thin-film of latex on the former are generated. Then, the uniform coating former is dipped into a leaching tank that filled with warm water. Next, the thin layer on the former can be dried and vulcanized at low temperature at about 60-80 °C. This is the first drying stage. This step can be re-immersed the former in the latex if desired thickness of the deposit film. After that, the former is immersed in water that

containing a suitable de-tacking agent to increase the allergic reaction from natural latex gloves. Washing and drying on the inside and outside former. Then, the former is secondarily dried and vulcanized at temperature of 110-120 °C in an oven. Finally, the former is cooled down and is removed from the former.

2.7 Filler for Elastomers [24-25]

Filler of elastomers acts as significant role in the improvement of variety of the vulcanizate properties. For example tensile strength, tear resistance and abrasion resistance. All fillers are not equal, so that they can be typically classified into three broad categories:

- 1 Non-reinforcing or degrading fillers
2. Semi- reinforcing or extending fillers
3. Reinforcing fillers

Common reinforcing fillers are carbon black and silica. The filler used in largest volume is carbon black. This filler has low cost, good compatibility and increases the mechanical properties. However, carbon black can only be used in black product. For this reason non-black filler is applied as reinforcing filler for product that not only giving smart properties but also colorful products. The non-black fillers for elastomers are various types such as calcium carbonate, kaolin clay, silica talc, barite, wallastonite and mica. Among of non-black fillers, silica is widely used as reinforcing filler.

2.7.1 Particle Size of Filler

Improvements in the physical properties are directly related to particle size. Filler with the smaller particle size imparts greater reinforcement to rubber compound. The particle size of fillers ranges as shown in **Figure 2.5**. Fillers with particle size larger than 10,000 nm (10 μm) are evaded so they can decrease performance of reinforcing fillers and do not improve the rubber properties. Fillers with particle size between 1,000 and 10,000 nm (1 to 10 μm) are used primarily as diluents and usually have no significant effect on the rubber properties. The suitable reinforcing fillers at which its size ranges from 10 to 100 nm (0.01 to 0.1 μm), can directly improve the rubber properties.

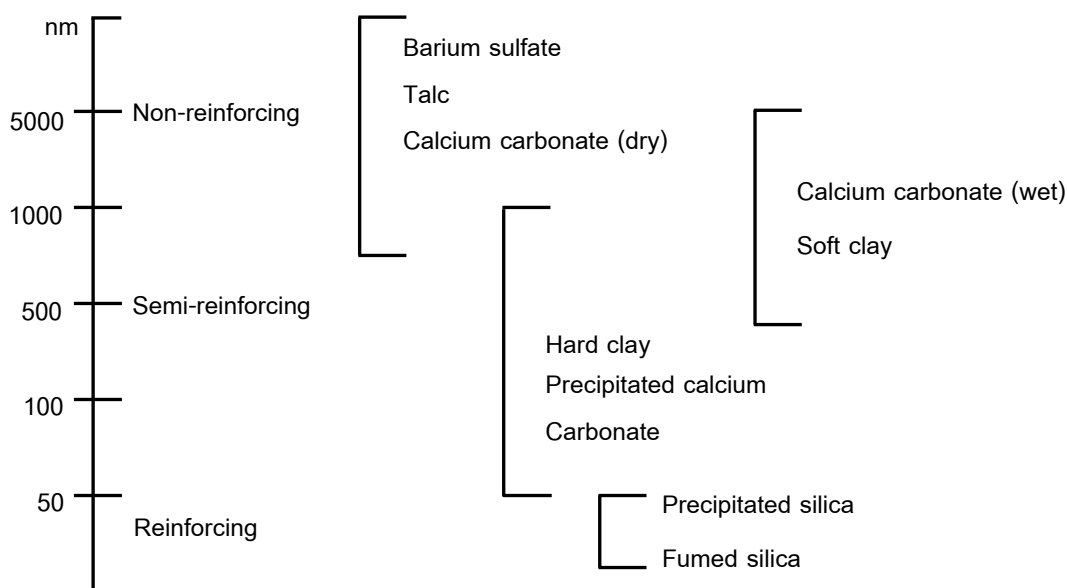


Figure 2.5 Classification of fillers based on their particle size [25]

2.7.2 Particle Surface Area

Fillers with a high surface area have more contact area available. Therefore, they have a higher potential to reinforce the rubber. The shape of the fillers and particle size distribution are also having significant effects on the reinforcement imparted by particulate fillers. Particle fillers with planar shapes have more surface area available for contacting the rubber than spherical particles with an equivalent average particle diameter. Particulate fillers with a broad particle-size distribution have better packing in the rubber matrix, which results in lower viscosity than that provided by an equal volume of fillers with a narrow particle-size distribution.

2.7.3 Structure of Filler

The primary particles of filler do not exist separately. They prefer to assemble to form a bigger particle called aggregate. Carbon black and precipitated silica usually form aggregate. The anisometry of these fillers is explained in term of structure, which incorporates aggregate shape, density and size.

2.7.4 Surface Activity

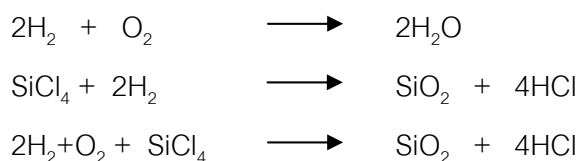
Even having a high surface area, high aspect ratio and small particle size, sometimes they still provide relatively poor reinforcement if they have low specific activity. The surface of filler has chemically or adsorptively bound functional groups that are called active site. The active site can be reacted chemically with rubber molecule. Thus, it can promote a high affinity of rubber to filler. For example, carbon black surface consists of carboxyl, lactone, quinine and other organic functional group which can form chemical reaction with molecule of the rubber.

2.8 Silica [26]

Chemical structure of silica is composed of ultimate particles of the inorganic polymer that are silicon and oxygen with the chemical formula of SiO_2 . Silica is occurred in several forms and is insoluble in water. Silica with pure form is colorless to white. Silica can be grouped into two major classes: natural and synthetic. Natural form is most commonly found as sand, quartz and walls of diatoms. Synthetic form is manufactured in several forms including fumed silica, fused quartz, gel and precipitated.

2.8.1 Fumed Silica or Pyrogenic Silica [27]

The fumed silica is prepared by the hydrolysis of silicon tetrachloride vapor in flame of hydrogen and oxygen at temperature of 1000°C or higher.



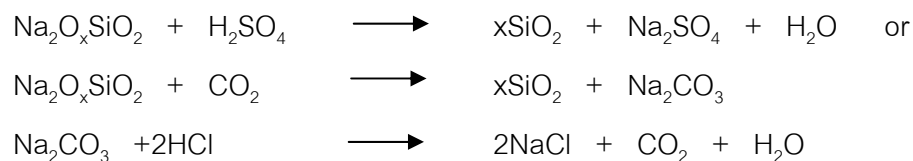
The primary particles of silica are formed when silicon tetrachloride is burned in a flame of hydrogen and oxygen. While still molten, the primary particles fuse irreversibly into secondary particles is called as aggregate. Fumed silica is amorphous structure. The particle of fumed silica is spherical morphology. The fumed silica has ultimate outstanding characteristics that are low density of silanol groups, low moisture content and high impurities. The general properties of the fumed silica are listed in **Table 2.2**.

Table 2.2 General properties of fumed silica [27]

| | |
|-----------------------|--------------------------|
| Color | white |
| Structure | amorphous |
| Surface area | 50-380 m ² /g |
| Silanol group density | 2-4 SiOH nm ² |
| Refractive index | 1.45 |
| Primary particle size | 7-40 nm |

2.8.2 Precipitated Silica

Precipitated silica is prepared by the acidulation of sodium silicate with either concentrated sulfuric acid, hydrochloric or carbonic acid. The reaction is conducted in a stirred reactor under alkaline pH conditions.



Reaction conditions are manipulated depending on the particle size required. Precipitated silica used as reinforcing filler generally has particle size at 10-40 nm. When the particle size is 40 or higher, this precipitated silica then is classified as semi-reinforcing filler.

2.9 Characteristics of Synthetic Silica [24-26]

2.9.1 Surface of Silica

Synthetic silicas are amorphous, submicron-size white powder. These are comprised of silicon. A silicon atom is covalent bonded in a tetrahedral structure arrangement to four oxygen atoms. The silica structure at surface terminates in siloxane group (-Si-O-Si) and one of the several forms of silanol group (-Si-O-H). Silica surface is densely covered with silanol (4-5 groups/100 Å²). The surface of silica can be divided into three silanol forms: isolated silanol, vicinal silanol and germinal silanol as shown in Figure 2.6.

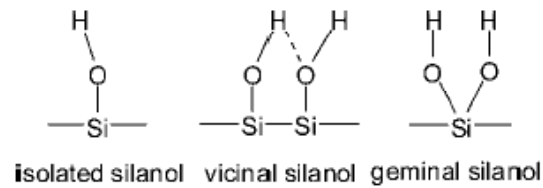


Figure 2.6 Illustration of three types of surface silanol [1]

2.9.2 Silica Structure and Surface Area

Naturally, silica does not like to stay as an individual particle but prefers to fuse together into bunch particle called aggregate. Thus the particles cannot be separated during compounding process. The silica aggregate built from primary particles are three-dimensional cluster and its size can range up to 500 nanometer in diameter. Besides, aggregates can physically agglomerate through intermolecular hydrogen bonding of silanol groups of one aggregate to a silanol group of another aggregate, forming agglomerate. Agglomerate size is approximately 100 micron in diameter. The median agglomerate particle size is generally 20 to 50 micron, but can be decreased by milling to about 1 micron. Figure 2.7 shows various structures of silica.

Surface area refers to the amount of silica surface available to interact with the elastomer. In general, surface is inversely to the size. The small particle has high surface area. And this is considered as excellent rubber reinforcing filler.

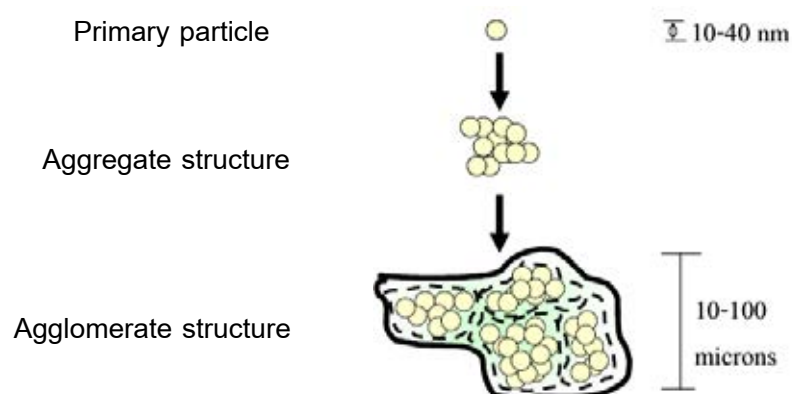


Figure 2.7 Illustration of silica morphology [26]

As mentioned above, the surface of the silica has a lot of silanol groups that induces aggregate to form agglomerate via hydrogen bonds. These bonds hold individual silica particles together and the aggregates remain intact even under the best mixing conditions. The interaction between the silanol groups (polar groups) on the surface of the silica aggregates with non-polar groups of hydrocarbon elastomer are weak compared with the hydrogen bonding interaction between surface silanol groups in silica itself (reinforcing filler), thus leading them to have low compatibility with rubber.

To improve mechanical properties of silica-filled rubber, the dispersion of silica in rubber matrix must be enhanced. A good dispersion may be completed by any surface modification of silica that can increase the compatibility between hydrocarbon rubber and silica. The surface modification of silica can be widely classified by either chemical or physical methods.

2.9.3 Chemical Modification Method [28-29]

Surface modification of the silica by chemical interaction can lead to strong interaction between rubber and silica. Modifier agents and grafting polymer are commonly used in chemical modification methods. Silane coupling agents are the most used modifier agents. The general formula of the silane coupling agents can exhibit two classes of functionality as $RSiX_3$ as shown in Figure 2.8.

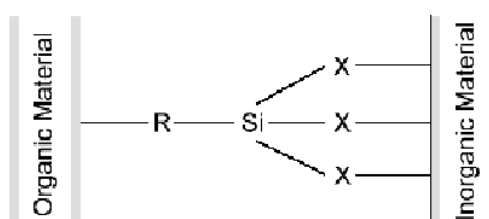


Figure 2.8 Chemical structure of silane coupling agent [29]

The "X" functional represents the hydrolysable groups. It can be attached to an inorganic material to achieve coupling reaction. The "X" group of the silane molecule will be hydrolyzed to produce silanol that form a metal hydroxide or siloxane bond with the inorganic material. Examples of "X" groups are methoxy, ethoxy

or chlorine. The “R” function represents the nonhydrolysable groups that can be reacted with the organic material to produce a covalent bond. The “R” groups have various functionalities such as vinyl, amino, chloro or epoxy.

Grafting of polymer chain to silica is an effective procedure to improve the adhesion of the silica surface with polymer matrix. Grafting method can be explained as the covalent process and can be increased the hydrophobicity of the particle. Generally, the grafting can be accomplished by either “grafting to” or “grafting from” approaches. For “grafting to” approach, functionalized monomers react as covalent bond with backbone polymer. For “grafting from” approach, it is obtained by treating a substrate with in situ polymerization to generate immobilized initiators.

2.9.4 Physical Modification Method [1]

Physical methods are based on the physical interaction between silica and polymer matrix. These methods usually use surfactants or macromolecules to adsorb onto surface of silica particles. A polar group of a surfactant can be absorbed to the surface of silica via electrostatic interaction. A surfactant can decrease interaction of silica particles in agglomerate structure and reduce the physical attraction, thus leading silica to incorporate into the polymer matrix.

2.10 Colloidal Composite Method

Colloidal polymer/silica composites exhibit a new method to improve silica dispersion in polymer matrix. These materials can have extraordinary properties such as mechanical, thermal or rheological properties when having the suitable combination between organic and inorganic components inside particles. To increase compatibility between silica surface and polymer, the synthetic methods of composite commonly require improving affinity. To establish a physicochemical or chemical link at the interface of the silica particle and polymer, there are various methods to prepare colloidal system such as sol-gel process, in situ polymerization and self-assembly technique. The important rule to achieve the physicochemical properties is the controlling of the morphology of colloidal particles. The colloidal polymer/silica composites can be

formed in many interesting morphologies such as raspberry-like, currant bun-like or core-shell structures as shown in Figure 2.9.

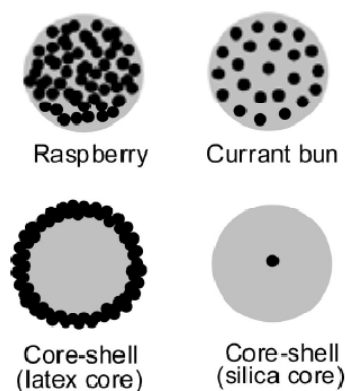


Figure 2.9 Illustration of morphologies of colloidal polymer/silica composite [1]

2.10.1 Self-assembly Technique [1, 30]

Self-assembly is a branch of nanotechnology which involves spontaneous and reversible organization of molecular units at which the molecules arrange themselves via their reciprocal interaction to form a larger functional unit by non-covalent interaction. Self-assembly may not represent simple method but give satisfied properties of polymer/silica nanocomposites. Silica nanoparticles are first prepared in colloidal form. The principal of self-assembly is to produce charges in the system to silica nanoparticles and polymer matrix. Then the self assembly between silica and polymer is occurred by electrostatic interaction.

Preparation of polymer/silica nanocomposites using Layer-by-layer technique was studied by Zhang et al [31]. The work showed the layer-by-layer technique was an effective method to synthesize composite of mesoporous silica shell on polystyrene (PS) sphere. PS beads were modified by polyelectrolyte acting as dispersing agent. Polyelectrolytes used in this work were poly (diallyldimethylammonium chloride) or PDDA and poly (styrenesulfonatesodium salt) or PSS. The preparation procedure of PS core-mesoporous silica nanoparticles shell composite is shown Figure 2.10. As seen, firstly, PDDA and PSS produced the positive charge around the PS beads by

electrostatic attraction. When mesoporous silica nanoparticles were added to the solution of modified-PS, the positive charge of modified-PS can react with negative charge on the surface of mesoporous silica nanoparticles, hence leading to form core-shell composite through strong electrostatic interaction.

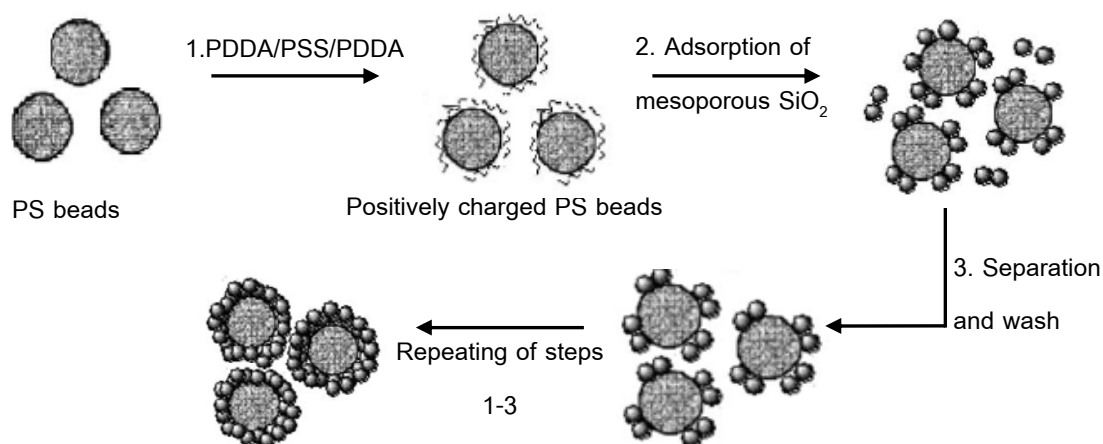


Figure 2.10 The schematic of PS core-mesoporous silica nanoparticle shell nanocomposites process [31]

Although electrostatic interactions between positive and negative charges are notable driving forces in the self-assembly technique, the self-assembly can be accomplished using other interactions such as hydrogen bonding, coordination bonding, or chemical bonding as the following work. Kong et al [8] lately prepared polyvinylalcohol (PVA)/silica nanocomposites by employing electrostatic attractive and hydrogen bonding interactions. Poly (allylamine hydrochloride) or PAH, that has positive charge throughout molecular chains, can be adsorbed onto the surface of negatively charged silica nanoparticles through electrostatic interactions. Then, the PVA molecular chains are assembled to the surface of silica nanoparticles through hydrogen bonding between their hydroxyl groups and amino groups of PAH. However, the result demonstrated that the silica content had direct influence on the formation of nanocomposites. When the content of silica used was at 5 wt% or higher, silica

nanoparticles tended to aggregate. Therefore, the formation of nanocomposites was limited by the optimal silica content.

The formation of PVA/silica nanocomposites through hydrogen bonding is shown in Figure 2.11.

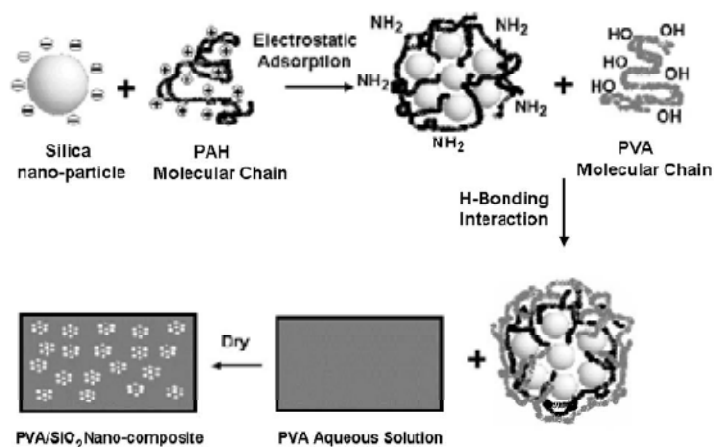


Figure 2.11 The schematic of PVA/silica nanocomposites process [8]

Although previous researches showed that self-assembly can be used to prepare polymer/silica nanocomposites. But silica content was a remarkable problem in this system. This was also observed by Peng et al [9]. They studied the preparation of natural rubber/silica nanocomposites through combining self-assembly and latex-compounding techniques. The effect of silica content was also discussed. The procedure of self-assembly is shown in Figure 2.12. Firstly, the positive charge of PDPA molecular chains was adsorbed onto the surface of negative charge of silica nanoparticles through electrostatic adsorption. Then the positive charge of silica/PDPA core-shell particles were assembled with negative charge of natural rubber particles.

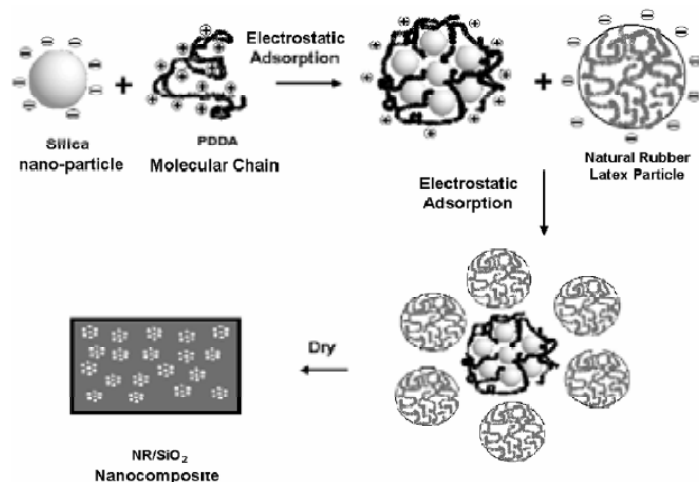


Figure 2.12 The schematic of self-assembly NR/silica nanocomposite process [9]

At different silica loadings, it was observed that when silica content was less than 4 wt%, the NR latex and silica nanoparticles can gather to form core-shell structure with slightly primary aggregation. As more silica was loaded, intensively secondary aggregation was produced.

Tensile and tear strength of nanocomposites were obviously increased with increasing silica content up to 4 wt% as shown in Table 2.3. This indicated that the silica dispersion played an important role on mechanical properties of NR/silica nanocomposites.

Table 2.3 Mechanical properties of NR/silica nanocomposite [9]

| | | | | | | | |
|-------------------------|------|------|------|------|------|------|------|
| Silica loading (wt%) | 0 | 0.5 | 1.0 | 2.5 | 4.0 | 6.5 | 8.5 |
| Tensile strength (MPa) | 15.1 | 18 | 19.8 | 22.7 | 26.3 | 21 | 1.06 |
| Tensile modulus (MPa) | | | | | | | |
| 100% elongation | 0.63 | 1.05 | 1.5 | 1.9 | 2.26 | 1.87 | 0.30 |
| 200% elongation | 0.96 | 1.54 | 2.03 | 2.48 | 3.08 | 2.35 | 0.65 |
| 300% elongation | 1.27 | 2.14 | 3.15 | 4.17 | 5.08 | 3.71 | 0.99 |
| Elongation at break (%) | 995 | 963 | 919 | 857 | 730 | 568 | 384 |
| Tear strength (kN/m) | 37.1 | 41.9 | 53 | 59 | 61.4 | 70.7 | 30.2 |

2.11 Particle Size Analysis [32-35]

Before discussion about the principle of particle size analysis, it is important to understand the particle sizes meaning. The particles are three-dimensional objects which three parameters are length, width and height that are required in a complete description. The particle size analysis technique can be explained them with only one number.

Particle size analysis is a measurement of the size distribution of individual particle in a soil sample. The major features of them are the destruction or dispersion of soil aggregates into discrete units by chemical, mechanical, or ultrasonic means and the separation of particles.

Particle size analysis data can be demonstrated in several techniques. Most techniques assume the material being measured is spherical. The spherical particle can be defined using a single number as diameter because every dimension is identical. Equivalent sphere is termed of particle size diameter when measuring in particle size analysis technique. This equivalent sphere approximation is useful in that it clarifies the way particle size distributions are represented. However, it does mean that different techniques can be produced different results when measuring non-spherical particles. So must be aware that each characterization technique will measure different properties of a particle (maximum length, minimum length, volume, surface area etc.) An example of the application of the equivalent sphere approximation work is shown in Figure 2.13.

2.11.1 Sample Dispersion Technique

Pretreatment of sample is very important step in particle size analysis. It can be enhanced the separation or dispersion of sample aggregate. Particle size analysis methods require that the soil particles must be dispersed in aqueous solution. Methods of the dispersion can be classified into two broad groups as chemical and physical dispersion. Dilute alkaline solution of sodium polyphosphate is frequency used in chemical dispersion. The effectiveness of the chemical dispersing agent depends on its

ability to create and maintain repulsive forces between soil particles. Physical dispersion of particles is carried out by shearing action such as mechanical shaker, electrical mixers or ultrasonic probe.

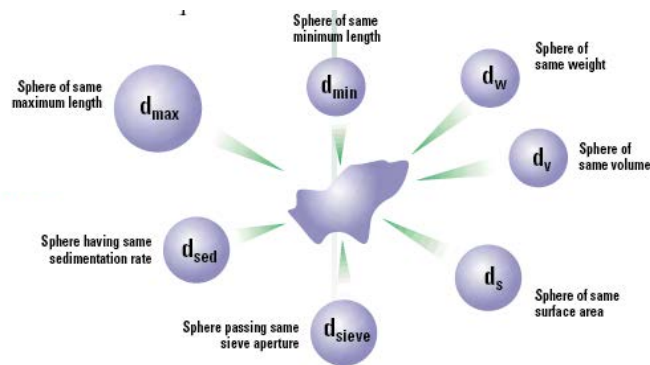


Fig. 2.13: Equivalent sphere representation for an irregularly shaped particle [32]

2.11.2 Laser Diffraction Particle Analysis

The principal of laser diffraction techniques is represented that particles passing through a laser beam will scatter light at an angle that is directly related to their size. As particle size decreases, the observed scattering angle increases logarithmically. Scattering intensity is also dependent on particle size, diminishing with particle volume. Large particles therefore scatter light at narrow angles with high intensity whereas small particles scatter at wider angles but with low intensity.

2.11.3 Interpretation of Particle Size Distribution Data

In laser diffraction, particle size distributions are calculated by comparing a sample's scattering pattern with an appropriate optical model. Traditionally two different models are used: Fraunhofer approximation and Mie theory.

Fraunhofer approximation was used in early diffraction instruments. It assumes that the particles being measured are opaque and scatter light at narrow angles. As a result, it is only applicable to large particles and will give an incorrect assessment of the fine particle fraction.

Mie theory provides a precise solution for the calculation of particle size distribution from light scattering data. It forecasts scattering intensities for all particles,

small or large, transparent or opaque. Mie theory predicts the primary scattering from the surface of the particle, with the intensity predicted by the refractive index difference between the particle and the dispersion medium. It also predicts the secondary scattering caused by light refraction within the particle. This is necessary important for particle which is transparent and below 50 microns in diameter.

Results of particle size analysis can usually display in logarithmic graph, a bell-shaped curve is generated as shown in **Figure 2.14**. Mean, median and mode that are basic terms in statistics are used in order to characterize the arithmetic mass distribution.

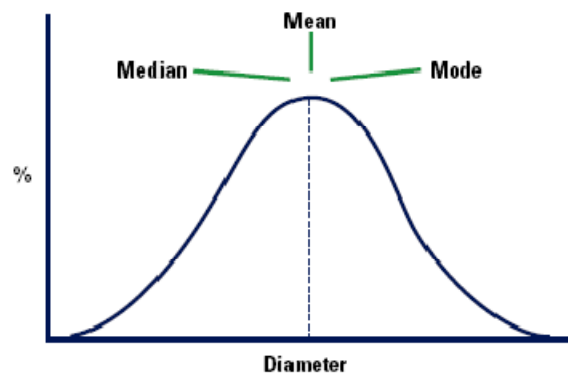


Figure 2.14 Symmetric distribution when mean, median and mode lie in the same position [35]

2.11.3.1 Mean

Mean value is some arithmetic average of the data. In particle size distribution, mean is the average particle diameter of distribution.

2.11.3.2 Median

Median value is defined that the particle diameter is divided the frequency distribution into two equal halves. For particle size distribution, the median is called D50 at which the size in microns splits the distribution with half above and half below this diameter. The Dv50 is the median for a volume distribution. Laser diffraction technique results are usually reported the data with D10, D50 and D90 values based on volume distribution as illustrated in **Figure 2.15**.

2.11.3.3 Mode

In particle size distribution, mode represents the particle diameter or size range that most commonly found in the distribution. The mode is the highest peak seen in the distribution. The mode is not commonly used, but can be described in particular if there is more than one peak to the distribution. The mode can be described the mod-point of the different peak.

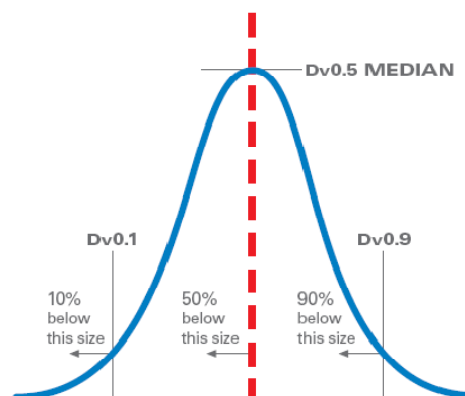


Figure2.15 Symmetric distribution: D10, D50 and D90 [35]

2.12 Polyelectrolyte [36]

Although the application of polyelectrolyte was already mentioned in the previous section when talking about the formation of polymer/silica nanocomposite via self assembly method, the more detail about polyelectrolyte is given here.

Polyelectrolyte is polymer that consists of repeating units of electrolyte group. In aqueous solution, electrolyte can dissociate, thus producing the charged polymer. Polyelectrolyte's properties are combined electrolyte and polymer properties. Polyelectrolyte is sometimes called polysalts. Electrolyte is salt that its solution is electrically conductive. Polymer represents a high molecular weight compound. Therefore, its solution is often viscous. Charged polymer chain plays a fundamental role in arbitrating structure, stability and interaction.

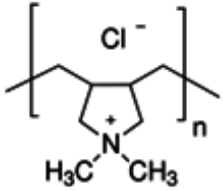
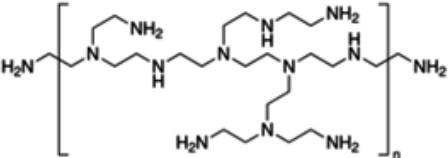
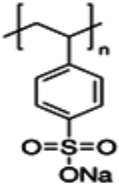
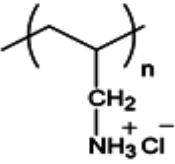
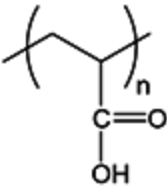
Degree of charging of polyelectrolyte solutions are directly affected in physical properties. Dissociation of polyelectrolyte releases counter-ions that significantly affect the solution's ionic strength and other properties such as electrical conductivity.

Polyelectrolyte can be applied in various applications. The polyelectrolyte can be represented to multiple types of surface due to the variety of ionic available and can be applied to surfaces in multilayer form to require a variety of design objectives. The uses of polyelectrolyte are grouped according to the following functions.

- Modifying flow in aqueous solution
- Stabilizing properties of aqueous solution and colloidal suspension
- Imparting surface charged
- Thickener
- Conditioner
- Flocculent
- Biocompatible polyelectrolyte

In commercial, polyelectrolytes can be used in various types and functions. **Table 2.4** illustrates examples of commercial polyelectrolyte.

Table 2.4 Commercial polyelectrolyte

| Name | Chemical Structure |
|---|---|
| Poly (diallyldimethylammonium chloride) or PDDA |  |
| Poly (ethyleneimine) or PEI |  |
| Poly (styrene sulfonate) or PSS |  |
| Poly (allylamine hydrochloride) or PAH |  |
| Poly (acrylic acid) or PAA |  |

CHAPTER III
EXPERIMENTAL

3.1 Materials and Chemical Agents

Materials and chemical agents used in this research along with their function are tabulated in Table 3.1.

Table 3.1 Materials and Chemical Agents

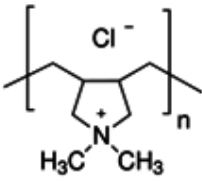
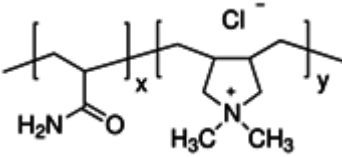
| Materials/Chemical Agents (Function) | Grade | Manufacturer / Resource |
|--|--|-------------------------------------|
| Natural rubber latex (composite matrix) | HA 60 wt% latex | Thai Rubber Latex PLC., Thailand |
| Silicon dioxide nanopowder (filler) | 10-20 nm (TEM) | Sigma Aldrich Co., LLC., USA |
| Poly(diallyldimethyl ammonium chloride) (dispersing agent)  | M _w 100,000-200,000 20 wt% in H ₂ O | Sigma Aldrich Co., LLC., USA |
| | M _w 250,000-350,000 20 wt% in H ₂ O | Sigma Aldrich Co., LLC., USA |
| | M _w 400,000-500,000 20 wt% in H ₂ O | Sigma Aldrich Co., LLC., USA |
| Poly(acrylamide-co-diallyl- dimethylammonium chloride) (dispersing agent)  | 10 wt% in H ₂ O | Sigma Aldrich Co., LLC., USA |
| Sodium hydroxide (pH modifier) | Commercial | RCI Labscan Ltd., Thailand |

Table 3.1 (cont.)

| Materials/Chemical Agents (Function) | Grade | Manufacturer / Resource |
|--|------------|--|
| Potassium hydroxide (stabilizer) | Commercial | Rubber Research Institute of Thailand |
| Surfactant c16-c18 alcohol ethoxylate (Teric 16 A 16) (stabilizer) | Commercial | Rubber Research Institute of Thailand |
| Sulfur (vulcanizing agent) | Commercial | Rubber Research Institute of Thailand |
| Zinc diethyl dithiocarbamate (cure accelerator) | Commercial | Rubber Research Institute of Thailand |
| Zinc-2 mercapto benzthiazole (cure accelerator) | Commercial | Rubber Research Institute of Thailand |
| Polyphenol antioxidant (Wingstay L) (antioxidant) | Commercial | Rubber Research Institute of Thailand |
| Zinc oxide (cure activator) | Commercial | Rubber Research Institute of Thailand |
| Toluene (rubber swelling solvent) | AR grade | RCI Labscan Ltd., Thailand |

3.2 Equipment

Equipment used to prepare NR/silica aqueous suspension and NR/silica nanocomposite sheet are listed in Table 3.2.

Table 3.2 The list of equipment

| Equipment | Model | Manufacture/Location |
|-------------------------------------|-----------------|--|
| High intensity ultrasonic processor | VCX-130 | Sonic & Materials, Inc., New South Wales |
| Magnetic stirrer | MR Hei-standard | Heidolph, Schabach, Germany |
| Mechanical stirrer | - | H.J.UNKEL (Tech.) Ltd., Thailand |
| Universal oven | UNB 400 | Memert, Germany |
| Test sieve | Mesh No. 200 | Endecotts, England |

3.3 Characterization and Testing

The physical and mechanical properties of the NR/silica aqueous suspension and NR/silica nanocomposite sheet were characterized and tested by the following instruments as shown in **Table 3.3**.

Table 3.3 The list of instruments

| Instruments | Model | Manufacture/Location |
|------------------------------------|--------------------------|--|
| Laser diffraction analyzer | Mastersizer 2000 | Malvern Instruments Co. Ltd., Malvern, England |
| Scanning electron microscope (SEM) | JSM-6400 | JEOL Ltd., Tokyo, Japan |
| Thermogravimetric analyzer (TGA) | TGA/SDTA851 ^e | Mettler Toledo, Greifensee, Switzerland |
| Universal Testing Machine | 5843 | Instron, Massachusetts |

3.4 Experiment Procedure

The NR/silica nanocomposite was prepared here by a self assembly and latex compounding technique using two types of dispersing agent including homopolymer

which is poly (diallyldimethylammonium chloride) or **PDDA** and copolymer which is poly (acrylamide-co-diallyl-dimethylammonium chloride) or **co-PDDA**. Moreover, there were three different molecular weights PDDA used here to study the effect of the size of dispersing agent on the properties of NR/silica nanocomposite sheet. The first PDDA has MW 100,000-250,000 and was named as low MW PDDA or **l-PDDA**. The second one has MW 200,000-350,000 and designated here as medium MW PDDA or **m-PDDA**. The last one is PDDA with 400,000-500,000 named as high MW or **h-PDDA**. The concentration of silica in the nanocomposite was varied from 1, 2, 3 and 4 wt%. The effects of different dispersing agent concentrations on ability to form the NR/silica nanocomposite were also investigated here. The concentrations of dispersing agent used here were 1 and 3 wt% of silica.

The preparation of the NR/silica nanocomposite was divided into two main steps as follows.

3.4.1 Preparation of the Silica/Dispersing Agent Aqueous Suspension

The silica nanopowder was added into the distilled water. Then, it was dispersed by high intensity ultrasonic processor (VCX-130, Sonic & Materials Inc., New South Wales) for 30 min. The operating condition was 130 watt at frequency of 20 kHz. The diameter and length of tip is 6 and 113 mm, respectively. Then, the pH of silica suspension was adjusted to 10 with 1 M NaOH in order to form negative charge on the silica surface. Next, the silica suspension was stirred for 20 min while dispersing agent was slightly added into it. In this step, the positive charge silica/dispersing agent aqueous suspension was obtained according to the schematic of self assembly NR/silica nanocomposite as shown in previous part (**Figure 2.12**). And **Figure 3.1** show the feature of a high intensity ultrasonic processor used in this study.



Figure 3.1 VCX-130, Sonic & Materials high intensity ultrasonic processor

3.4.2 Preparation of NR/Silica Nanocomposite

The prevulcanized natural rubber latex was prepared according to the formulation shown in **Table 3.4**. The positively charged silica/dispersing agent aqueous suspension was slowly added into the prevulcanized natural rubber latex and then mixed together using mechanical stirrer as shown in **Figure 3.2** at the constant speed of 150 rpm. Then obtained latex compound was filtrated by a 200 μm sieve to remove the dust. After that, the NR/Silica dispersion was casted in a mold of glass plates (20x20x1.5 cm) and pre-dried at 40 $^{\circ}\text{C}$ for 36 hours and post-dried at 100 $^{\circ}\text{C}$ for 15 min. Finally, the NR/silica nanocomposite sheet with thickness of 1 mm was obtained.

The outline of the overall experiment procedure for preparation and characterization of NR/Silica nanocomposite is described in **Figure 3.3**.



Figure 3.2 H.J.UNKEL (Tech), Mechanical stirrer

Table 3.4 Formation of pre vulcanized natural rubber latex.

| Ingredients | (phr) |
|-------------------------------|-------|
| Natural rubber | 100 |
| Potassium hydroxide | 2 |
| Teric 16A16 | 0.29 |
| Sulfur | 1.6 |
| Zinc diethyl dithiocarbamate | 0.8 |
| Zinc-2-mercapto benzothiazole | 0.8 |
| Wingstay L | 2 |
| Zinc oxide | 2 |

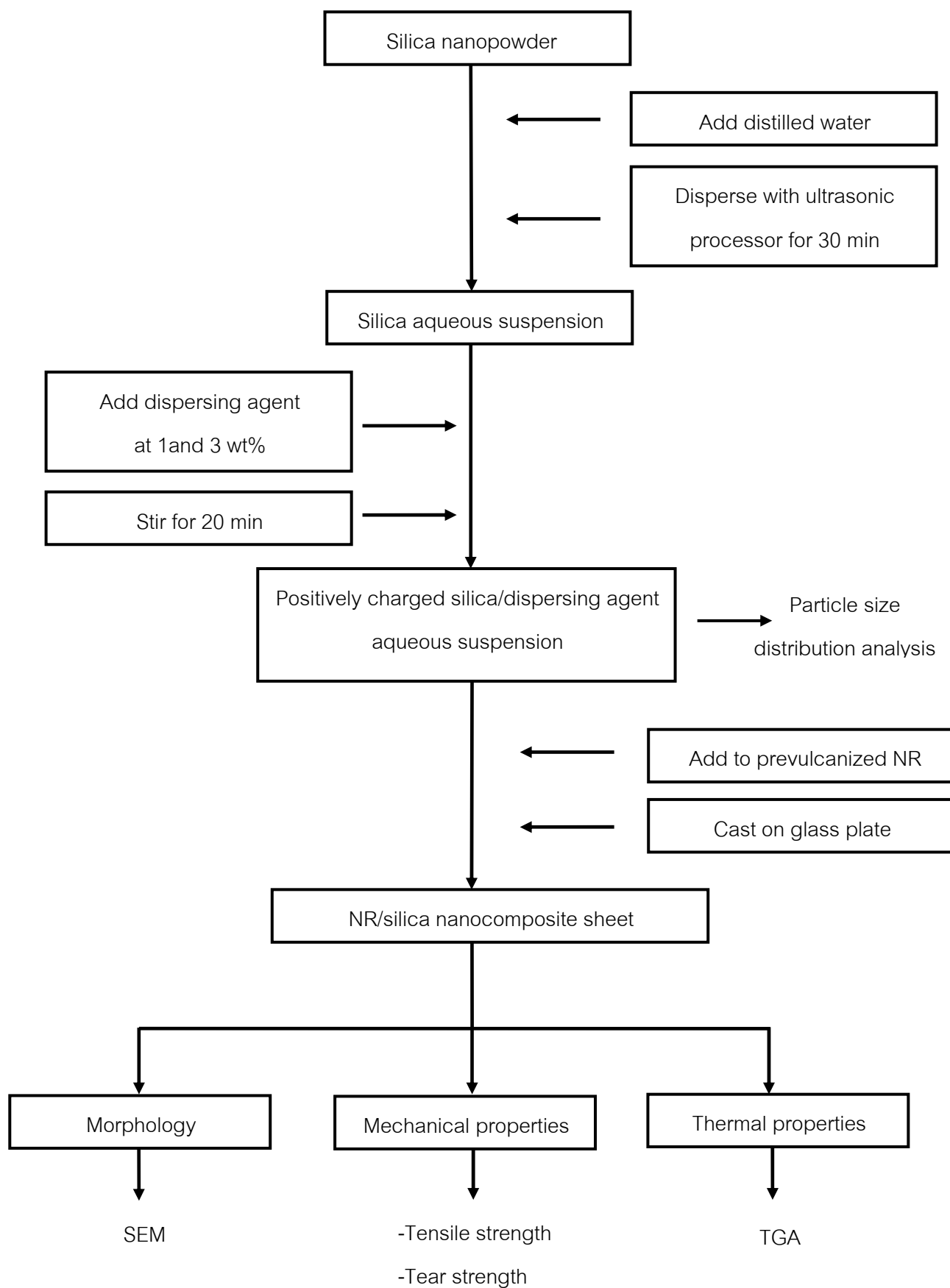


Figure 3.3 The outline of the experiment

3.5 Characterization and Testing

3.5.1 Particle Size Distribution of Silica/Dispersing Agent Aqueous Suspension

The particle size distribution of silica nanoparticles was measured by laser diffraction analyzer (Mastersizer 2000, Malvern Instruments Ltd., Malvern, England) as shown in **Figure 3.4** using small volume sample unit and dynamic range is 0.02 μm -2000 μm . Water is used as a dispersion medium and the refractive index of silica is 0.01. The average particle size distribution was adjudged from three replicates for each sample.



Figure 3.4 Mastersizer 2000, Malvern particle size distribution analyzer

3.5.2 Morphology of NR/Silica Nanocomposite

The morphology of NR/silica nanocomposite was taken using a scanning electron microscope; SEM (JSM-6400, JEOL Ltd., Tokyo, Japan) as shown in **Figure 3.5**. The cross-section of sample was prepared by breaking sample after quenching with liquid nitrogen. The fracture surface was coated with conductive gold before observation.



Figure 3.5 JSM-6400, JEOL Scanning electron microscope

3.5.3 Thermal Properties of NR/Silica Nanocomposite

Decomposition temperature of the NR/silica nanocomposite were analyzed using thermogravimetric analyzer (TGA/SDTA 851^o, Mettler Toledo, Greifensee, Switzerland) as shown in **Figure 3.6**. Measurement was carried out under nitrogen atmosphere. The sample was heated from 50 to 600 °C at heating rate of 20 °C/min. The flow rate of transporting gas was 20 ml/min. Weight of sample was in range of 8-10 mg. The onset and endset temperature of degradation were reported.



Figure 3.6 TGA/SDTA 851^o, Mettler Toledo Thermogravimetric instrument.

3.5.4 Tensile Strength

Tensile properties of NR/silica nanocomposite sheet were measured according to ISO 37 using an universal testing machine model (5843, Instron Ltd., Massachusetts) with a crosshead speed of 500 mm/min. The NR/Silica nanocomposite sheet was cut by applying type II die with dumb-bell shape as shown in **Figure 3.7**. The 100% and 300% modulus, tensile strength and elongation at break were determined. Five specimens were tested for each compound and the average value was reported.

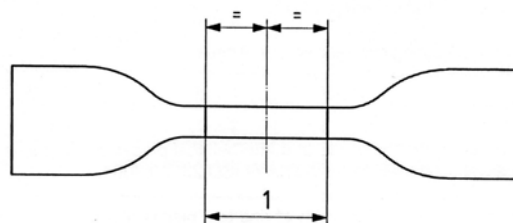


Figure 3.7 Tensile specimen type II according to ISO 37

The tensile properties were calculated as following:

1.100% modulus = stress at 100% elongation

2.300% modulus = stress at 300% elongation

3.Tensile strength (TS) = stress at break

$$\text{when Stress} = \frac{F}{A} \quad (3.1) \text{where}$$

F = observed force (N)

A = cross-sectional area of unstrained specimen (mm^2)

Percent elongation at break (EB)

$$EB = \left[\frac{L - L_0}{L_0} \right] \times 100 \quad (3.2)$$

where L = observed distance between grip of extended specimen

L_0 = original distance between the extensometer

3.5.5 Tear Strength

Tear strength of NR/silica nanocomposite sheet was measured according to ISO 34 using an universal testing machine (5843, Instron Ltd., Massachusetts) with a crosshead speed of 500 mm/min. Specimen was cut by applying type C die as shown in Figure 3.8. The tear strength can be calculated from maximum force required to tear specimen into two pieces per unit of thickness as shown in **equation 3.3**. The average tear strength from five specimens was reported.

$$\text{Tear strength (N/mm)} = \frac{F}{d} \quad (3.3)$$

where F = the maximum force (N)

d = the thickness of the specimen (mm)



Figure 3.8 Tear specimen type C according to ISO 34

3.5.6 Crosslink Density

The crosslink density can be measured from swelling method. The NR/silica nanocomposite sheet was cut into square shape, weighing approximately 0.2 gram. Then it was soaked in 50 ml of toluene and preserved in the dark for 7 days at room temperature. Then the swollen sample was taken out and wiped with tissue paper. It was quickly transferred to the weighing bottle to measure the weight. The swollen sample was dried at room temperature until the constant weight was achieved. After that the weight of dried sample was gauged. At least three samples for each compound were measured. The crosslink density (η_{swell}) was then calculated using the Flory-Rehner equation as shown in equation 3.4.

$$-\ln(1-v_r) - v_r \chi V_r^2 = 2V_t \eta_{\text{swell}} V_r^{1/3} - \frac{2V_r}{f} \quad (3.4)$$

when

$$v_r = \frac{\left[\frac{W_d}{\rho_d} - \frac{W_f}{\rho_t} \right]}{\left[\frac{W_d}{\rho_d} - \frac{W_f}{\rho_t} \right] - \left[\frac{W_s - W_d}{\rho_t} \right]}$$

where W_d = weight of dried sample (g)

| | | |
|-----------------------|---|--|
| W_f | = | weight of filler in sample (g) |
| W_s | = | weight of swollen sample (g) |
| ρ_d | = | density of rubber (g/cm^3) |
| ρ_f | = | density of filler |
| ρ_t | = | density of toluene ($0.862 \text{ g}/\text{cm}^3$) |
| V_r | = | volume fraction of rubber in the swollen gel |
| V_t | = | molar fraction of toluene ($106.2 \text{ cm}^3/\text{mol}$) |
| χ | = | rubber-solvent interaction parameter (0.39 for NR-toluene) |
| f | = | function of crosslink with sulfur vulcanization (4) |
| η_{swell} | = | number of moles of crosslink per unit volume (mol/cm^3) |

CHAPTER IV

RESULTS AND DISCUSSION

The effects of molecular weight, chemical structure (homo- or copolymer), and loading of dispersing agent and also loading of nanosilica on mechanical and thermal properties of the NR/silica nanocomposites were studied in this work. This Chapter was divided into three parts in order to clearly and easily understand. The first part was focused on the optimal preparing condition of the silica/dispersing agent aqueous suspension. The second part showed the effects of molecular weight, chemical structure, and loading of dispersing agent and also loading of nanosilica on the particle size distribution of nanosilica in the aqueous suspension. And the last part studied about the effects of all previous factors on the morphology, mechanical and thermal properties of the NR/silica nanocomposite sheets.

4.1 Optimal Preparing Condition for The Silica/Dispersing Agent Aqueous Suspension

For the preparation of the silica/dispersing agent aqueous suspension by self-assembly technique, nanosilica has to be well suspended in the distilled water first in order to form colloid. There were two factors, ultrasonicate time and pH value that played an important role in this step.

This part was a preliminary work to design the suitable condition to prepare the silica aqueous suspension.

4.1.1 Effect of Ultrasonicate Time for Preparing Silica Aqueous Suspension

To obtain well-dispersed nanosilicas in the aqueous, ultrasonic processor was used here. Ultrasonicate time for preparing suspensions was varied from 30 to 40, 50 and 60 minutes. Laser diffraction analysis technique giving the size distribution curve and median diameter was used to investigate the distribution of nanosilica in the aqueous media. The physical appearance of the 1 wt% silica aqueous suspensions, which was ultrasonicated for 30, 40, 50 and 60 minutes, is shown in **Figure 4.1**. Common to all four different ultrasonicate times, the suspensions were observed as white cloudy liquid.



Figure 4.1 Physical appearance of the 1wt% silica aqueous suspension at different ultrasonic times

The size distributions of the 1 wt% silica in the aqueous acquired from the suspensions with different ultrasonic times of 30, 40, 50 and 60 minutes were displayed in Figure 4.2.

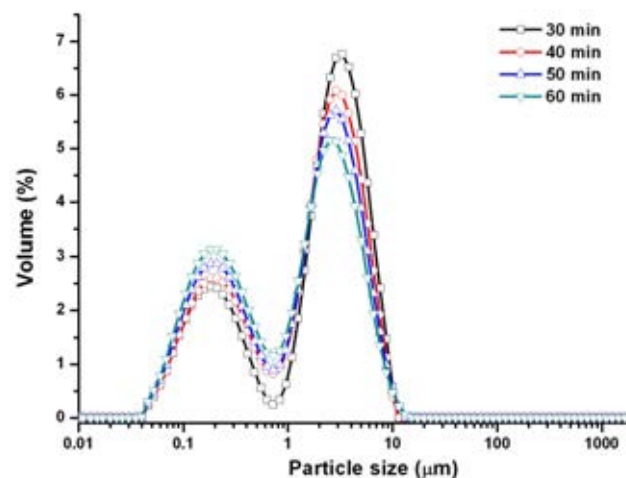


Figure 4.2 Effect of ultrasonic time on the particle size distribution of the 1 wt% silica aqueous suspension

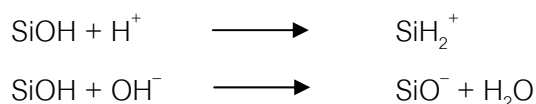
From Figure 4.2, all samples prepared from different ultrasonic times showed bimodal particle size distribution at which particle size was ranged roughly from 0.04 to 1 and 1 to 10 micron. Increasing ultrasonic time seemed to decrease the population of large particles and increased the population of particle with diameter less than 1

micron. However, the particle size distribution still appeared as a bimodal curve when increasing ultrasonicate time from 30 to 60 minutes. Therefore, the ultrasonicate time with 30 minutes was selected and used throughout this work in order to prepare the silica aqueous suspension.

4.1.2 Effect of pH Value for Preparing Silica Aqueous Suspension

To prepare the NR/silica nanocomposite, core-shell of the silica/dispersing agent (homo-PDDA and co-PDDA) must be formed first via a self-assembly process as described in **Figure 2.12**. To form this, the most important factor that extremely affects is the pH value of the medium. It must facilitate silica particle to form negative charge at its surface and dispersing agent to form positive charge along its chain.

Figure 4.3 shows the Zeta potential of a very fine 10 wt% silica as a function pH [37]. As can be seen, the pH of isoelectric point for silica is between 2 and 3. The isoelectric point for the oxide surfaces involves the particle charge is determined by a competition between two reactions: one that makes the surface positive and one that makes it negative:



At low pH values, the first reaction dominates and the surface becomes positive, while at high pH the second reaction prevails and the surface turns into negative. However, a positive silica surface is believed not to exist for the silica surface. Therefore, it is estimated that the region of stability against aggregation would start from about pH = 7.0 and goes higher. This is due to the repulsion of negative charge. However, increasing pH much above 10 will decrease in the magnitude of the zeta potential. This occurs as the ionic strength increases with the pH. As mentioned earlier, the pH value must also be suitable for dispersing agent to form the positive charge along its chain. Kunitake et al [38] reported that the suitable pH value for PDDA to form one positive charge per monomer unit is 10. Therefore, to make sure that the nanosilica particle will be well dispersed at this pH without causing any severe aggregation, the effect of pH value ranging 7 to 10 on the particle size distribution was studied. The pH value was

adjusted by 1 M NaOH. Figure 4.4 shows the particle size distribution of 1 wt% silica suspension when varying pH values.

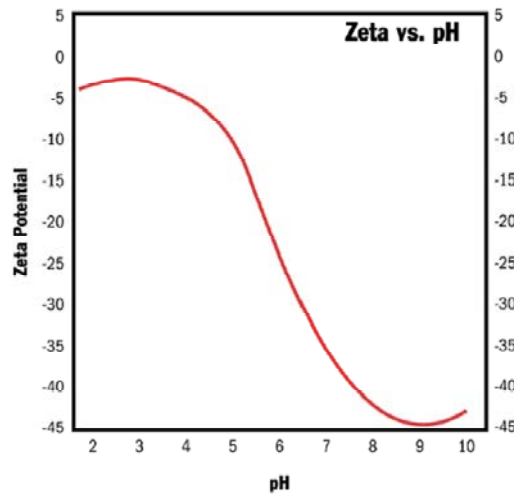


Figure 4.3 Zeta potential vs. pH of a very fine 10 wt% silica system [37]

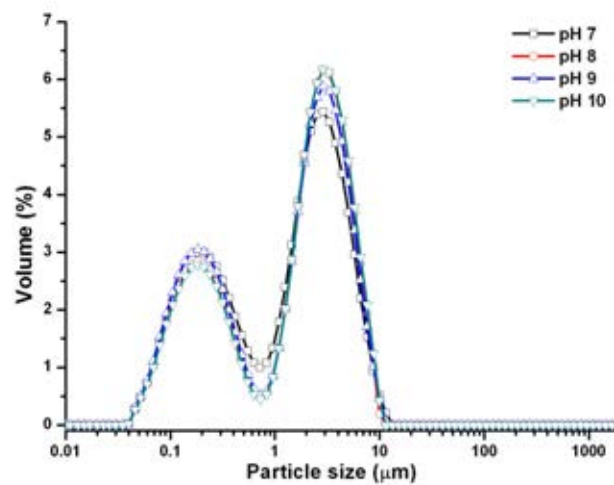


Figure 4.4 Particle size distribution of 1 wt% silica suspensions when varying pH values

It can be seen that all samples in the different pH mediums varying from pH 7 to 10 showed bimodal particle size distribution. When increasing pH value from 7 to 10, the population of particle with bigger size just slightly increased. Varying pH value from 7 up to 10 had no significant effect on the particle size distribution of silica, especially at pH

of 10. Therefore, in this work, the preparation of silica/dispersing agent aqueous suspension was performed at pH 10.

It was expected that the use of suitable ultrasonic time and pH value to prepare the silica/dispersing agent aqueous suspension could lead to the formation of well-dispersed silica nanoparticles in the aqueous suspension. This is to reduce silica agglomerate, inhibit silica sediment, thus increasing the compatibility between NR latex and silica when dried.

4.2 Characterization of The Silica/Dispersing Agent Aqueous Suspension

4.2.1 The Stability of The Silica/Dispersing Agent Aqueous Suspension

In this study, it was observed that the pure silica and silica/dispersing agent precipitated over storing time. The influences of the presence of dispersing agent and nature of dispersing (molecular weight and chemical structure) on the precipitation were discussed here.

First, let take a look the influence of the presence of dispersing. It was observed that no matter what type of dispersing agent was used the silica/dispersing agent system caused the precipitation of silica faster than the pure silica system. This might be due to the heavier weight of the silica/dispersing agent particle compared with that of the pure silica particle. However, interestingly, it was found that after shaking the silica/dispersing agent particle can be completely re-dispersed again and looked just like the initial form. On the other hand, the complete re-dispersion of the pure silica precipitating could not be reached. Moreover, the big particle was observed with naked eyes. This indicated the formation of tight agglomeration of silica particle. To describe this phenomenon, at first the colloidal stability should be comprehensible.

Colloidal particles in the dispersion medium always show Brownian motion and particles may adhere together and form aggregates of increasing size. An initially formed aggregate is called flocculation and this is reversible process. If the aggregate changes to a denser form, it is called coagulation which is an irreversible process. The general behavior of colloid is shown in **Figure 4.5** [39].

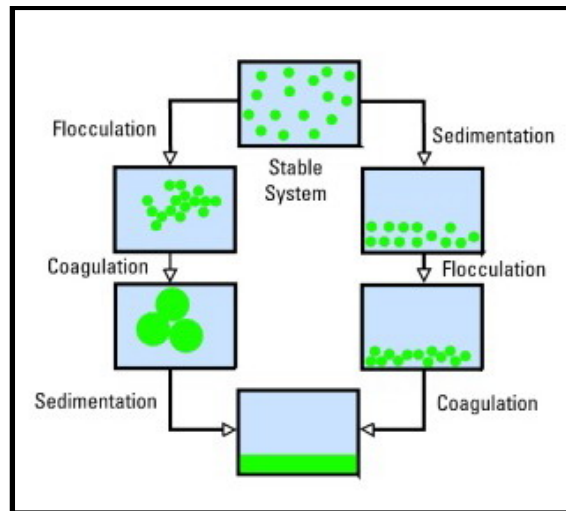


Figure 4.5 The schematic of colloidal stability [39]

The stability of colloids is determined by the interaction between the particles. There are two basic interactions: one being attractive and the other repulsive [40]. A colloidal dispersion can be stable when repulsion force is balanced with attraction force. The fundamental mechanisms that affect colloidal stability are: electrostatic stabilization and steric stabilization. Electrostatic stabilization is the mechanism at which the colloidal particle can be stable by the particle interaction due to distribution of charge species in the dispersion [39, 41]. Steric stabilization is the mechanism at which dispersing polymer added to the dispersion adsorbs onto the surface and then causes the repulsive force, thus separating particles from each other. The steric stabilization sometimes is called polymeric stabilization [41]. Electrostatic stabilization can be combined with steric stabilization, leading to something called as electrosteric stabilization. When polymer covers the particle surface, a polymer layer would be a net charge on the particle surface and is sketched in **Figure 4.6**. When particles tend to be close together, either electrostatic repulsion or steric restriction would prevent agglomerate [40]. However, if there are extra charges left on the polymer chain, the electrosteric stabilization will be taken place.

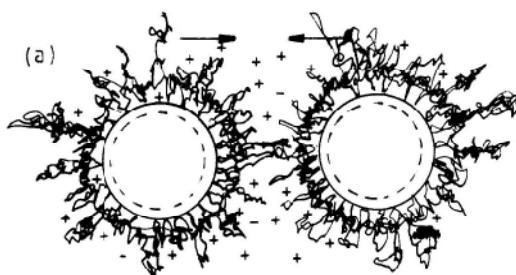


Figure 4.6 Illustration of electrosteric stabilization of polyelectrolyte attached to the particles [40]

For this study when using PDDA both homo- and co-polymer as dispersing agent, it can be explained that the electrosteric stabilization was occurred. PDDA is a polyelectrolyte, so it can be fragmented to form the positively charged chain in the system. The positively-charged PDDA can be assembled with the negatively-charged surface of silica nanoparticles. Now PDDA chain covering the surface of silica implied steric part. Furthermore, the extra positive charge of PDDA then implied electrostatic repulsion, preventing the silica particle from getting closer to each other. However, the silica/PDDA dispersing agent precipitated with time due to the gravity. But it can be re-dispersed again by shaking due to its loose agglomerate. The complete re-disperse was not observed in the case of pure silica suspension. This was due to the formation of agglomeration between silica particles via hydrogen bonding which is difficult to be destroyed.

Second, the influence of the nature of PDDA on the colloid stability was not observed with the naked eyes. However, to be more precise on this, the influence of the nature of PDDA will be discussed in term of the particle size distribution using a laser diffraction analysis in the next part.

4.2.2 Particle Size Distribution of The Silica/Dispersing Agent Aqueous Suspension

Poly (diallyldimethylammonium chloride) or PDDA and poly (acrylamide-co-diallyldimethylammonium chloride) or co-PDDA were used here as dispersing agent. Particle size distribution of the silica/dispersing agent aqueous suspension was focused

here. Although the presence of dispersing agent will prevent silica from the coalescence, there is a chance for it to wrap few silica particles together due to its long length. However, at the same time, its long length might enhance the steric stabilization which in turn gives more colloid stability. Therefore, besides using two different chemical structures of PDDA (homo- and co-polymer), in this study homo-PDDA with different molecular weights were also used. The suitable type and optimal loading of dispersing agent must be carefully concerned. The concentration of silica in suspension was varied from 1 to 2, 3 and 4 wt% when concentration of dispersing agent was fixed at 1 and 3 wt% of silica. To clearly understand, the results were divided according to the concentration of silica and dispersing agent used.

For 1 wt% silica, the particle size distributions and their corresponding median values were shown in Figures 4.7-4.8

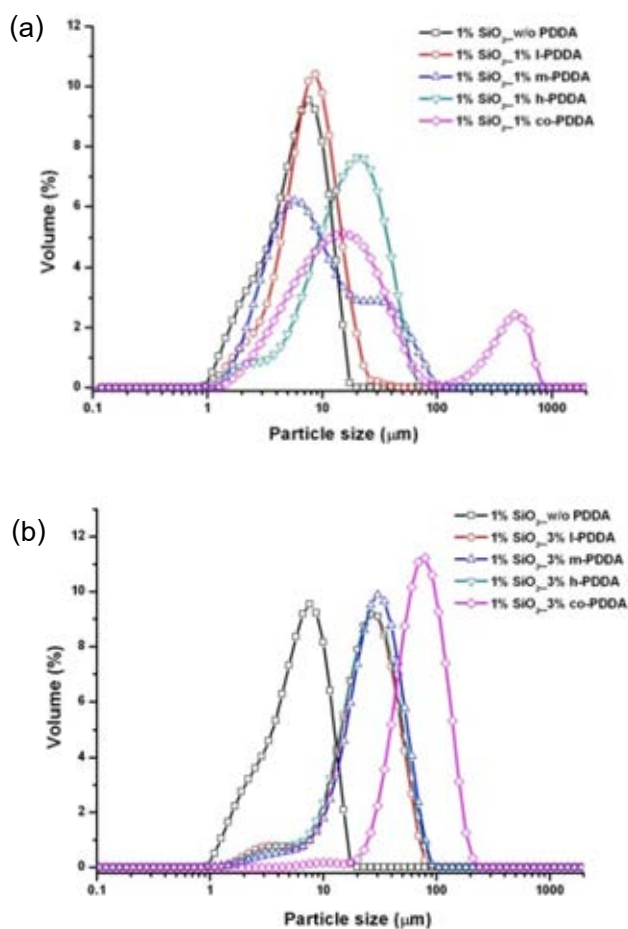


Figure 4.7 Particle size distributions of 1 wt% silica aqueous suspensions with dispersing agent at (a) 1wt% and (b) 3 wt% of silica

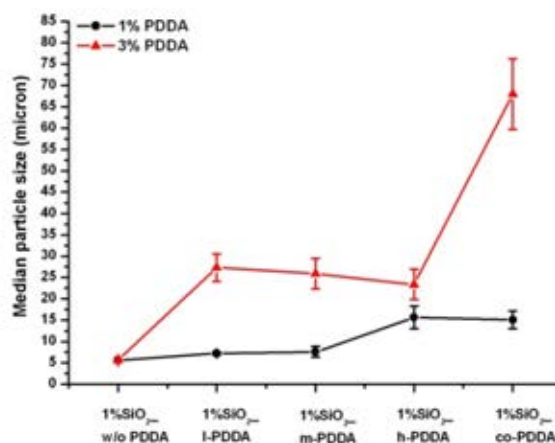


Figure 4.8 Median particle sizes of 1 wt% silica suspension at dispersing agent 1 and 3 wt% of silica

When considering silica suspension with dispersing agent 1 wt% of silica (Figure 4.7(a)), it can be found that both monomodal peak with and without shoulder and bimodal peak were observed depending on the nature of dispersing agent. The particle size distribution of 1 wt% I-PDDA system was very similar to that of the pure silica system. The peaks of the particle size distribution for these two systems were nearly the same. However, when using higher molecular weight homo-PDDA, m-PDDA, h-PDDA and also co-PDDA, it was found that the particle size distribution was shifted to the higher size with gradually forming of clear bimodal size distribution.

For silica suspension with dispersing agent 3 wt% of silica (Figure 4.7(b)), all different dispersing agents gave particle size distribution as monomodal peak with small shoulder. Moreover, regardless of the nature of dispersing agent, the addition of 3 wt% dispersing agent extremely caused increase in the particle size distribution when compared with the pure silica system. The significant increase in the particle size when using 3 wt% dispersing agent implied that there was more agglomeration of silica particle. The position of peak was independent of the molecule weight of dispersing agent but significantly affected by the chemical architecture of dispersing agent. Using co-PDDA gave the silica/disperse agent with the biggest size.

The median particle size as given in Figure 4.8 also clearly showed the effect of the nature of dispersing agent on the size of silica. At dispersing agent 1 wt% of silica, the particle size was not strongly affected by both the presence of dispersing agent and also the nature of dispersing agent. The size was not much different from that of the pure silica. However when increasing loading of dispersing agent to 3 wt% of silica, bigger particles were clearly formed. The effect of size of dispersing agent on the median particle size was not observed. But changing from homopolymer to copolymer significantly increased the median particle size.

For 2 wt% silica, the particle size distributions and their corresponding median values were shown in Figures 4.9-4.10.

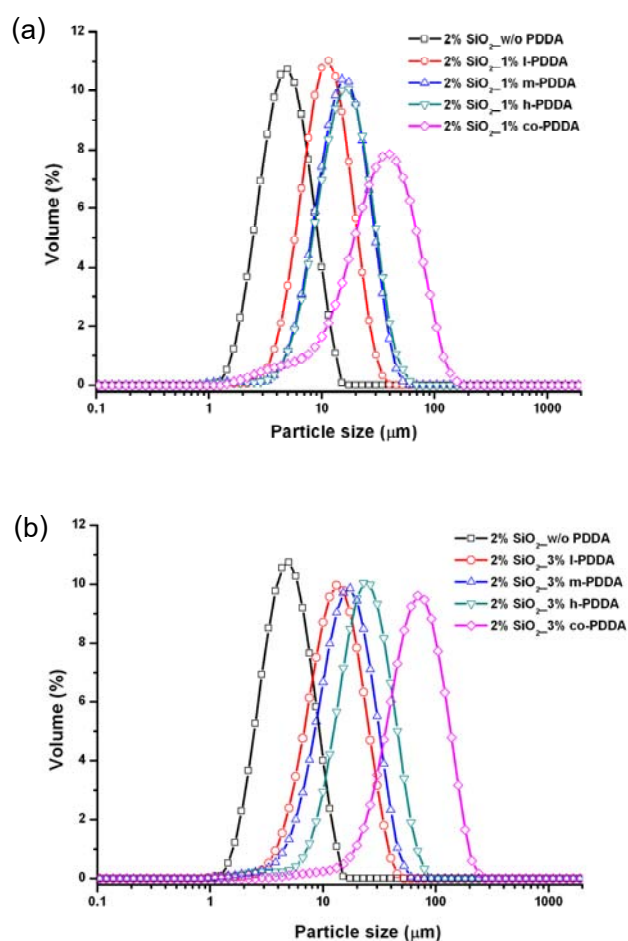


Figure 4.9 Particle size distributions of 2 wt% silica aqueous suspensions with dispersing agent at (a) 1wt% and (b) 3 wt% of silica

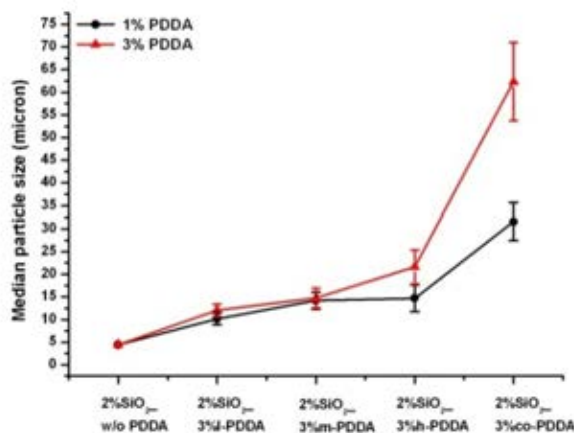


Figure 4.10 Median particle sizes of 2 wt% silica suspension at dispersing agent 1 and 3 wt% of silica

When increasing amount of silica from 1 to 2 wt%, the particle size distribution of the pure silica in the aqueous did not change. The monomodal peak roughly ranging from 1 to 20 micron was still observed. But in the case of 2 wt% of silica, there was no shoulder at the smaller size found. For both dispersing agent loadings, 1 and 3 wt% of silica, the bigger particle was formed. Similar to the 1 wt% silica system, the increase in particle size was significantly observed when using co-PDDA. At the 2 wt% silica, increasing amount of homo-PDDA dispersing agent from 1 to 3 wt% of silica did not increase the median particle size at all. However, the huge increase in the median particle size when increasing amount of co-PDDA was observed.

When increasing amount of silica from 2 to 3 and 4 wt%, the similar influences of amount and nature of dispersing agent on the particle size distribution and the median particle size were observed. The results were shown in Figures 4.11-4.14.

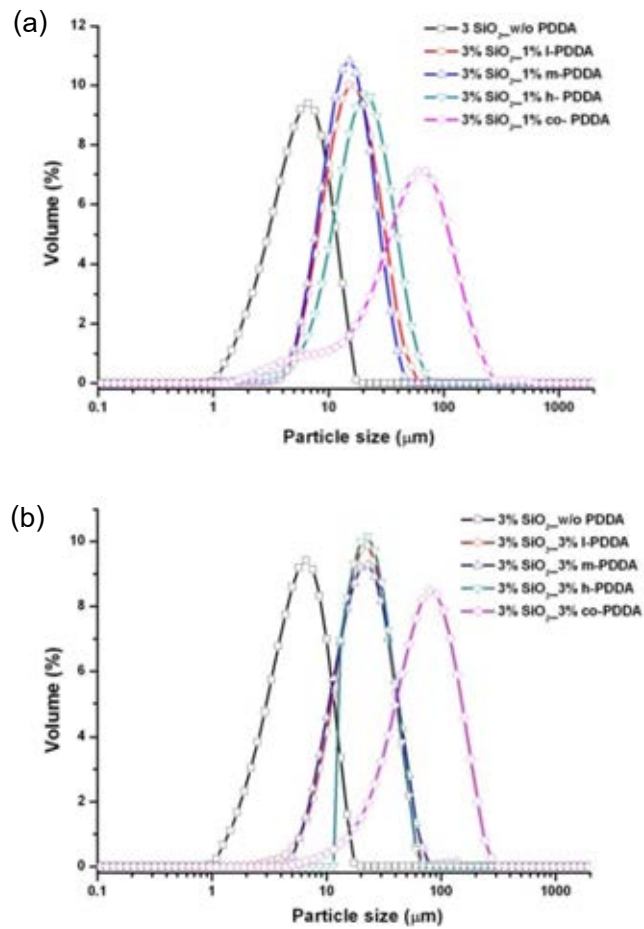


Figure 4.11 Particle size distributions of 3 wt% silica aqueous suspensions with dispersing agent at (a) 1wt% and (b) 3 wt% of silica

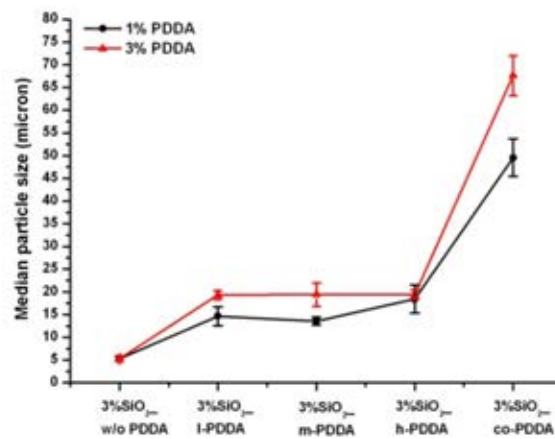


Figure 4.12 Median particle sizes of 3 wt% of silica suspension at dispersing agent 1 and 3 wt% of silica

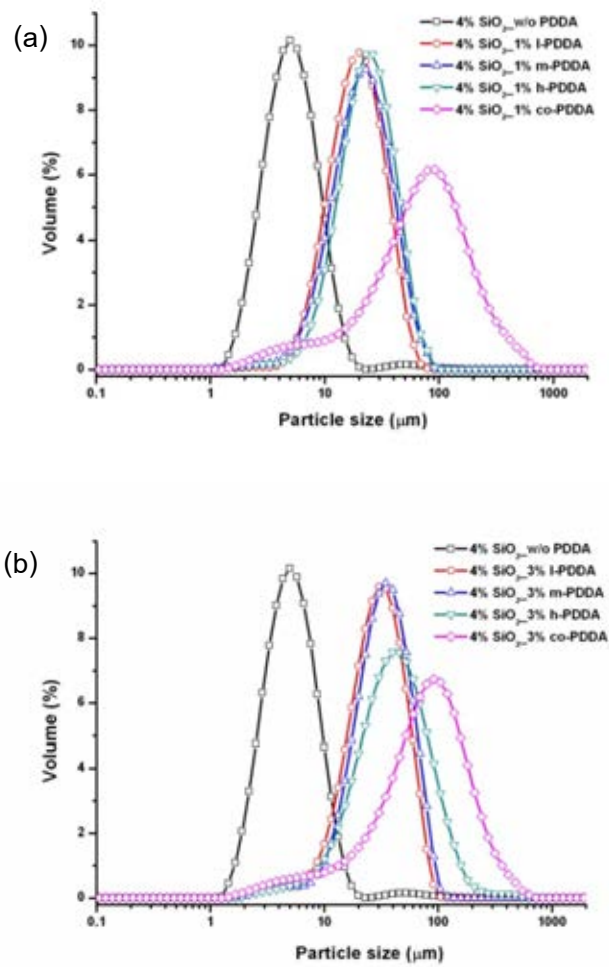


Figure 4.13 Particle size distributions of 4 wt% silica aqueous suspensions with dispersing agent at (a) 1 wt% and (b) 3 wt% of silica

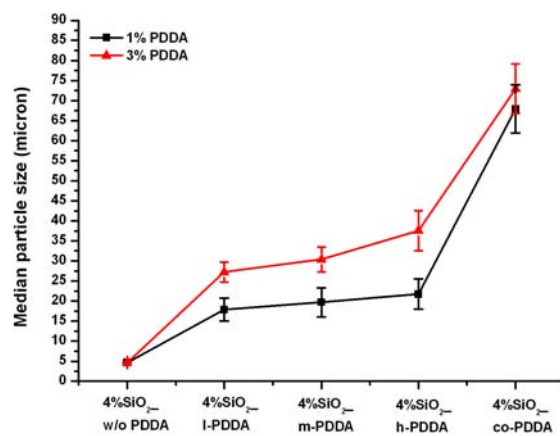


Figure 4.14 Median particle sizes of 4 wt% of silica suspension at dispersing agent 1 and 3 wt% of silica

The effect of silica loading on the median particle size was shown in Figure 4.15.

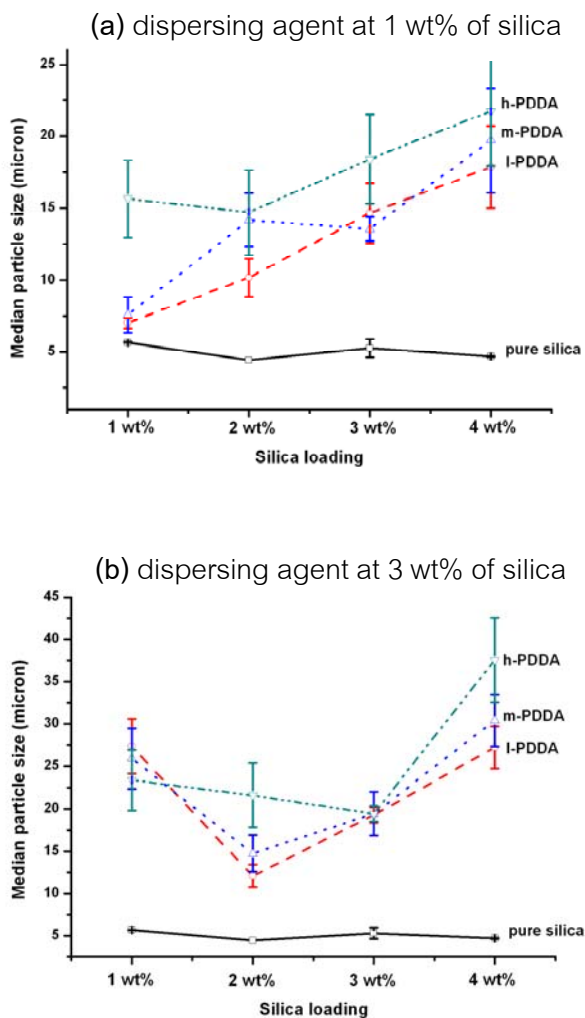


Figure 4.15 Median particle sizes of the silica aqueous suspension at various silica loadings with dispersing agent (a) 1 and (b) 3 wt% of silica

From above results, it was observed that without dispersing agent the increase of silica loading did not effect on the median particle size of silica in the aqueous medium at all. However, with the presence of dispersing agent, the opposite effect was found. The mean particle size of silica in the aqueous medium increased with increasing silica loading. This effect was augmented when increasing amount of dispersing agent.

4.3 Crosslink Density, Mechanical and Thermal Properties and Morphology of the Pure NR and NR/Silica Nanocomposites

The effects of molecular weight, chemical structure, and loading of dispersing agent and also loading of nanosilica on the crosslink density, mechanical and thermal properties and morphology of the NR/silica nanocomposite were focused here.

4.3.1 Crosslink Density

The crosslink density of the pure NR was compared to that of the NR/silica nanocomposites containing various silica loadings as shown in Figure 4.16 to 4.19.

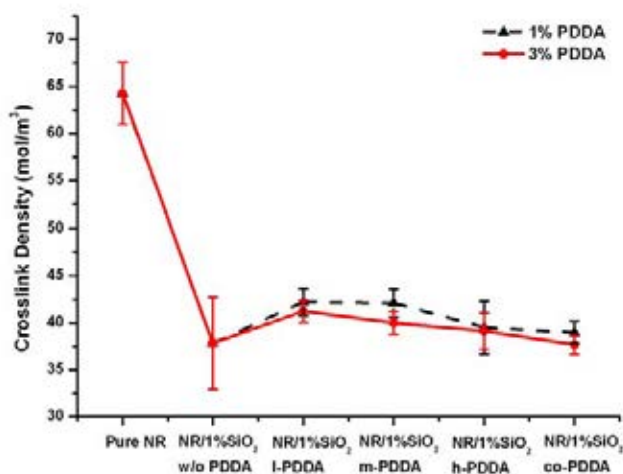


Figure 4.16 Crosslink densities of the pure NR and the NR/1 wt % silica with different dispersing agents at 1 and 3 wt% of silica

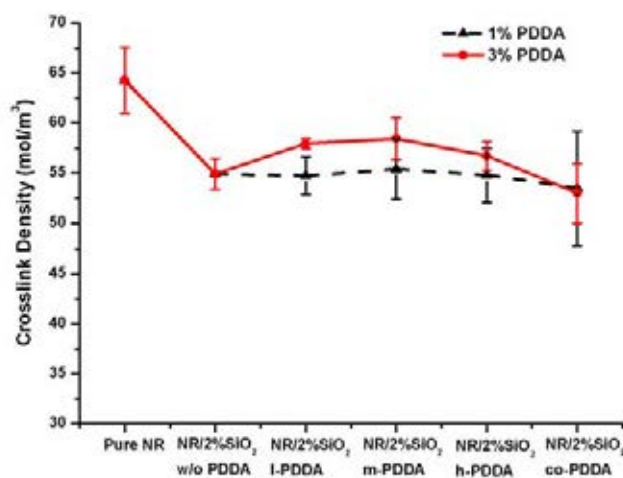


Figure 4.17 Crosslink densities of the pure NR and the NR/2 wt% silica with different dispersing agents at 1 and 3 wt% of silica

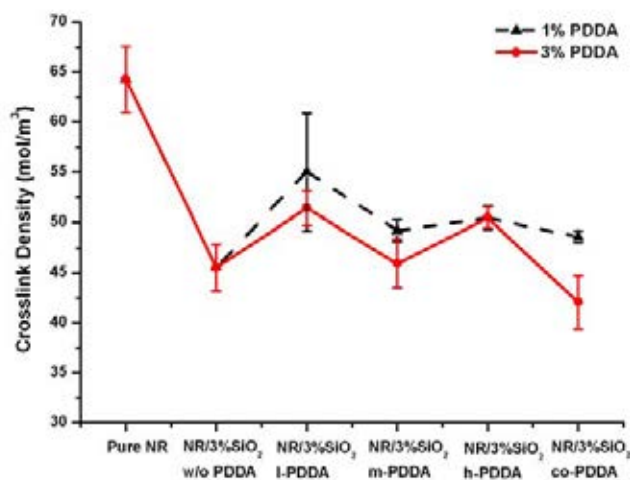


Figure 4.18 Crosslink densities of the pure NR and the NR/3 wt% silica with different dispersing agents at 1 and 3 wt% of silica

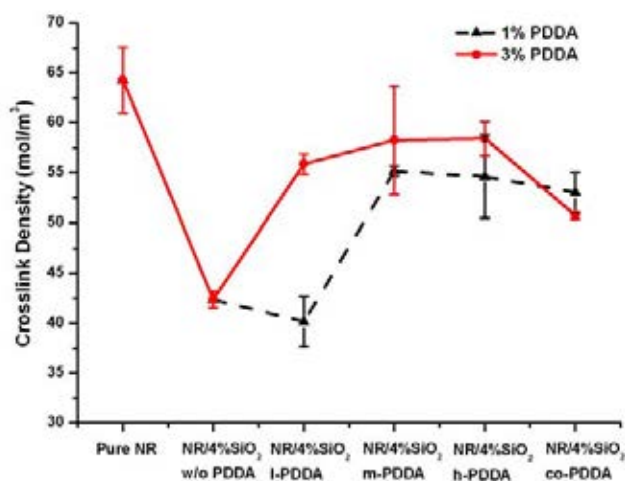


Figure 4.19 Crosslink densities of the pure NR and the NR/4 wt% silica with different dispersing agents at 1 and 3 wt% of silica

The crosslink density of the pure NR and the NR/silica nanocomposites at 1 wt% silica with different dispersing agents at 1 and 3 wt% of silica is demonstrated in **Figure 4.16**. Generally, it was observed that the crosslink density significantly decreased when adding silica no matter with or without dispersing agent. For silica loading from 2 to 4 wt%, it was observed that the increase in silica loading without adding dispersing agent further decreased the crosslink density of the NR/silica nanocomposites. The reason for the reduction in the crosslink density when adding silica in the absence of dispersing

agent was due to the adsorption of curing agent onto the silica surface. The more silica, the lower curing agent. So the lower crosslink density was observed at high silica loading.

However, after adding dispersing agent regardless of type and loading, the crosslink density of the NR/silica nanocomposites was gradually increased. The dispersing agent was wrapped up the silica particles, inhibiting them not only from interacting with each other to form agglomerate but also from absorbing the curing agent. Thus, this led to the increasing in crosslink density. The I-PDDA and m-PDDA showed comparable effect on the increase in crosslink density. However, their effect on the increase in crosslink density was much more pronounced than that of h-PDDA and co-PDDA.

The effect of amount of dispersing agent was also studied. However, the conclusion for how it affected on the crosslink density was inconsistent. At silica loading of 2 and 4 wt%, increasing amount of dispersing agent gave the NR/silica nanocomposites with higher crosslink density. However, the opposite behavior was observed at silica loading of 3 wt%. Moreover, at 1 wt% silica, the crosslink density was independent of the amount of dispersing agent.

4.3.2 Mechanical Properties

Tensile properties including tensile strength, modulus and elongation at break and tear strength of the NR/silica nanocomposite were investigated here.

4.3.2.1 Tensile Strength

The tensile strength of the pure NR was compared to those of the NR/silica nanocomposites containing various silica loadings as shown in **Figures 4.20-4.23**.

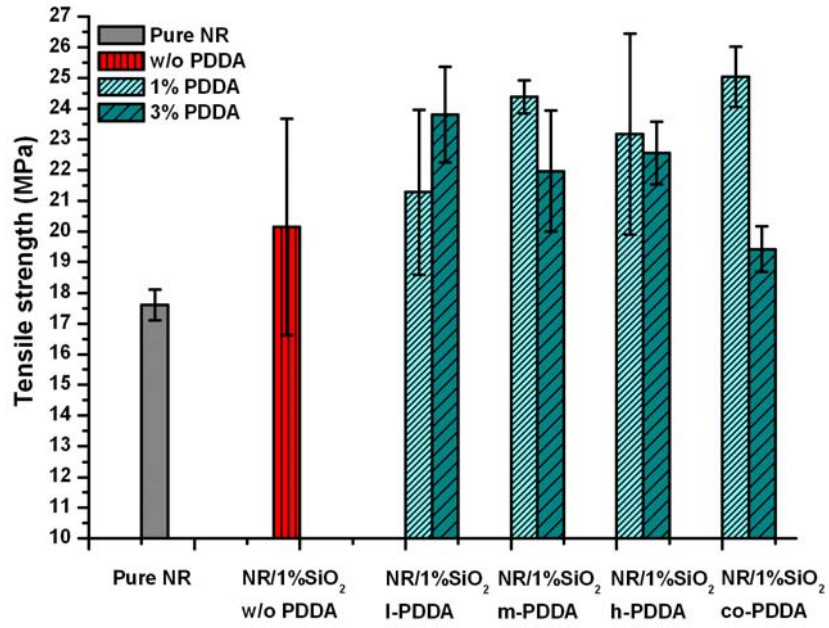


Figure 4.20 Tensile strengths of the pure NR and the NR/1 wt% silica with different dispersing agents at 1 and 3 wt% of silica

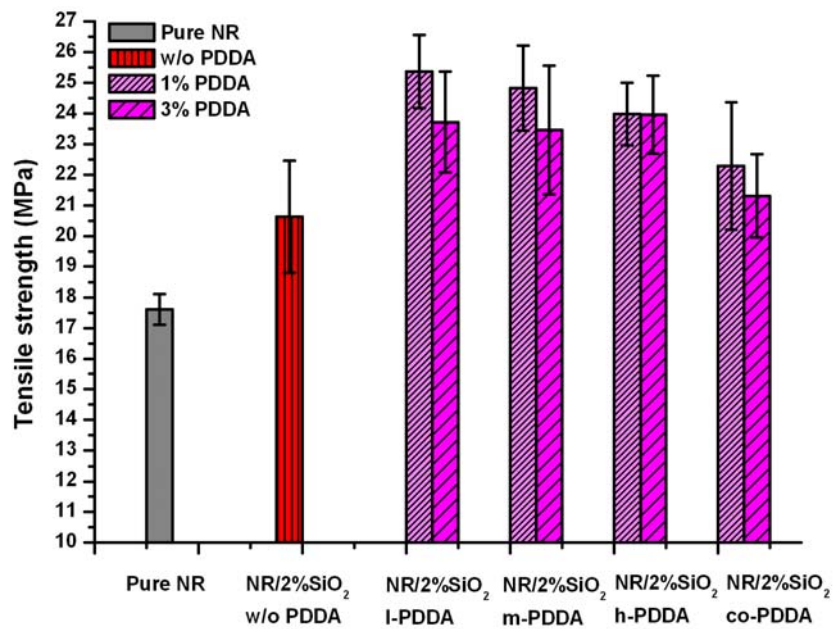


Figure 4.21 Tensile strengths of the pure NR and the NR/2 wt% silica with different dispersing agents at 1 and 3 wt% of silica

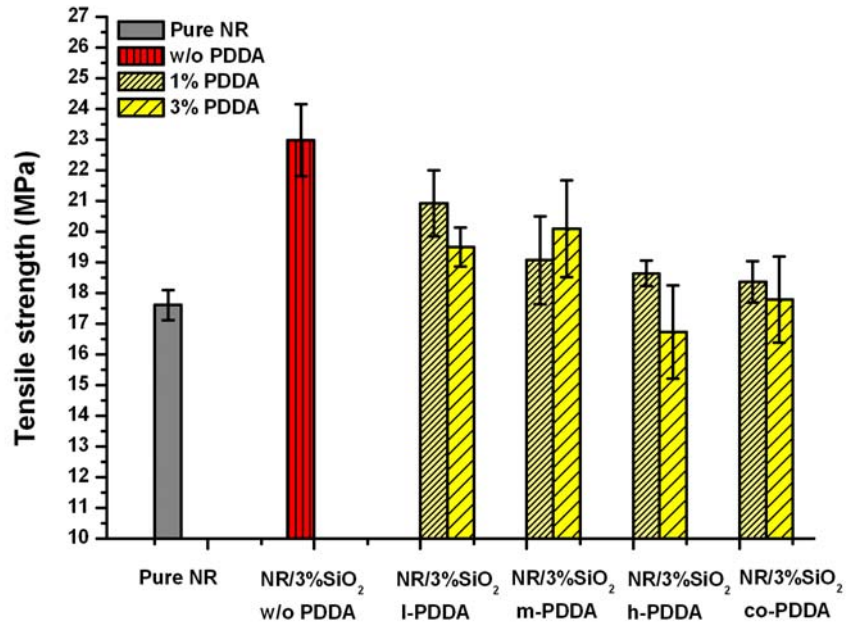


Figure 4.22 Tensile strengths of the pure NR and the NR/3 wt% silica with different dispersing agents at 1 and 3 wt% of silica

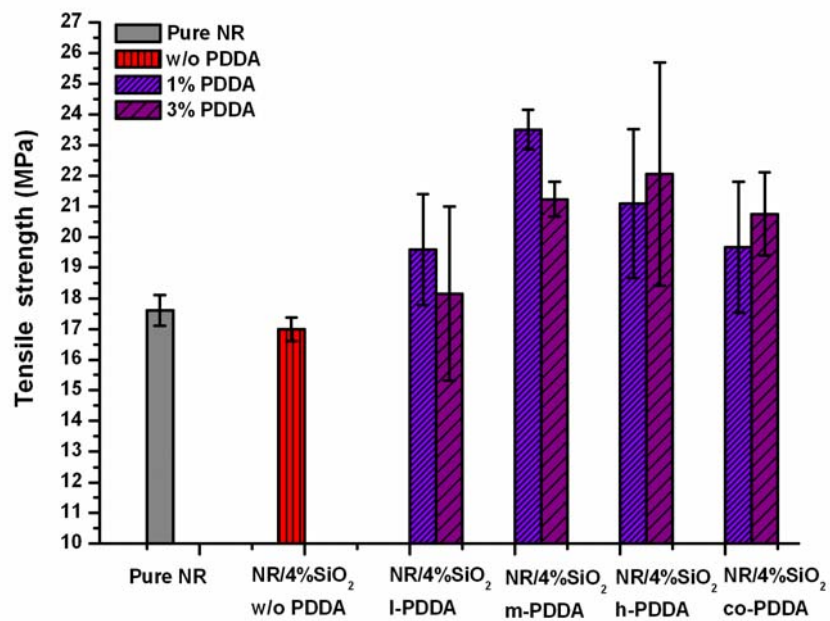


Figure 4.23 Tensile strengths of the pure NR and the NR/4 wt% silica with different dispersing agents at 1 and 3 wt% of silica

As shown above, the tensile strength of the pure NR was approximately 17 MPa. The presence of silica at 1-3 wt% without any dispersing agent can enhance tensile strength of the NR matrix. But in the case of 4 wt% silica with no dispersing agent, the tensile strength of the NR/silica nanocomposite was lower than that of the pure NR. Additionally, the tensile strength was further increased if dispersing agent was added. As can be seen, tensile strength of the NR/silica nanocomposites was strongly dependent of type and loading of dispersing agent. Moreover, at different silica loadings, the difference in behavior was also observed.

As demonstrated in **Figure 4.20**, the addition of silica at 1 wt% without any dispersing agent could increase tensile strength of the NR matrix. However, the tensile strength was further increased, if dispersing agent was added. This was due to the increase of silica stability and the prohibition of silica agglomeration in the aqueous. Moreover, the PDDA dispersing agent also acted as a bridge between the silica and rubber matrix through the electrostatic interaction between positive charge of PDDA and negative charge of rubber particle. This action can make the stronger interfacial interaction and improve the mutual compatibility which in turn resulted an enhancement of the tensile strength of the nanocomposites [42]. The increase in tensile strength varied with the type and amount of dispersing agent. With dispersing agent 1 wt% of silica, surprisingly, it was found that co-PDDA gave the NR/silica nanocomposite with highest tensile strength though it led to the formation of the biggest silica/dispersing aqueous suspension (see **Figure 4.8**). Homo-PDDA with different molecular weights seemed to give the NR/silica nanocomposites with comparable tensile strengths. For all dispersing agents but I-PPDA, increasing amount of dispersing agent to 3 wt% of silica diminished tensile strength of the NR/silica nanocomposite. Co-PDDA showed the highest effect on the reduction of tensile strength and gave even worse tensile strength than the one without dispersing agent.

At 2 wt% silica, it was found that at this silica content the presence of dispersing agent no matter what type or which loading led to the increase in tensile strength as seen in **Figure 4.21**. Although I-PDDA gave higher tensile strength than the other two

homo-PDDA (m-PPDA and h-PDDA) at 1 wt% of dispersing agent, the comparable tensile strengths were observed at 3 wt% of dispersing agent. Co-PDDA at both concentrations gave lowest efficiency to enhance the tensile strength. This might be due to it caused highest median particle size.

At 3 wt% silica, surprisingly, it was observed that at this silica loading, the presence of dispersing agent caused the reduction of tensile strength as shown in **Figure 4.22**. At 1 wt% of dispersing agent, using I-PDDA gave the highest tensile strength while using co-PDDA gave the lowest tensile strength. And at this dispersing agent loading, the tensile strength can be placed from the highest to lowest in the order of I-PPDA, m-PPDA, h-PPDA, and co-PPDA. At 3 wt% of dispersing agent, using m-PDDA gave the highest tensile strength while using h-PDDA gave the lowest tensile strength.

At 4 wt% silica (the highest silica loading in this study), the presence of silica gave the lower tensile strength than the pure NR as seen in **Figure 4.23**. However, the tensile strength of the NR/silica nanocomposite at this silica loading can be improved by the addition of dispersion agent. All dispersing agents at both concentrations showed the higher tensile strength than both the pure NR and the NR/silica nanocomposite without any dispersing agent. In this silica loading, it was found that at both dispersing agent concentrations homo-PDDA with lowest molecular weight, I-PDDA, showed the lowest ability to enhance tensile strength. Increasing of molecular weight of homo-PDDA or using co-PDDA lead to the higher tensile strength. At 1 wt% of dispersing agent, m-PPDA gave highest tensile strength, while at 1 wt% of dispersing agent, m-PDDA and h-PDDA showed comparable tensile strength and their tensile strength were highest.

In this part, it was observed that the best condition to obtain the highest tensile strength, 25 MPa, was the NR compound consisting of 2 wt% silica with I-PDDA at 1 wt% of silica. Further increase in silica loading did not give higher tensile strength at all. Comparing amongst homo-PDDA, generally, I-PDDA and m-PDDA gave the comparable tensile strength and higher than h-PDDA, whereas co-PDDA seemed to

have the lowest ability to enhance tensile strength. However, it was useful to note that even though co-PDDA formed the silica/dispersing agent particle with median particle size much higher than the homo-PDDA, the tensile strength of the obtained NR/silica nanocomposite was not significantly lower than that of the ones prepared from homo-PDDA as expected. In fact, at some circumstance, it even gave the higher tensile strength than the other systems. Therefore, it might not be only the particle size of silica/dispersing agent particle playing an important role on the tensile strength of the NR/silica nanocomposite. The ability to form interaction between the positively charged silica/PDDA particle and the negatively charged NR particle may be also influenced on the tensile strength. However, its influence on the tensile strength was clearly understood here. Moreover, it was also observed that the increase in dispersing agent concentration seemed to cause the reduction of tensile strength even at high silica loading. This may be due to the formation of larger silica/dispersing agent particle in the aqueous suspension as mentioned earlier.

4.3.2.2 Tensile Modulus

The tensile modulus at 100 and 300% strain of the pure NR was compared to those of the NR/silica nanocomposites containing various silica loadings as shown in Figures 4.24 to 4.27.

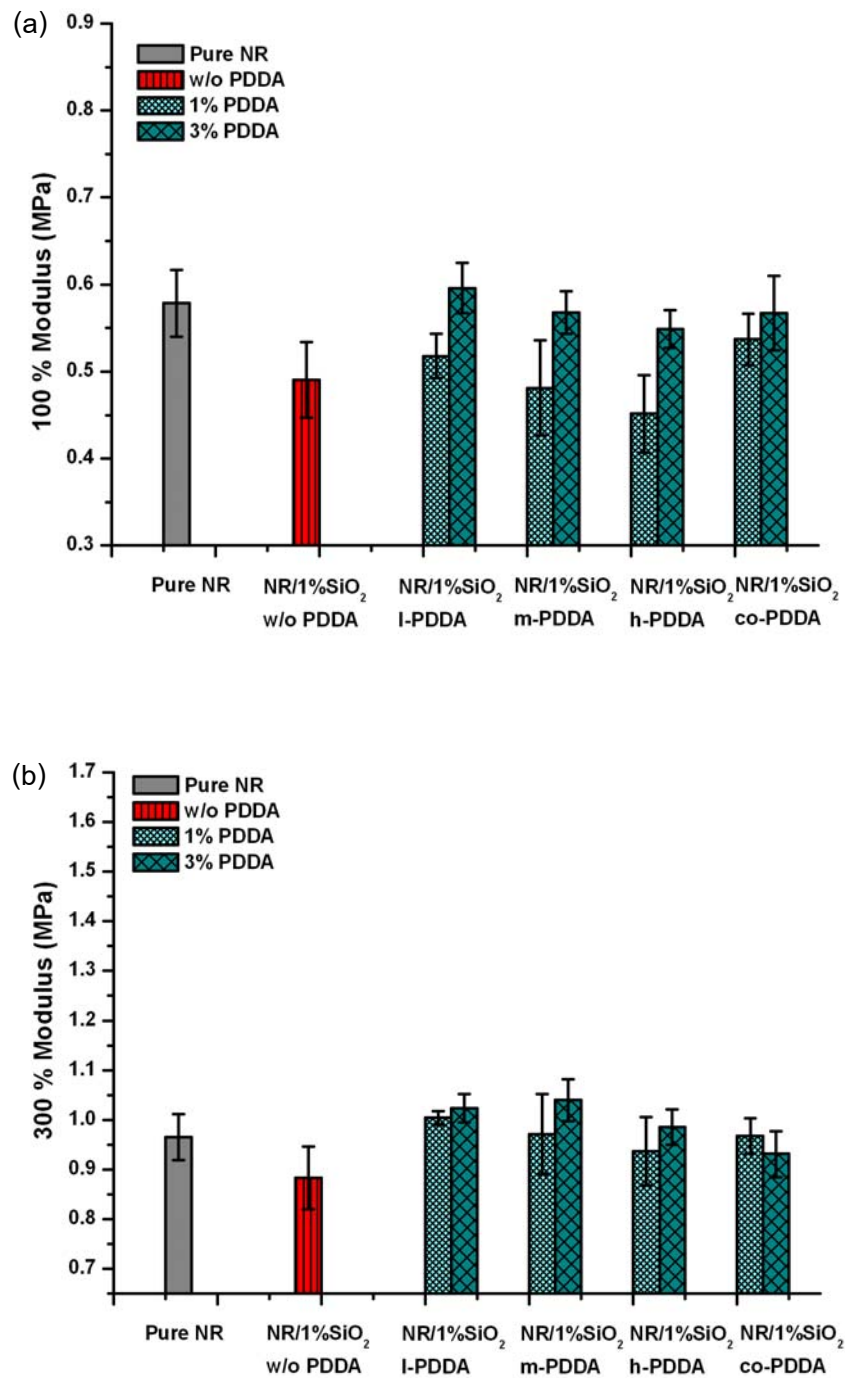


Figure 4.24 Tensile modulus at (a) 100% strain and (b) 300% strain of the pure NR and the NR/1 wt% silica with different dispersing agents at 1 and 3 wt% of silica

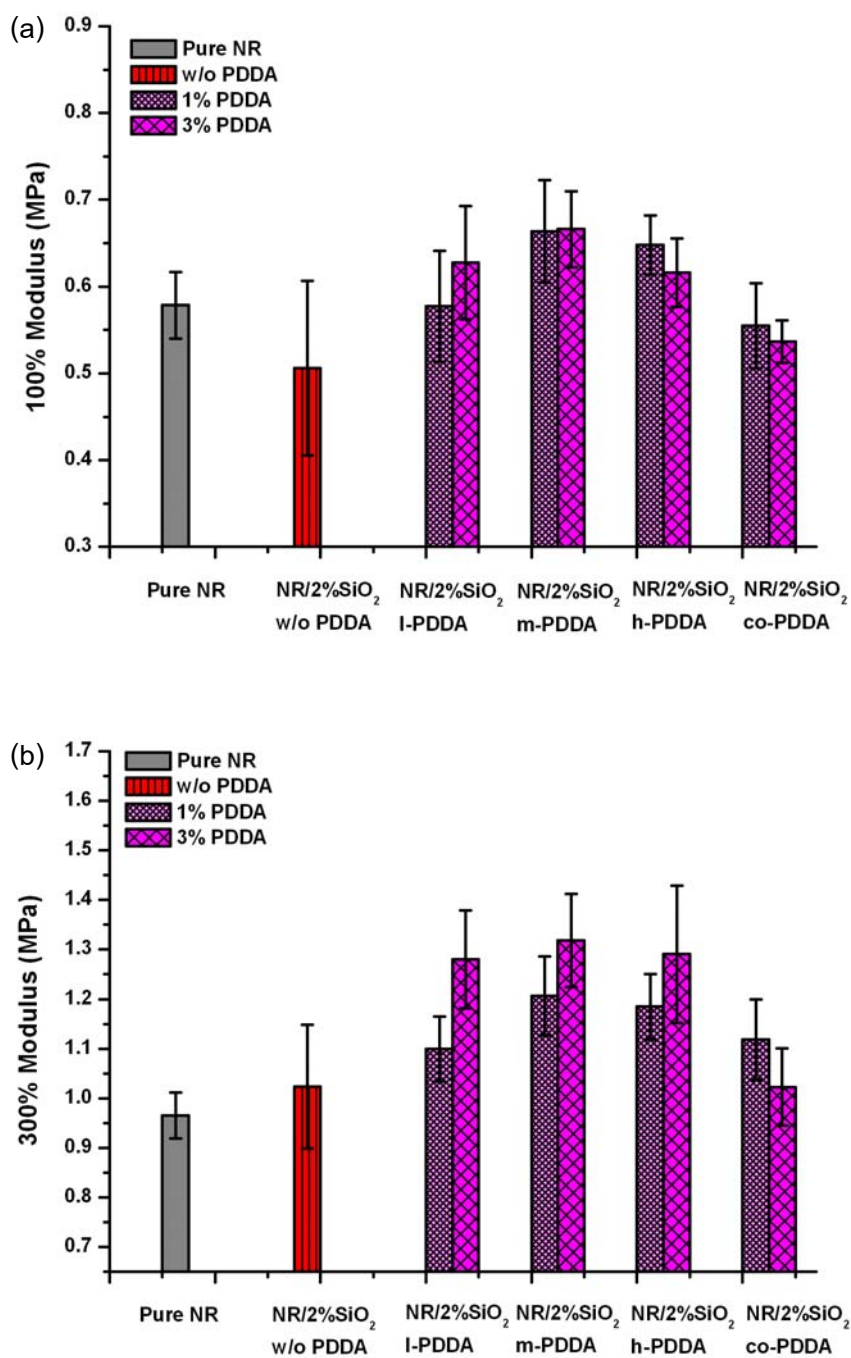


Figure 4.25 Tensile modulus at (a) 100% strain and (b) 300% strain of the pure NR and the NR/2 wt% silica with different dispersing agents at 1 and 3 wt% of silica

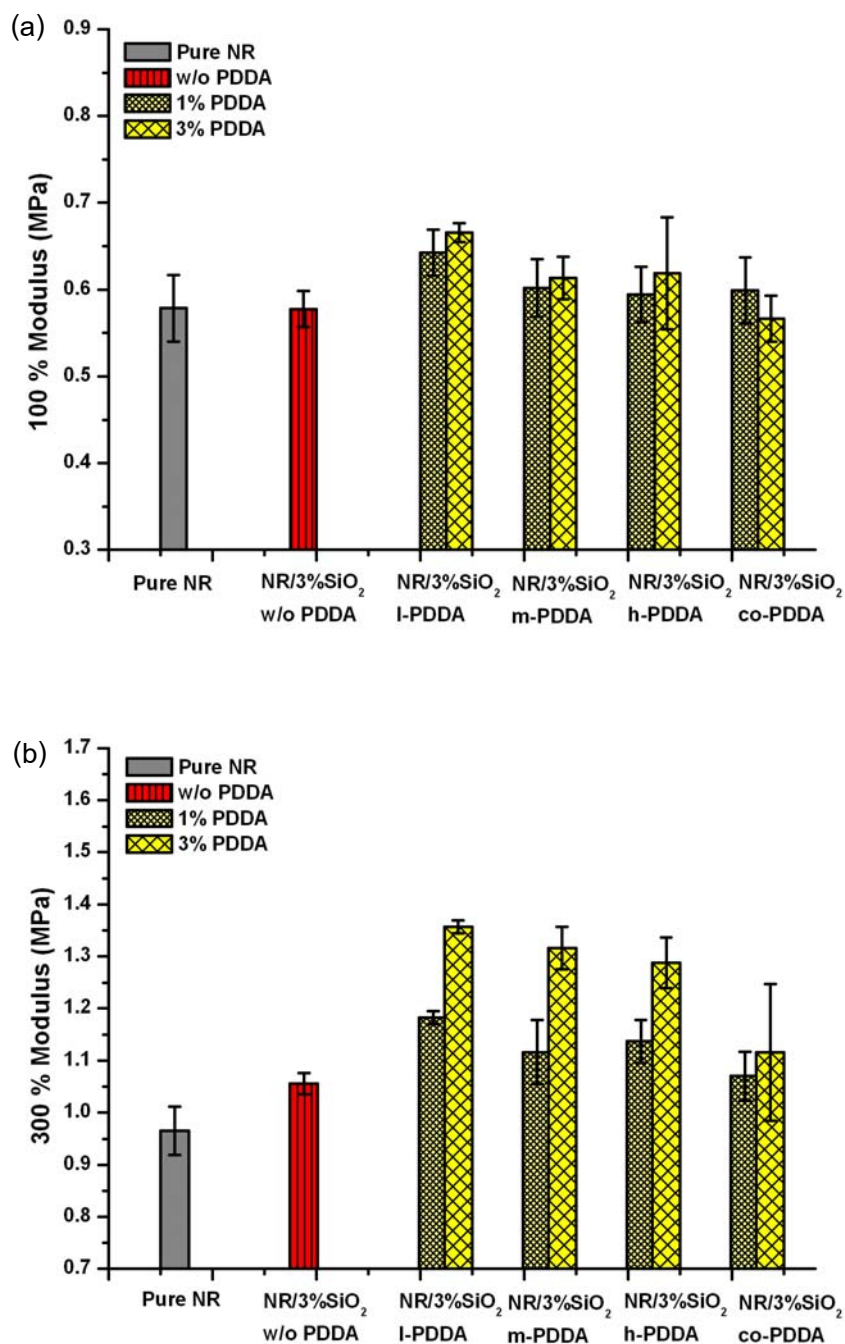


Figure 4.26 Tensile modulus at (a) 100% strain and (b) 300% strain of the pure NR and the NR/3 wt% silica with different dispersing agents at 1 and 3 wt% of silica

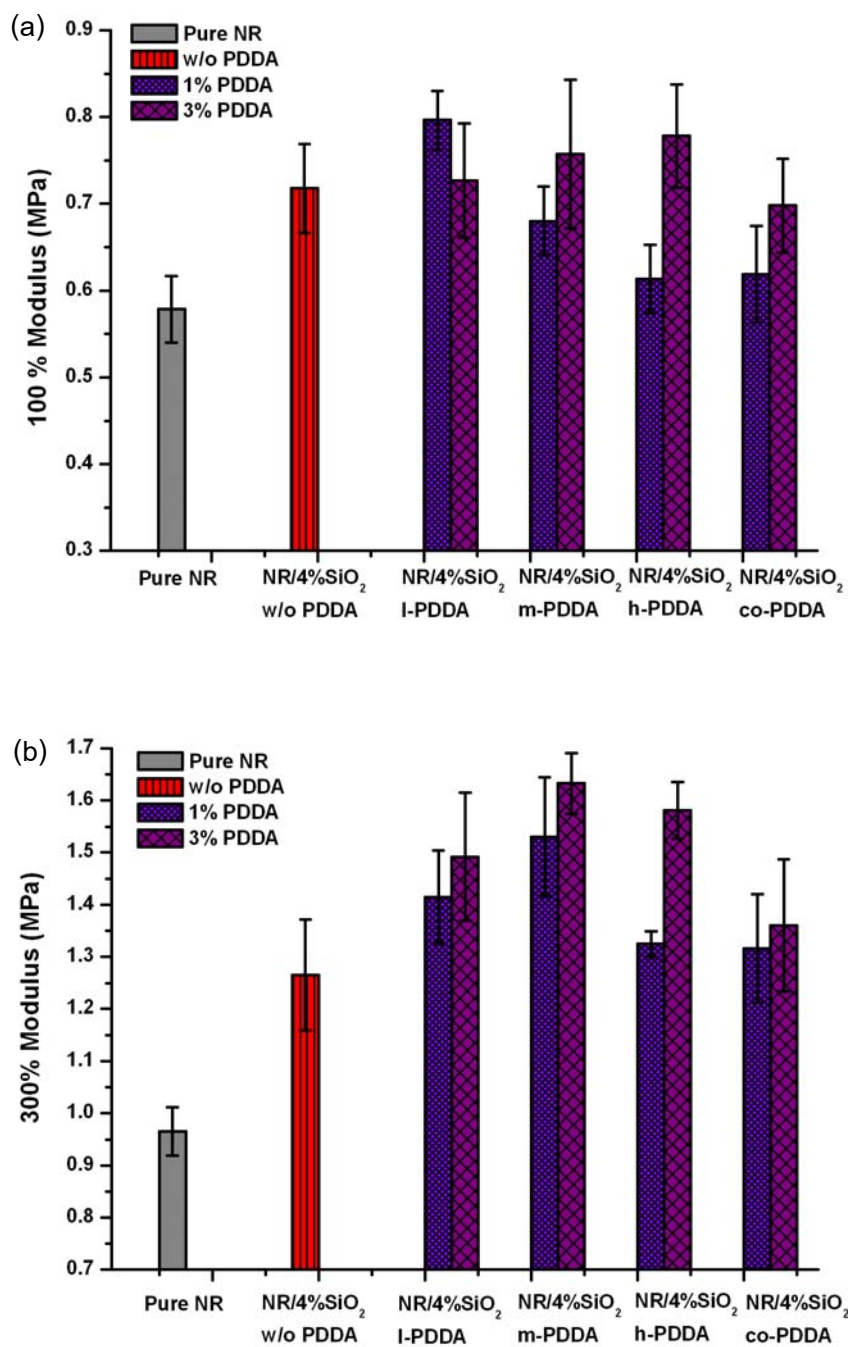


Figure 4.27 Tensile modulus at (a) 100% strain and (b) 300% strain of the pure NR and the NR/4 wt% silica with different dispersing agents at 1 and 3 wt% of silica

From above figures, first it was observed that at low silica loading, 1 and 2 wt%, the presence of silica without any dispersing agent reduced both 100 and 300% modulus of the NR matrix. The opposite behavior was observed at the higher silica loading. The presence of silica at higher loadings (3 and 4 wt%) gave the NR matrix with higher 100 and 300% modulus than those of the pure NR matrix. In general, the addition of rigid particle into the rubber will give the rubber matrix with higher modulus. This is due to the hydrodynamic volume. Moreover, if the filler can form a good interaction with the rubber matrix, it will give even higher modulus due to the strain amplification effect. However, as known that silica has very active surface which can absorb or interact with curing agent such as zinc oxide, the modulus of the rubber matrix may be reduced due to the lower crosslink density. At low silica loading, the decrease of crosslink density due to the presence of silica may be dominant, thus leading to the reduction of tensile modulus. At higher silica loading, the hydrodynamic effect might become more vital, thereby giving the rubber matrix with higher modulus than that of the pure NR.

The increase of tensile modulus when adding dispersing agent was a clear evident to confirm that the dispersing agent did not only prevent the agglomeration of silica but also do enhance interaction between silica particle and the rubber matrix. The interaction between these two components was occurred via the electrostatic interaction between the positive charge of the silica/dispersing agent particle and the negative charge of rubber particle. The formation of electrostatic interaction between the silica/dispersing agent and the NR particle can stiffen the NR matrix by restricting the mobility of the NR chain. Therefore, the NR/silica nanocomposite will be more rigidity [43]. The enhancement of modulus was dependent of type and amount of dispersing agent. It was found that with only few exception conditions, for homo-PDDA, tensile modulus passed though the maximum with increasing molecular weight of PDDA. The reason at which tensile modulus initially increased with increasing molecular weight of PDDA might be due to the more positive charges of silica/PDDA particle to interaction with the negative charges of the NR particle. However, the further increase in molecular weight of PDDA tended to reduce tensile modulus. This may be due to the poor

dispersion of silica when using large dispersing agent as indicated in Figures 4.24-4.27. Co-PDDA seemed to have the lowest ability to enhance tensile modulus. This was because its chemical structure consists lesser positive charge than homo-PDDA. However, the tensile modulus of the NR/silica nanocomposite prepared from co-PDDA was not much lower than that of the one prepared from I-PDDA. Besides, the higher tensile modulus can be obtained when using higher amount of dispersing agent. Clearly, it was due to the higher available positive charges.

4.3.2.3 Elongation at Break

The elongation at break of the pure NR was compared to that of the NR/silica nanocomposites containing various silica loadings as shown in Figure 4.28 to 4.41.

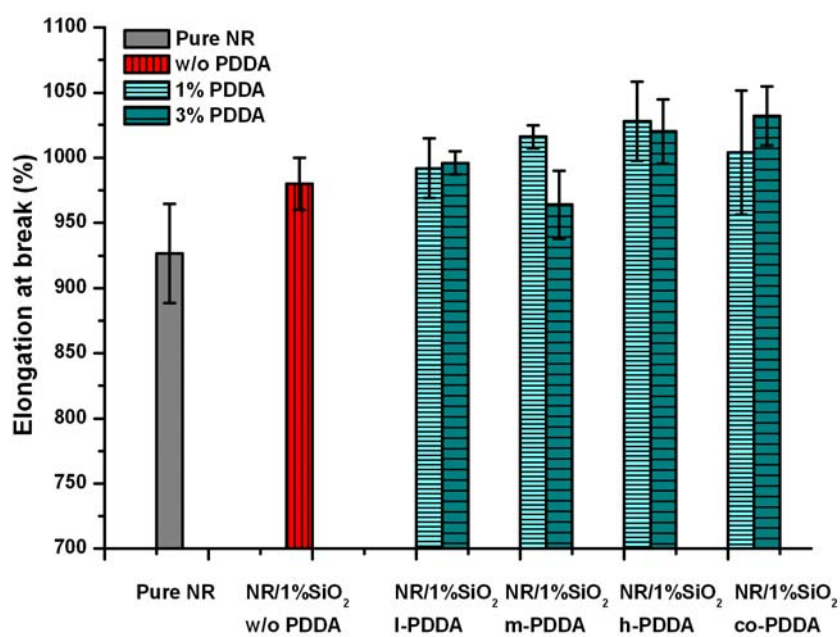


Figure 4.28 Elongations at break of the pure NR and the NR/1 wt% silica with different dispersing agents at 1 and 3 wt% of silica

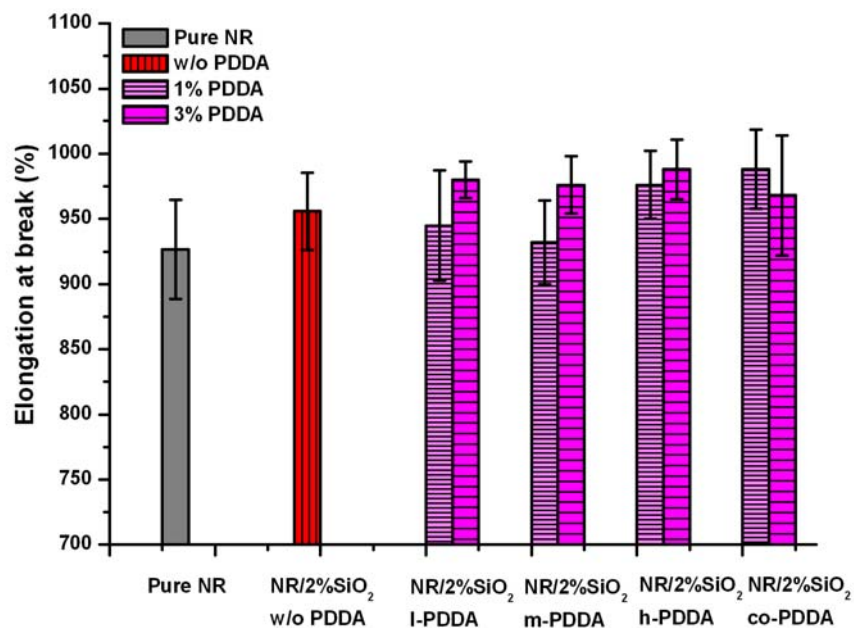


Figure 4.29 Elongations at break of the pure NR and the NR/2 wt% silica with different dispersing agents at 1 and 3 wt% of silica

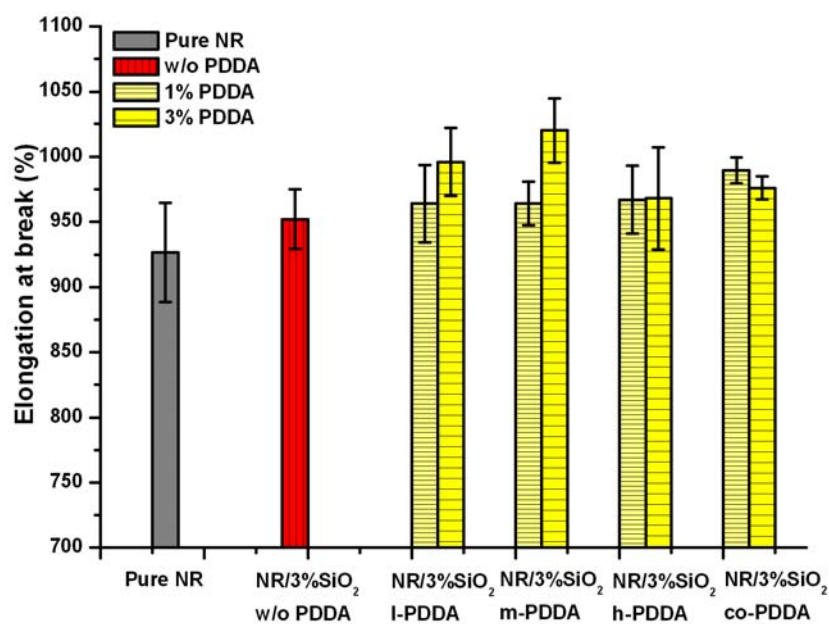


Figure 4.30 Elongations at break of the pure NR and the NR/3 wt% silica with different dispersing agents at 1 and 3 wt% of silica

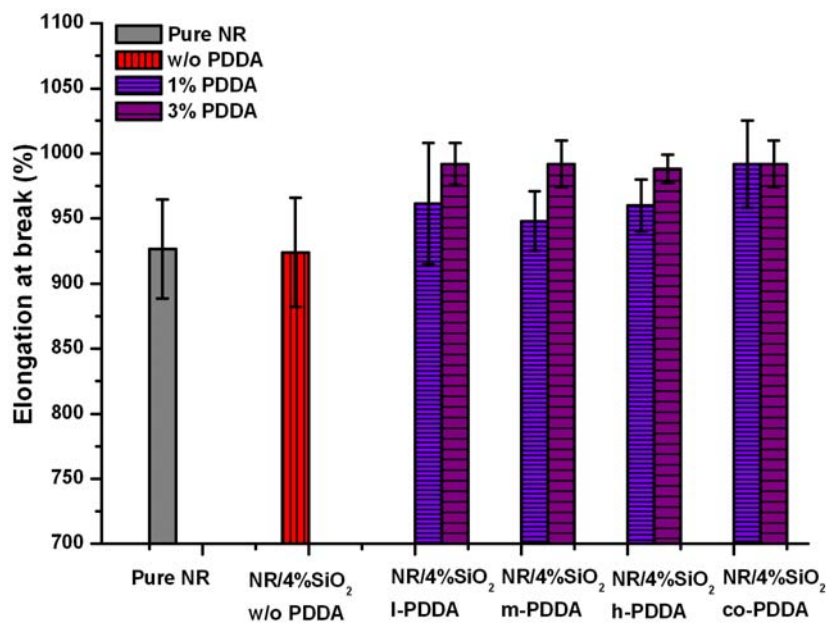


Figure 4.31 Elongations at break of the pure NR and the NR/4 wt% silica with different dispersing agents at 1 and 3 wt% of silica

First of all, it was clearly observed from above figures that the addition of silica except at 4 wt% without adding any dispersing agent led to the increase in the elongation at break of the NR/silica nanocomposites. This was due to the reduction in the crosslink density of the NR/silica nanocomposites as seen in Figures 4.16-4.19. As mentioned earlier, the decrease in the crosslink density was caused by the absorption of curing agents specially ZnO onto the silica surface. The rubber network with lesser crosslink density can be elongated more than the one with denser crosslink. Therefore, the higher elongation at break is obtained.

When considering the effect of dispersing agent on the elongation at break, it was found that the presence of dispersing agent no matter which type or how much further increased the elongation at break of the NR/silica nanocomposites. This seemed to be unusual when considering the amount of their crosslink density in parallel. Generally, the rubber chains of the tight network cannot move much, thus causing them break at low strain. However, in the case of the NR/silica nanocomposite with the presence of dispersing agent, it was found that the NR/silica nanocomposite had higher

crosslink density but it broke at higher elongation at break than the one without dispersing agent. It will be much easier to understand if first considering the deformation of the unfilled vulcanizate. Upon stretching, the rubber chain will be gradually stretched out until the rubber chain is tightened. Further stretching will cause the breaking of chain. In the case of adding filler, after constricted, the rubber chain will detach from the filler surface and then break. However, in the presence of dispersing agent, the rubber chain interacts with filler through the dispersing agent which is the long chain polymer. So before detaching from the filler, the chain of dispersing agent must be stretched until tightening. The stretching out of the dispersing agent causes the whole matrix breaks at higher elongation. This is a reason why even having higher crosslink density; the NR/silica nanocomposite with the presence of dispersing agent had higher elongation at break.

When considering the effect of the type of dispersing agent, with few excluding cases, it was found that in general the increase in molecular weight of PDDA, resulting the NR/silica nanocomposite in having more or less higher elongation at break. The reason for this was because the longer chain of dispersing agent reached the fully stretching point at the higher elongation. Thus, it caused the whole rubber matrix break at higher elongation as well. When replacing homo-PDDA with co-PDDA, it was found the elongation at break seemed to shift to slightly higher elongation at break. Again this observation consisted of few exception cases. The result might be these composites consisted of the lower crosslink densities as seen in **Figures 4.28-4.31**.

Comparing the elongation at break of the NR/silica nanocomposites with dispersing agent at 1 and 3 wt% of silica, it was found that at every silica loading but 1 wt%, the addition of dispersing agent at 3 wt% of silica gave the nanocomposites with higher elongation at break.

4.3.2.4 Tear Strength

The tear strength of the pure NR was compared to that of the NR/silica nanocomposites containing various silica loadings as shown in Figures 4.32 to 4.35.

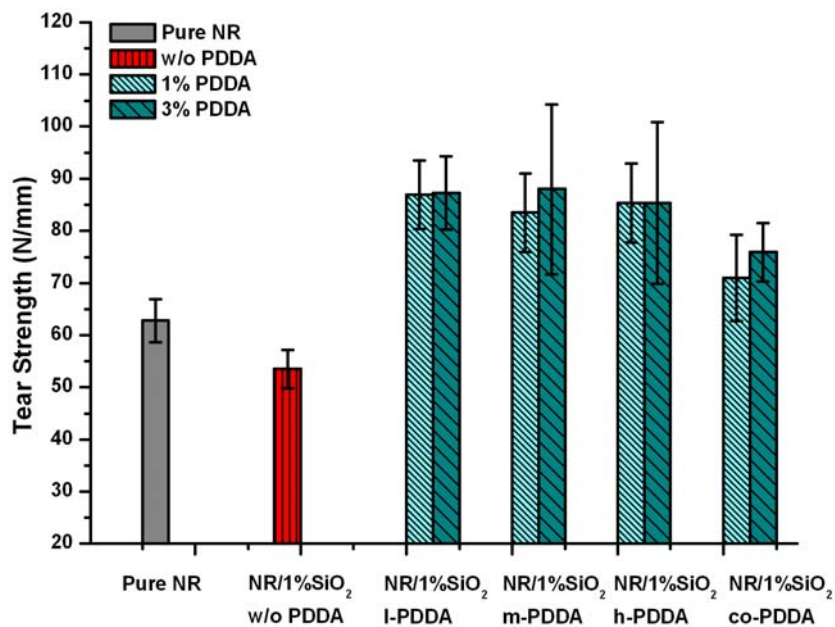


Figure 4.32 Tear strengths of the pure NR and the NR/1 wt% silica with different dispersing agents at 1 and 3 wt% of silica

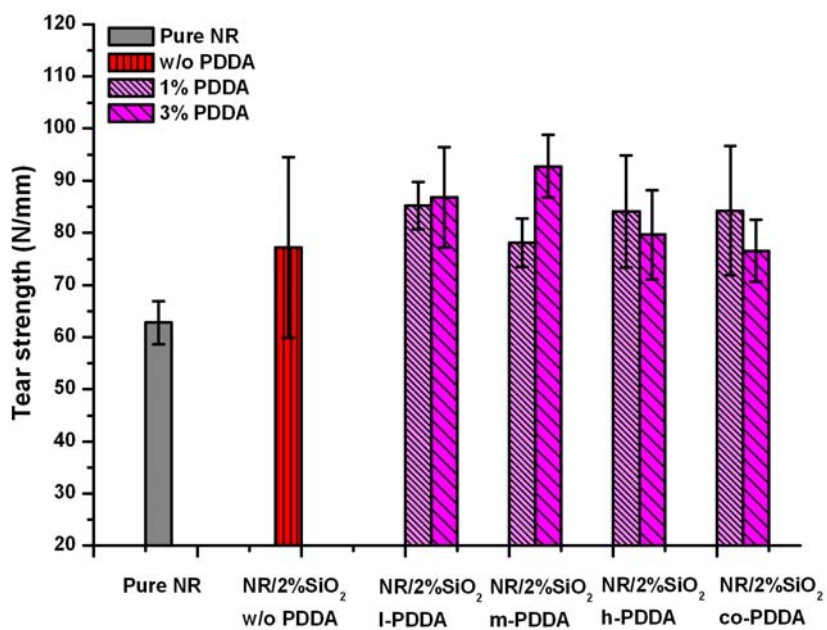


Figure 4.33 Tear strengths of the pure NR and the NR/2 wt% silica with different dispersing agents at 1 and 3 wt% of silica

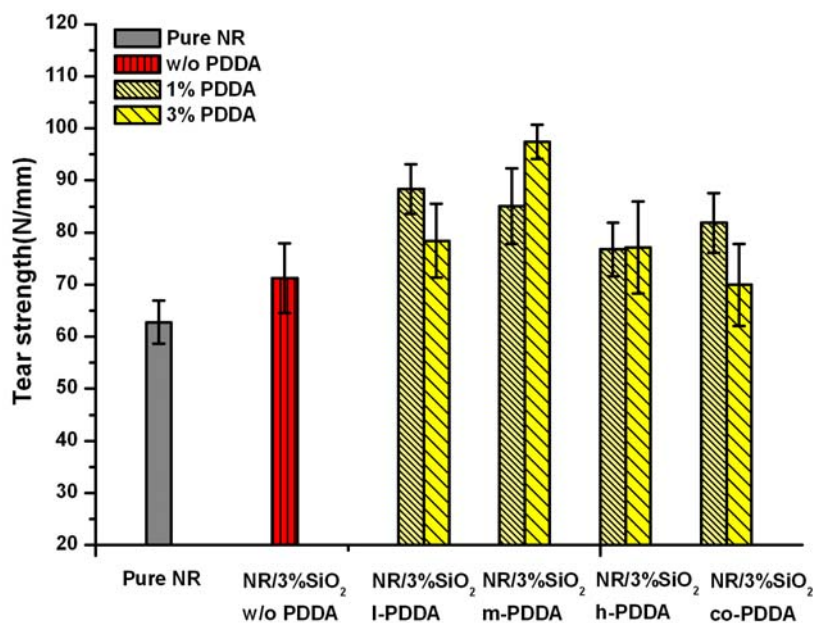


Figure 4.34 Tear strengths of the pure NR and the NR/3 wt% silica with different dispersing agents at 1 and 3 wt% of silica

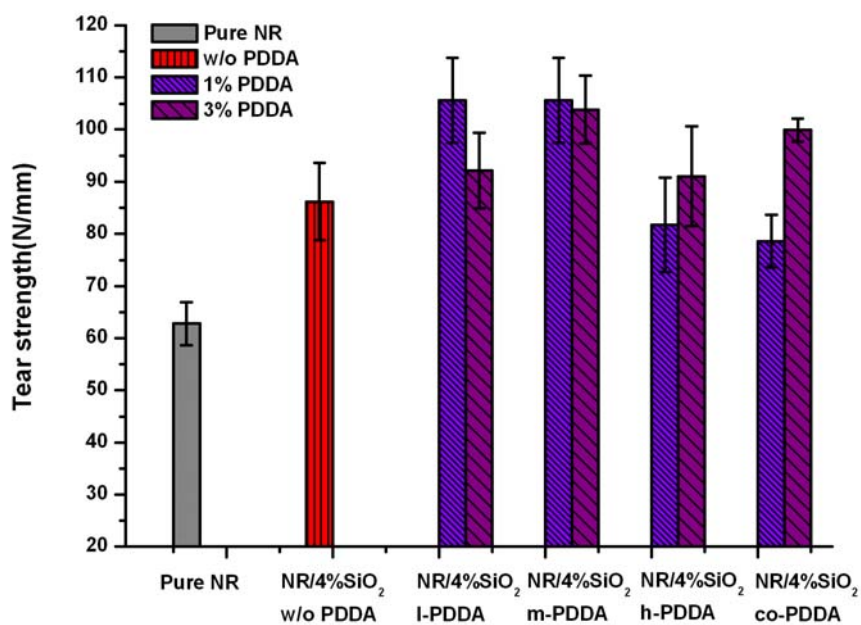


Figure 4.35 Tear strengths of the pure NR and the NR/4 wt% silica with different dispersing agents at 1 and 3 wt% of silica

From the result shown above, it was observed that the addition of silica at 2-4 wt% could significantly improve tear strength of the NR matrix. The tear strength increased with increasing silica loading. This improvement can be explained that the network of silica mutually penetrated within the rubber matrix and hindered the slide of NR molecules [9]. So, the tear strength of the NR/silica nanocomposite became higher. However, the better tear strength could be achieved when adding dispersing agents at 1 or 3 wt%. This was due to the better interaction between silica and NR. The influence of dispersing type on tear strength showed similar trend as that on tensile strength and modulus described as follows. I-PDDA and m-PDDA had the comparable ability to enhance tear strength and their ability were higher than that of h-PDDA and co-PDDA. The presence of h-PDDA and co-PDDA did not show any significant increase in tear strength but do not worsen it. The variation of dispersing agent concentration did not show any certain pattern on the improvement of the tear resistance. The highest tear strength at silica loading of 1 wt%, 2 wt%, 3 wt% and 4 wt% were shown as a following order: 88, 92, 97 and 105 N/mm, respectively. All of these were obtained when using m-PDDA as dispersing agent.

4.3.3 Thermal Properties

The thermal stability of the NR/silica nanocomposite was determined by thermal gravity analyzer (TGA). The onset temperature indicating the starting decomposition temperature confirmed by the observation of the weight loss and the endset temperature indicating the complete decomposition confirmed by the constant weight loss were focused here. All of samples were measured under the nitrogen atmosphere. The TGA curves of the NR/silica nanocomposites with various silica contents of 1, 2, 3, and 4 wt% were shown in **Figure 4.35-4.38**, respectively. It can be seen that all the nanocomposite samples with different silica contents showed similar thermal degradation pattern. The TGA curves clearly presented one stage thermal decomposition mechanism of NR matrix, primarily initiated by thermal separation of C-C chain bonds accompanying transfer of hydrogen at the site of the separation [9]. The decomposition of NR started at about 360°C. The similar behavior was also observed when the different core-shell structure.

silica-poly(methyl methacrylate), were used to prepare the NR/silica nanocomposite [42].

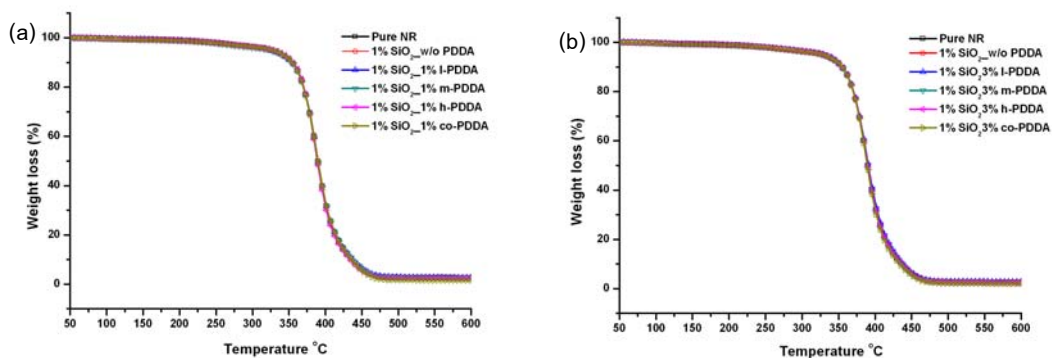


Figure 4.36 TG curves of the NR/1wt% silica nanocomposite with different dispersing agents at (a) 1 and (b) 3 wt% of silica

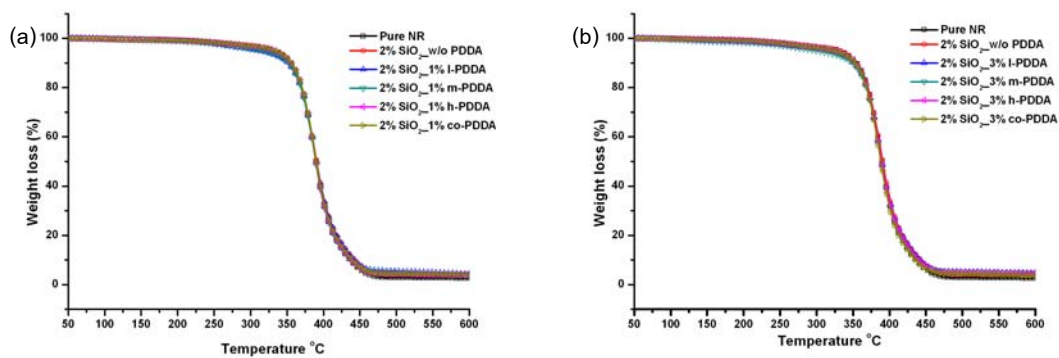


Figure 4.37 TG curves of the NR/2 wt% silica nanocomposite with different dispersing agents at (a) 1 and (b) 3 wt% of silica

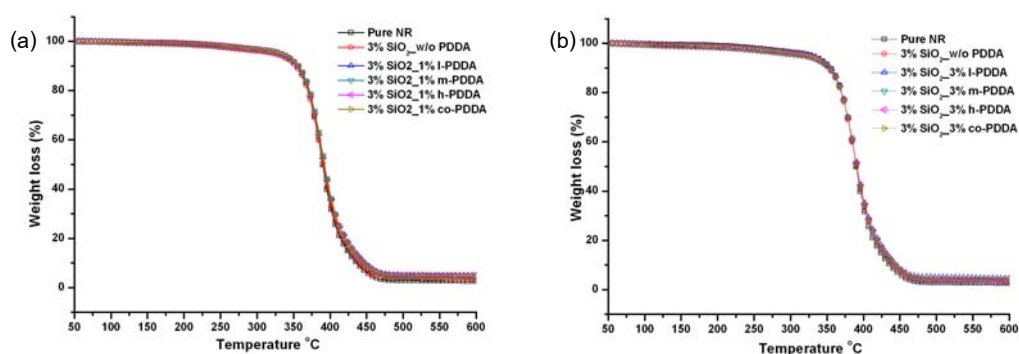


Figure 4.38 TG curves of the NR/3 wt% silica nanocomposite with different dispersing agents at (a) 1 and (b) 3 wt% of silica

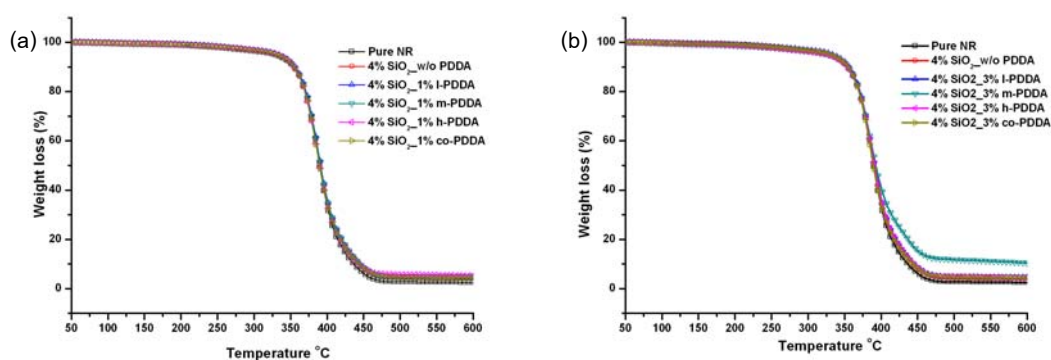


Figure 4.39 TG curves of the NR/4 wt% silica nanocomposite with different dispersing agents at (a) 1 and (b) 3 wt% of silica

Table 4.1 summarizes the TGA data of the pure NR compound and its nanocomposites. The data induced the temperatures indicating the onset (T_d^{onset}) and endset (T_d^{endset}) of thermal degradation. It can be observed that the onset and endset temperature of degradation for the NR/silica nanocomposite were shifted toward higher temperature when adding silica whether with or without dispersing agent. The onset temperature of degradation increased around 3-5 °C compared with that of the pure NR. The maximum onset degradation temperature that can be achieved in this work was 367.8 °C. The endset temperature of degradation also increased from 410 °C (pure NR)

to 417 °C (maximum). The endset temperature was increased approximately as 3-7 °C. These indicated an improvement the thermal stability of the nanocomposite material even only small loading of nanosilica was introduced into the matrix. However, when considered the effect of silica loadings on the onset degradation temperatures, the slight difference was observed. The difference of the onset degradation temperatures altered in range of 1-3 °C.

From all data, the onset temperatures of degradations can be divided into two groups accordingly to silica loading. The 1 and 2 wt% silica loadings were referred as low silica loading while 3 and 4 wt% silica loading were referred to high silica loading here. As can be seen, the onset temperature of the NR/silica nanocomposite filled with low silica loading was slightly higher than that of the NR/silica nanocomposite filled with high silica loading. Especially, the 2 wt% silica seemed to have the highest ability to enhance thermal stability for the nanocomposite. Although it has been explained in the literature that the distribution and interaction of silica nanoparticles were also dominate factors effecting on the thermal stability of nanocomposite. If silica nanoparticles are homogeneously distributed throughout the NR matrix as nano-cluster and has strongly interacts with NR chains, the diffusion of degradation products from the bulk polymer to gas phase has been slow down, thus leading to the higher thermal stability of the NR matrix [9]. However, in this study, it was found that the type and concentration of dispersing agent did not play any role on the onset temperature. Using different dispersing agent at 1 or 3 wt% of silica gave nearly the same onset temperature.

When considering the factor influencing on the the endset temperature, from **Table 4.1** it was found that the endset temperature trended to increase with increasing amount of silica. This may be due to the higher proportion of inorganic filler having much higher thermal stability than the organic component like NR in the matrix. Similar to the onset temperature, both dispersing type and loading seemed to have no significant effect on this property.

Table 4.1 The onset degradation temperatures of the pure NR and NR/silica nanocomposites with various silica contents

| Sample | Dispersing agent | Silica loading (wt%) | | | |
|-------------------------|------------------|----------------------|--------|--------|--------|
| | | 1 | 2 | 3 | 4 |
| Pure NR | N/A | 362.90 | 362.90 | 362.90 | 362.90 |
| NR/silica nanocomposite | N/A | 366.09 | 365.12 | 364.21 | 364.65 |
| NR/silica nanocomposite | 1% I-PDDA | 366.10 | 366.35 | 365.91 | 365.11 |
| NR/silica nanocomposite | 1% m-PDDA | 366.23 | 367.83 | 365.61 | 365.43 |
| NR/silica nanocomposite | 1% h-PDDA | 365.04 | 367.44 | 365.48 | 363.97 |
| NR/silica nanocomposite | 1% co-PDDA | 365.88 | 367.18 | 365.66 | 365.80 |
| NR/silica nanocomposite | 3% I-PDDA | 366.30 | 365.77 | 364.55 | 365.10 |
| NR/silica nanocomposite | 3% m-PDDA | 367.80 | 365.63 | 364.21 | 365.02 |
| NR/silica nanocomposite | 3% h-PDDA | 365.83 | 365.04 | 354.43 | 365.01 |
| NR/silica nanocomposite | 3% co-PDDA | 365.91 | 365.48 | 364.65 | 365.39 |

Table 4.2 The endset degradation temperatures of the pure NR and NR/silica nanocomposites with various silica contents

| Sample | Dispersing agent | Silica loading (wt%) | | | |
|-------------------------|------------------|----------------------|--------|--------|--------|
| | | 1 | 2 | 3 | 4 |
| Pure NR | N/A | 410.99 | 410.99 | 410.99 | 410.99 |
| NR/silica nanocomposite | N/A | 414.30 | 416.53 | 415.15 | 417.66 |
| NR/silica nanocomposite | 1% I-PDDA | 413.62 | 415.29 | 417.80 | 416.93 |
| NR/silica nanocomposite | 1% m-PDDA | 414.10 | 412.24 | 418.09 | 416.43 |
| NR/silica nanocomposite | 1% h-PDDA | 413.69 | 412.47 | 417.47 | 413.76 |
| NR/silica nanocomposite | 1% co-PDDA | 416.50 | 413.26 | 417.85 | 412.62 |
| NR/silica nanocomposite | 3% I-PDDA | 416.25 | 414.65 | 415.51 | 417.48 |
| NR/silica nanocomposite | 3% m-PDDA | 412.99 | 414.95 | 415.66 | 417.48 |
| NR/silica nanocomposite | 3% h-PDDA | 415.20 | 414.88 | 416.00 | 416.98 |
| NR/silica nanocomposite | 3% co-PDDA | 413.48 | 412.66 | 415.63 | 417.05 |

4.3.4 Morphology

4.3.4.1 Physical Appearance

Figure 4.40 shows top view of the obtained NR/silica nanocomposite sheet at silica loading of 2 wt%. The smooth surface, opaque, and yellow color was observed. At the other silica loadings with and without dispersing agent, the same appearance was found. However, at the bottom view, the difference appearance dependent of the amount of silica and the presence of dispersing agent was observed.

Figure 4.41 shows the bottom view of the NR/silica nanocomposite consisting of 4 wt% silica. As seen, without dispersing agent, silica tended to agglomerate and then deposited on the bottom of the rubber sheet, giving a rough surface as shown in Figure 4.41 (a). However, when adding dispersing agent, only slight deposition of silica was observed, thus giving the rubber sheet with smooth surface as shown in Figure 4.41 (b). At the lower silica loading, the smoother bottom surface was observed. This indicated the less precipitation of silica.



Figure 4.40 Physical appearance of the NR/silica nanocomposite sheet

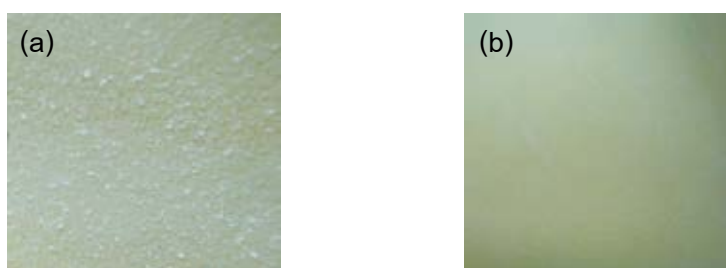


Figure 4.41 Images of the NR/silica nanocomposite surface

(a) without PDDA (b) with PDDA

4.3.4.2 SEM Pictures

As mentioned in the previous part, silica nanopowder does not exist as individual silica nanoparticle but as aggregate silica as shown in **Figure 4.42**. To enhance the strength of the matrix, the better dispersion of silica must be performed.

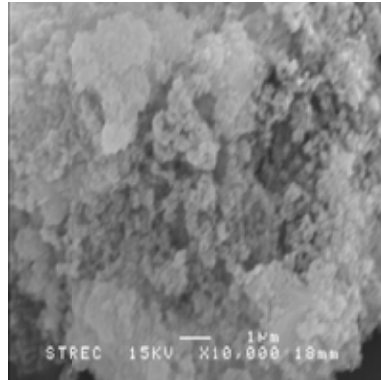


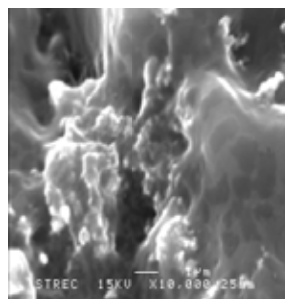
Figure 4.42 SEM image of silica nanopowder

To study the morphology of silica in the rubber matrix, the fracture surface of the NR/silica nanocomposite sheet was observed by scanning electron microscopy as shown in **Figure 4.43**. As seen, when increasing silica concentration, the aggregation of silica was generated gradually and then can be clearly seen at high silica content. The silica/dispersing agent particle thoroughly dispersed inside natural rubber matrix as cluster forms. The dark area presented NR matrix and the bright area presented silica clusters. At low silica loading, the intensive aggregations was not clearly seen (**Figure 4.43 (a)-1 to (a)-3**). The aggregation being started in some areas of natural rubber matrix and assumed that the size of silica clusters was smaller. At high silica content, size and density of silica clusters dramatically increased until they were push outside and appeared in bright phase as obviously seen in **Figure 4.43 (c)-2 and (d)-2**. The aggregation of silica at the loading of 2, 3, and 4 wt% showed the same features as that at 1 wt% silica loading. However, at low silica loading with co-PDDA **Figure 4.43 (a)-4 and (b)-4**, the silica cluster seemed to have higher size and showed larger aggregation on NR matrix surface compared with high silica loading.

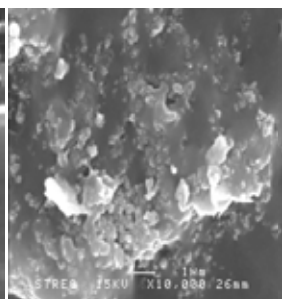
Increasing silica loading \longrightarrow

I-PDDA

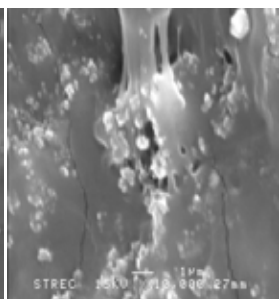
(a)-1 1% silica_I-PDDA



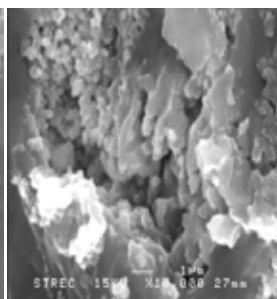
(b)-1 2% silica_I-PDDA



(c)-1 3% silica_I-PDDA

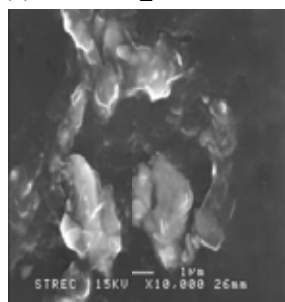


(d)-1 3% silica_I-PDDA

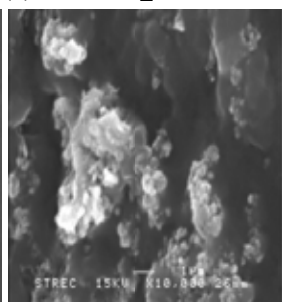


m-PDDA

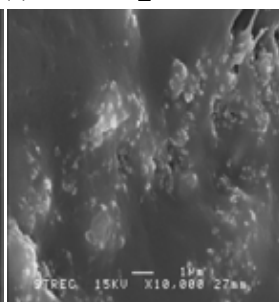
(a)-2 1% silica_m-PDDA



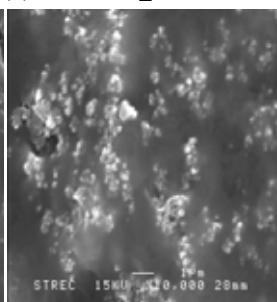
(b)-2 2% silica_m-PDDA



(c)-2 3% silica_m-PDDA

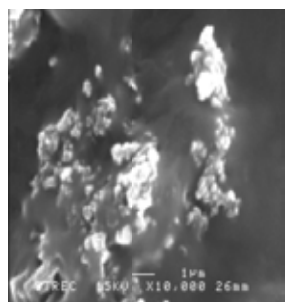


(d)-2 4% silica_m-PDDA

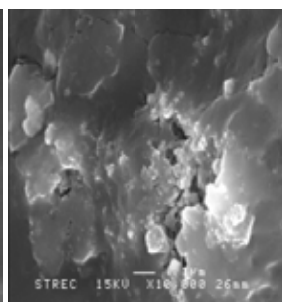


h-PDDA

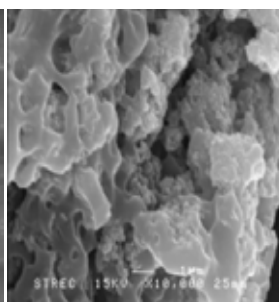
(a)-3 1% silica_h-PDDA



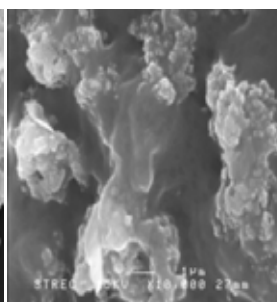
(a)-3 2% silica_h-PDDA



(a)-3 3% silica_h-PDDA

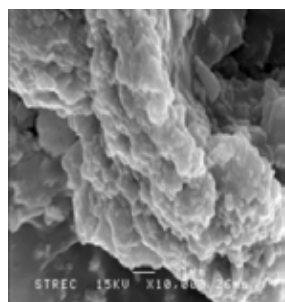


(a)-3 4% silica_h-PDDA

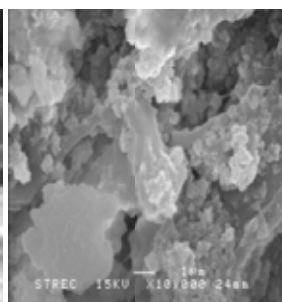


co-PDDA

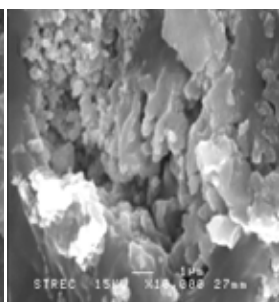
(a)-4 1% silica_co-PDDA



(b)-4 2% silica_co-PDDA



(c)-4 3% silica_co-PDDA



(d)-4 4% silica_co-PDDA

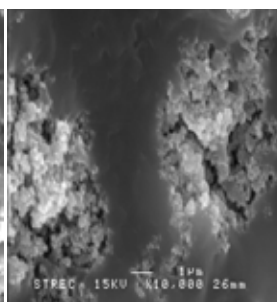


Figure 4.43 SEM micrograph of NR/silica nanocomposites:

(a) 1% silica_PDDA

(b) 2% silica_PDDA

(c) 3% silica_PDDA

(d) 4% silica_PDDA

When considering the different of molecular weight of PDDA dispersing agents, it can be found that either 1wt% silica or 2% silica contents, when using l-PDDA, m-PDDA and h-PDDA, there was no distinguished difference as shown in **Figure 4.43 (a)1-3** and **(b)1-3**. The size of silica clusters in the rubber matrix was just about the same. However, when using co-PDDA, the difference was observed. The aggregate structures were found in most area and intensively took place in natural rubber matrix as shown in **Figure 4.43 (a)-4**.

CHAPTER V

CONCLUSIONS

The influences of molecular weight, chemical structure, and loading of dispersing agent and also loading of silica on the mechanical and thermal properties of the NR/silica nanocomposites were focused here. Homo-PDDA with three different molecular weights including l-PDDA (MW = 100,000-200,000), m-PDDA (MW = 200,000-350,000), and h-PDDA (MW = 400,000-500,000) and co-PDDA at 1 and 3 wt% of silica were used here as dispersing agent. The concentration of silica was varied from 1 to 2, 3, and 4 wt%. According to this study, the obtained results including not only how those factors played a role on the mechanical and thermal properties of the NR/silica nanocomposites but also the optimal preparing condition and physical properties of the silica/dispersing agent aqueous suspension are summarized as follows:

1. With respect of practical part and particle size distribution of silica as well, the 30 min ultrasonicate time and pH value of the aqueous at 10 were the optimal condition to prepare the silica/dispersing agent aqueous suspension.

2. For homo-PDDA, it seemed like all three different molecular weight PDDAs gave the silica/dispersing agent aqueous suspension with comparable median particle size. When replacing homo-PDDA with co-PDDA, it was found that the median particle size of the silica/dispersing agent aqueous suspension increased significantly. Interestingly, with the absence of dispersing agent, increasing amount of silica did not increase the median particle size of the silica aqueous suspension. On the other hand, with the presence of dispersing agent, increasing amount of silica significantly increased the median particle size of the silica/dispersing agent aqueous suspension. Moreover, increasing amount of dispersing agent from 1 to 3 wt% of silica also increased the median particle size.

3. Although the presence of dispersing agent led to the bigger silica particle size distribution, it gave the silica aqueous suspensions better colloid stability indicating by

completely re-dispersing after coagulation and slowed down the precipitation during preparing the rubber sheet.

4. When considering crosslink density, it was observed that the crosslink density significantly decreased when adding silica no matter with or without dispersing agent. However, after adding dispersing agent regardless of type and loading, the crosslink density of the NR/silica nanocomposites was gradually increased. The I-PDDA and m-PDDA showed comparable effect on the increase in crosslink density and their effect on the increase in crosslink density was much more pronounced than that of h-PDDA and co-PDDA. The effect of amount of dispersing agent was also studied. However, the conclusion for how it affected on the crosslink density was inconsistent.

5. The presence of silica at 1-3 wt% without any dispersing agent can enhance tensile strength of the NR matrix. But the opposite behavior was observed at 4 wt% silica. The presence of dispersing agent further enhanced the tensile strength. The best condition to obtain the highest tensile strength, 25 MPa, was the NR compound consisting of 2 wt% silica with I-PDDA at 1 wt% of silica. Further increase in silica loading did not give higher tensile strength at all. Comparing amongst homo-PDDA, generally, I-PDDA and m-PDDA gave the comparable tensile strength and higher than h-PDDA, whereas co-PDDA seemed to have the lowest ability to enhance tensile strength.

6. For tensile modulus, it was observed that at low silica loading, 1 and 2 wt%, the presence of silica without any dispersing agent reduced both 100 and 300% modulus of the NR matrix. The opposite behavior was observed at the higher silica loading. At low silica loading, the decrease of crosslink density due to the presence of silica led to the reduction of tensile modulus. At higher silica loading, the hydrodynamic effect might become more vital, thereby giving the rubber matrix with higher modulus than that of the pure NR. The increasing of tensile modulus was observed when adding dispersing agent. The enhancement of modulus was dependent of type and amount of

dispersing agent. It was found that with only few exception conditions, for homo-PDDA, tensile modulus passed through the maximum with increasing molecular weight of PDDA. However, the further increase in molecular weight of PDDA tended to reduce tensile modulus. Co-PDDA seemed to have the lowest ability to enhance tensile modulus.

7. The addition of silica except at 4 wt% without adding any dispersing agent led to the increase in the elongation at break of the NR/silica nanocomposites. This was due to the reduction in the crosslink density of the NR/silica nanocomposites. The presence of dispersing agent no matter which type or how much further increased the elongation at break of the NR/silica nanocomposites. When considering the effect of the type of dispersing agent, with few excluding cases, it was found that in general the increase in molecular weight of PDDA, resulting the NR/silica nanocomposite in having more or less higher elongation at break. When replacing homo-PDDA with co-PDDA, it was found the elongation at break seemed to shift to slightly higher elongation at break. The addition of dispersing agent at 3 wt% of silica gave the nanocomposites with higher elongation at break except at 1 wt% silica.

8. For tear strength, it was observed that the addition of silica at 2-4 wt% could significantly improve tear strength of the NR matrix. The tear strength increased with increasing silica loading. However, the better tear strength could be achieved when adding dispersing agents at 1 or 3 wt%. The influence of dispersing type on tear strength showed similar trend as that on tensile strength and modulus described as follows. l-PDDA and m-PDDA had the comparable ability to enhance tear strength increased and their ability were higher than that of h-PDDA and co-PDDA. The presence of h-PDDA and co-PDDA did not show any significant increase in tear strength but did not worsen it. The variation of dispersing agent concentration did not show any certain pattern on the improvement of the tear resistance. The highest tear strength, 105 N/mm, was obtained when adding silica 4 wt% with m-PDDA 3 wt% of silica.

9. The presence of silica no matter with or without dispersing agent shifted the onset and endset decomposition temperature toward higher temperature. The onset and endset temperature of the NR/silica nanocomposite increased from 362 to 367 °C and 410 to 417 °C, respectively. However, varying silica loading from 1 upto 4 wt% gave insignificantly difference on the increase of the onset decomposition temperature. On the other hand, the endset decomposition temperature slightly increased with increasing silica loading. The presence of dispersing agent did not further enhance the thermal property of the NR/silica nanocomposite at all. Changing either molecular weight or chemical structure of dispersing agent gave the NR/silica nanocomposite nearly the same thermal property.

10. SEM micrographs showed that when increasing silica concentration, the aggregation of silica was generated gradually and then can be clearly seen at high silica content. For homo-PDDA, increasing of molecular weight of PDDA did not affect much on the formation of silica aggregate in the rubber matrix. But replacing homo-PDDA with co-PDDA led to the severe aggregate formation of silica.

REFERENCES

- [1] Zou, H., Wu, S., and Shen, J. Polymer/Silica Nanocomposites : Preparation, Characterization, Properties, and Applications. Chemical Reviews 108 (2008): 3897-3957.
- [2] Yu, T., Lin, J., Xu, J., and Ding, W. Nanocomposites of Vinyl Chloride-Acrylonitrile Copolymer and Silica. Journal of Polymer Science: Part B: Polymer Physics 43 (2005) : 3127-3134.
- [3] Kemal, L. et al. Toughening of Unmodified Polyvinylchloride Through the Addition of Nanoparticulate Calcium Carbonate. Polymer 50 (2009) : 4066-4079.
- [4] Habibi, S. et al. Preparation and Flame Retardancy of Poly(ethyleneterephthalate)/Montmorillonite Nanocomposites. Asian Journal of Chemistry 21 (2009) : 4881-4888.
- [5] Nakasorn, C, Pechurai, W., Sahakaro, K., and Kaesaman, A. Rheological, Thermal, and Curing Properties of Natural-g-Poly (methyl methacrylate). Journal of Applied Polymer Science 99 (2006) : 1600-1614.
- [6] Schadler, L. S. Nanotube/Polymer Composites. In, Polymer-based and Polymer-filled Nanocomposites, pp 100-101. Germany : Federal Republic, 2004.
- [7] Peng, Z., Kong, L. X., and Li, S.D. Thermal Properties and Morphology of a Poly(vinylalcohol)/Silica Nanocomposite Prepared with a Self-Assembled Monolayer Technique. Journal of Applied Polymer Science 96 (2005) : 1436-1442.
- [8] Kong, L. X., Peng, Z., and Li, S.D. Non-Isothermal Crystallisation Kinetics of Self-Assembled Polyvinylalcohol/Silica Nano-Composite. Polymer 46 (2005) : 1949-1955.
- [9] Peng, Z., Kong, L. X., Li, S. D., Chen, Y., and Huang, M. F. Self-Assembled Natural Rubber/Silica Nanocomposites: Its Preparation and Characterization. Composite Science and Technology 67 (2007) : 3130-3139.

- [10] UNCTAD secretariat. Description and technical features [online]. Available from : <http://r0.unctad.org/infocomm/anglais/rubber/characteristics.htm> [2011, November 27]
- [11] Daranee Nuntivanich. Silica Reinforcement of Natural Rubber by Sol-Gel Process in Latex. Master's Thesis, Department of Petrochemistry and Polymer Science, Faculty of Science, Chulalongkorn University, 2003.
- [12] Aungsutorn Mahittikul. Structure and Properties of Hydrogenated Natural Rubber Latex Using $\text{OsHCl}(\text{CO})(\text{O})_2(\text{PCl}_2)_2$ as a Catalyst and Diimide Reduction. Doctoral dissertation, Department of Chemical technology, Faculty of Science, Chulalongkorn University, 2005.
- [13] Resing, W. Production, Processing and Properties. Naturalrubber 17 (2000) : 2-3.
- [14] จิตต์ลัดดา ศักดาภิพาณิชย์. เทคโนโลยียางธรรมชาติ. กรุงเทพมหานคร : เทคโนโลยีคอมมิวนิเคชันส์, 2553.
- [15] Jacob, J.L., Auzac, J., and Prevot, J.C. The Composition of Natural Rubber Latex from Hevea Brasiliensis. Clinical Reviews in Allergy 11 (1993) : 325-332.
- [16] Gazeley, K. F., Gorton, A. D. T., and Pendle, T. D. The Production of NR Latex Concentrate. In A.D. Roberts (ed.), Latex Concentrates : Properties and Composition, pp.63-66. New York : Oxford University Press, 1988.
- [17] Blackley, D. C. Polymer Latices Science and Technology. Second edition. Volume 2 Type of Latices. London : Chapman & Hall, 1997.
- [18] Rubber board. Latex Preservation and Concentration [Online]. Available from : <http://rubberboard.org.in/ManageCultivation.asp?Id=192> [2012, January 27]
- [19] LaL, L., Raju, S., and Shanker, R. Studies on Factors Affecting the Quality of the Radiation-Vulcanized Latex [Online]. Available from: <http://polymerprojecttopicsblogspot.com/2010/08/radiation-vulcanized-latex.html> [2011, January 27]
- [20] Dzikowicz, B. Latexes [Online]. Available from : <http://www.Rtvanderbilt.com/Latex%20by%20Bob%20Dzikowicz%20onWebMast.pdf> [2012, March 6]
- [21] ธาณินทร์ ไลปนนานนท์. การทำน้ำยางข้น. วารสารยางพารา 2 (2529) : 60-71.

- [22] ณพรัตน์ วิชิตชลชัย. การผลิตผลิตภัณฑ์จากน้ำยาง. กลุ่มอุตสาหกรรมผลิตภัณฑ์ยาง สำนักวิจัยและพัฒนาวิทยาการหลังการเก็บเกี่ยวและแปรรูปผลิตผลเกษตร. (เอกสารไม่ตีพิมพ์)
- [23] Naus, I. H., Collard, F., and Winkel H. T. Natural Rubber Latex Technology. Naturalrubber 17 (2000) : 10-14.
- [24] Walter, H., Waddell, and Evans, R. Introduction. In D. S. John (ed.), Precipitated Silica and Non-Black Filler, pp.325 Canada : Hanser Gardner Publications.
- [25] Non-black filler for rubber [Online]. Available from: <http://www.rtvanderbilt.com/NonBlackFillers.pdf>, [2012, May 30]
- [26] พงษ์ธร แซ่อูย การใช้ซิลิกาเป็นสารตัวเติมในยาง [Online]. Available from : <http://rubber.sc.mahidol.ac.th/rubbertech/Silica.pdf> [2012, March 2]
- [27] Wason, S.K. Synthetic Silica-Overview. In, Synthetic Silica, pp.166-182. New York : Van Nostrand Reinhold, 1987.
- [28] Unitedchem. Silane Coupling Agent Guide [Online]. Available from : <http://www.amchro.com/PDFs/Silane/Neu-SilaneCouplingAgents08.pdf> [2012, January 15]
- [29] SiSiB R Silanes. Silane Coupling Agent Guide [Online]. Available from : <http://www.powerchemcorp.com/library/public/Silane%20Coupling%20Agents.pdf> [2012, January 15]
- [30] Wikipedia. Self-assembly [Online]. Available from : <http://en.wikipedia.org/wiki/Self-assembly> [2012, January 30]
- [31] Zhang, Y.B., Qian, X.F., Xi, H.A., Yin, J., and Zhu, Z K. Preparation of Polystyrene Core–Mesoporous Silica Nanoparticles Shell Composite. Materials Letters 58 (2003) : 222– 225.
- [32] Rawle, A. Basic Principles of Particle Size Analysis [Online]. Available from http://golik.co.il/Data/BasicPrinciplesofParticlesize_1126925513.pdf [2012, March 18]
- [33] Kippax, P. Particle Size Distribution [Online]. Available from : <http://www.chemeurope.com/en/whitepapers/61205/measuring-particle-size-using-modern-laser-diffraction-techniques.html> [2012, March 18]

- [34] Gee , G. W. Particle-Size Analysis [Online]. Available from : http://www.cprl.ars.usda.gov/pdfs/2_4%20Particle%20Size%20Analysis%202002.pdf [2012, March 18]
- [35] Horiba Scientific. A Guidebook to Particle Size Analysis [Online]. Available from : http://www.horiba.com/fileadmin/uploads/Scientific/Documents/PSA/PSA_Guidebook.pdf [2012, March 18]
- [36] Wikipedia. Polyelectrolyte [Online]. Available from : <http://en.wikipedia.org/wiki/Polyelectrolyte> [2012, March 22]
- [37] Dosramos, J.G. Characterizing Particles in Nano-Powder Regimes [Online]. Available from : <http://www.matec.com/mas/applications/particlecharacterization/> [2012, March 28]
- [38] Kunitake, T., Lvov, Y., Ariga, K., Onda, M., and Ichinose, I. Alternate Assembly of Ordered Multilayers of SiO₂ and Other Nanoparticles and Polyions. Langmuir 13 (1997) : 6195-6203.
- [39] Silver Colloids. An Introduction to Zeta Potential and its Measurement [Online]. Available from : <http://www.silver-colloids.com/Tutorials/Intro/pcs7.html> [2012, March 28]
- [40] Shi, J. Steric Stabilization. Center for Industrial Sensors and Measurements Department Materials Science & Engineering Group Inorganic Material Science Literature Review. 29 (August 2009) : 1-15.
- [41] Kopeliovich, D. Stabilization of Colloids [Online]. Available from : http://www.substech.com/dokuwiki/doku.php?id=stabilization_of_colloids&DokuWiki=1a7660dc-ed264b04eed3e7f [2012, March 28]
- [42] Wang, Q. et al. Reinforcement of Natural Rubber with Core-Shell Structure Silica-Poly (Methyl Methacrylate) Nanoparticles. Journal of Nanomaterials. (2012) : 2-10.
- [43] Boonmahitthisud, A. Natural Rubber Filled with Nanoparticles of Polystyrene and PS-encapsulated Silica. Pure and Applied Chemistry International Conference. (2009) : 231-234.

APPENDICES

APPENDIX A

APPENDIX A

CROSSLINK DENSITIES OF NR/SILICA NANOCOMPOSITES

Table A-1 Crosslink densities of Pure NR

| Sample | Crosslink density (mol/m ³) |
|---------|---|
| 1 | 62.10 |
| 2 | 62.71 |
| 3 | 68.07 |
| Average | 64.29 |
| SD | ±3.301 |

Table A-2 Crosslink densities of NR/1% silica without PDDA

| Sample | Crosslink density (mol/m ³) |
|---------|---|
| 1 | 39.35 |
| 2 | 32.31 |
| 3 | 41.78 |
| Average | 37.81 |
| SD | ±4.915 |

Table A-3 Crosslink densities of NR/1% silica with 1% PDDA

| Sample | Crosslink density (mol/m ³) | | | |
|---------|---|--------|--------|---------|
| | I-PDDA | m-PDDA | h-PDDA | co-PDDA |
| 1 | 43.34 | 41.35 | 36.55 | 40.20 |
| 2 | 40.58 | 41.13 | 42.16 | 37.90 |
| 3 | 42.71 | 43.84 | 39.8 | 38.70 |
| Average | 42.21 | 42.10 | 39.50 | 38.94 |
| SD | ±1.443 | ±1.500 | ±2.817 | ±1.165 |

Table A-4 Crosslink densities of NR/1% silica with 3% PDDA

| Sample | Crosslink density (mol/m ³) | | | |
|---------|---|--------|--------|---------|
| | I-PDDA | m-PDDA | h-PDDA | co-PDDA |
| 1 | 41.45 | 41.24 | 40.89 | 38.78 |
| 2 | 42.26 | 39.96 | 39.36 | 37.17 |
| 3 | 39.93 | 38.79 | 37.08 | 36.98 |
| Average | 41.21 | 39.99 | 39.11 | 37.65 |
| SD | ±1.183 | ±1.226 | ±1.907 | ±0.989 |

Table A-5 Crosslink densities of NR/2% silica without PDDA

| Sample | Crosslink density (mol/m ³) |
|---------|---|
| 1 | 53.13 |
| 2 | 55.80 |
| 3 | 55.78 |
| Average | 54.90 |
| SD | ±1.538 |

Table A-5 Crosslink densities of NR/2% silica with 1% PDDA

| Sample | Crosslink density (mol/m ³) | | | |
|---------|---|--------|--------|---------|
| | I-PDDA | m-PDDA | h-PDDA | co-PDDA |
| 1 | 52.70 | 58.59 | 57.77 | 58.40 |
| 2 | 56.44 | 54.89 | 52.44 | 54.76 |
| 3 | 54.99 | 52.64 | 54.10 | 47.29 |
| Average | 54.71 | 55.37 | 54.77 | 53.48 |
| SD | ±1.883 | ±3.004 | ±2.730 | ±5.661 |

Table A-6 Crosslink densities of NR/2% silica with 3% PDDA

| Sample | Crosslink density (mol/m ³) | | | |
|---------|---|--------|--------|---------|
| | I-PDDA | m-PDDA | h-PDDA | co-PDDA |
| 1 | 58.46 | 56.056 | 57.65 | 53.06 |
| 2 | 57.81 | 59.27 | 57.40 | 49.97 |
| 3 | 57.47 | 60.00 | 55.04 | 55.87 |
| Average | 57.91 | 58.44 | 56.69 | 52.96 |
| SD | ±0.500 | ±2.098 | ±1.439 | ±2.950 |

Table A-7 Crosslink densities of NR/3% silica without PDDA

| Sample | Crosslink density (mol/m ³) |
|---------|---|
| 1 | 46.04 |
| 2 | 47.60 |
| 3 | 42.9 |
| Average | 45.54 |
| SD | ±2.347 |

Table A-8 Crosslink densities of NR/3% silica with 1% PDDA

| Sample | Crosslink density (mol/m ³) | | | |
|---------|---|--------|--------|---------|
| | I-PDDA | m-PDDA | h-PDDA | co-PDDA |
| 1 | 52.74 | 49.90 | 51.10 | 49.20 |
| 2 | 50.62 | 47.99 | 51.08 | 48.11 |
| 3 | 61.66 | 49.71 | 49.13 | 48.43 |
| Average | 55.01 | 49.20 | 50.43 | 48.58 |
| SD | ±5.858 | ±1.047 | ±1.133 | ±0.557 |

Table A-9 Crosslink densities of NR/3% silica with 3% PDDA

| Sample | Crosslink density (mol/m ³) | | | |
|---------|---|--------|--------|---------|
| | I-PDDA | m-PDDA | h-PDDA | co-PDDA |
| 1 | 51.89 | 48.20 | 51.2 | 44.51 |
| 2 | 49.54 | 46.24 | 50.92 | 39.19 |
| 3 | 52.78 | 43.36 | 49.29 | 42.54 |
| Average | 51.40 | 45.93 | 50.47 | 42.07 |
| SD | ±1.675 | ±2.431 | ±1.028 | ±2.688 |

Table A-10 Crosslink densities of NR/4% silica without PDDA

| Sample | Crosslink density (mol/m ³) |
|---------|---|
| 1 | 43.27 |
| 2 | 42.25 |
| 3 | 41.58 |
| Average | 42.37 |
| SD | ±0.849 |

Table A-10 Crosslink densities of NR/4% silica with 1% PDDA

| Sample | Crosslink density (mol/m ³) | | | |
|---------|---|--------|--------|---------|
| | I-PDDA | m-PDDA | h-PDDA | co-PDDA |
| 1 | 38.45 | 54.75 | 50.159 | 50.85 |
| 2 | 38.96 | 55.76 | 55.23 | 53.35 |
| 3 | 43.05 | 54.86 | 58.44 | 54.79 |
| Average | 40.15 | 55.13 | 54.61 | 53.00 |
| SD | ±2.522 | ±0.546 | ±4.177 | ±1.994 |

Table A-10 Crosslink densities of NR/4% silica with 3% PDDA

| Sample | Crosslink density (mol/m ³) | | | |
|---------|---|--------|--------|---------|
| | I-PDDA | m-PDDA | h-PDDA | co-PDDA |
| 1 | 56.77 | 55.67 | 59.60 | 50.99 |
| 2 | 54.79 | 54.57 | 57.22 | 50.88 |
| 3 | 55.9 | 64.51 | 59.60 | 50.30 |
| Average | 55.85 | 58.25 | 58.41 | 50.72 |
| SD | ±0.998 | ±5.451 | ±1.682 | ±0.367 |

APPENDIX B

APPENDIX B

MECHANICAL PROPERTIES OF NR/SILICA NANOCOMPOSITES

Table B-1 Mechanical properties of NR/1% silica without PDDA

| Sample | 100% Modulus (MPa) | 300% Modulus (MPa) | % Elongation | Tensile strength (MPa) | Tear strength (MPa) |
|---------|--------------------|--------------------|--------------|------------------------|---------------------|
| 1 | 0.49 | 0.98 | 1000 | 26.16 | 54.68 |
| 2 | 0.43 | 0.81 | 960 | 17.49 | 57.08 |
| 3 | 0.48 | 0.88 | 960 | 20.15 | 56.66 |
| 4 | 0.50 | 0.85 | 980 | 17.91 | 49.83 |
| 5 | 0.55 | 0.89 | 1000 | 19.01 | 49.39 |
| Average | 0.49 | 0.88 | 980 | 20.14 | 53.5 |
| SD | ± 0.043 | ± 0.060 | ± 20.000 | ± 3.518 | ± 3.692 |

Table B-2 Mechanical properties of NR/1% silica with 1% I-PDDA

| Sample | 100% Modulus (MPa) | 300% Modulus (MPa) | % Elongation | Tensile strength (MPa) | Tear strength (MPa) |
|---------|--------------------|--------------------|--------------|------------------------|---------------------|
| 1 | 0.55 | 0.99 | 980 | 21.53 | 95.62 |
| 2 | 0.48 | 1.02 | 960 | 18.77 | 90.31 |
| 3 | 0.52 | 0.99 | 1020 | 24 | 87.63 |
| 4 | 0.52 | 0.99 | 1000 | 23.78 | 79.52 |
| 5 | 0.50 | 1.01 | 1000 | 18.31 | 81.53 |
| Average | 0.52 | 1.00 | 992 | 21.28 | 86.92 |
| SD | ± 0.026 | ± 0.014 | ± 22.804 | ± 2.684 | ± 6.548 |

Table B-3 Mechanical properties of NR/1% silica with 1% m-PDDA

| Sample | 100% Modulus (MPa) | 300% Modulus (MPa) | % Elongation | Tensile strength (MPa) | Tear strength (MPa) |
|---------|--------------------|--------------------|--------------|------------------------|---------------------|
| 1 | 0.45 | 0.90 | 1020 | 24.63 | 94.86 |
| 2 | 0.44 | 0.93 | 1020 | 23.84 | 76.17 |
| 3 | 0.43 | 0.93 | 1000 | 24.51 | 78.23 |
| 4 | 0.53 | 1.00 | 1020 | 23.83 | 81.34 |
| 5 | 0.55 | 1.09 | 1020 | 25.07 | 86.89 |
| Average | 0.48 | 0.971 | 1016 | 24.37 | 83.498 |
| SD | ±0.054 | ±0.080 | ±8.944 | ±0.536 | ±7.528 |

Table B-4 Mechanical properties of NR/1% silica with 1% h-PDDA

| Sample | 100% Modulus (MPa) | 300% Modulus (MPa) | % Elongation | Tensile strength (MPa) | Tear strength (MPa) |
|---------|--------------------|--------------------|--------------|------------------------|---------------------|
| 1 | 0.42 | 0.88 | 1000 | 19.54 | 83.93 |
| 2 | 0.39 | 0.84 | 1060 | 23.87 | 77.07 |
| 3 | 0.50 | 0.98 | 1000 | 25.48 | 95.37 |
| 4 | 0.48 | 0.99 | 1020 | 26.92 | 90.58 |
| 5 | 0.46 | 0.99 | 1060 | 20.06 | 79.85 |
| Average | 0.45 | 0.93 | 1028 | 23.17 | 85.36 |
| SD | ±0.044 | ±0.068 | ±30.331 | ±3.268 | ±7.550 |

Table B-5 Mechanical properties of NR/1% silica with 1% co-PDDA

| Sample | 100% Modulus (MPa) | 300% Modulus (MPa) | % Elongation | Tensile strength (MPa) | Tear strength (MPa) |
|---------|--------------------|--------------------|--------------|------------------------|---------------------|
| 1 | 0.53 | 0.91 | 940 | 23.81 | 65.19 |
| 2 | 0.52 | 0.96 | 1060 | 25.12 | 84.02 |
| 3 | 0.55 | 0.99 | 980 | 25.00 | 67.11 |
| 4 | 0.58 | 1.00 | 1040 | 26.52 | 64.34 |
| 5 | 0.50 | 0.98 | 1000 | 24.72 | 74.08 |
| Average | 0.53 | 0.96 | 1004 | 25.034 | 70.948 |
| SD | ±0.029 | ±0.035 | ±47.740 | ±0.970 | ±8.240 |

Table B-6 Mechanical properties of NR/1% silica with 3% I-PDDA

| Sample | 100% Modulus (MPa) | 300% Modulus (MPa) | % Elongation | Tensile strength (MPa) | Tear strength (MPa) |
|---------|--------------------|--------------------|--------------|------------------------|---------------------|
| 1 | 0.58 | 1.00 | 1000 | 24.29 | 89.46 |
| 2 | 0.64 | 1.04 | 1000 | 23.1 | 87.61 |
| 3 | 0.59 | 1.01 | 980 | 26.04 | 76.00 |
| 4 | 0.58 | 1.00 | 1000 | 21.82 | 87.91 |
| 5 | 0.59 | 1.07 | 1000 | 23.79 | 95.36 |
| Average | 0.59 | 1.023 | 996 | 23.81 | 87.27 |
| SD | ±0.028 | ±0.029 | ±8.944 | ±1.550 | ±7.032 |

Table B-7 Mechanical properties of NR/1% silica with 3% m-PDDA

| Sample | 100% Modulus (MPa) | 300% Modulus (MPa) | % Elongation | Tensile strength (MPa) | Tear strength (MPa) |
|---------|--------------------|--------------------|--------------|------------------------|---------------------|
| 1 | 0.53 | 1.00 | 940 | 20.22 | 104.24 |
| 2 | 0.57 | 1.01 | 1000 | 24.15 | 90.78 |
| 3 | 0.59 | 1.06 | 940 | 21.44 | 69.37 |
| 4 | 0.57 | 1.02 | 960 | 20.09 | 72.96 |
| 5 | 0.58 | 1.11 | 980 | 23.93 | 102.7 |
| Average | 0.57 | 1.03 | 964 | 21.97 | 88.01 |
| SD | ±0.0244 | ±0.042 | ±26.077 | ±1.966 | ±16.285 |

Table B-8 Mechanical properties of NR/1% silica with 3% h-PDDA

| Sample | 100% Modulus (MPa) | 300% Modulus (MPa) | % Elongation | Tensile strength (MPa) | Tear strength (MPa) |
|---------|--------------------|--------------------|--------------|------------------------|---------------------|
| 1 | 0.57 | 1.03 | 980 | 20.89 | 108.94 |
| 2 | 0.53 | 1.00 | 1020 | 23.47 | 70.04 |
| 3 | 0.56 | 0.99 | 1040 | 23.19 | 91.87 |
| 4 | 0.52 | 0.94 | 1020 | 22.33 | 74.94 |
| 5 | 0.54 | 0.97 | 1040 | 22.87 | 80.97 |
| Average | 0.54 | 0.98 | 1020 | 22.55 | 85.352 |
| SD | ±0.021 | ±0.035 | ±24.495 | ±1.020 | ±15.499 |

Table B-9 Mechanical properties of NR/1% silica with 3% co-PDDA

| Sample | 100% Modulus (MPa) | 300% Modulus (MPa) | % Elongation | Tensile strength (MPa) | Tear strength (MPa) |
|---------|--------------------|--------------------|--------------|------------------------|---------------------|
| 1 | 0.59 | 1.0 | 1040 | 19.11 | 73.57 |
| 2 | 0.63 | 0.95 | 1000 | 20.33 | 74.27 |
| 3 | 0.55 | 0.90 | 1020 | 18.81 | 73.3 |
| 4 | 0.53 | 0.90 | 1060 | 20.1 | 72.62 |
| 5 | 0.53 | 0.89 | 1040 | 18.76 | 85.87 |
| Average | 0.56 | 0.93 | 1032 | 19.42 | 75.93 |
| SD | ±0.043 | ±0.046 | ±22.803 | ±0.740 | ±5.590 |

Table B-10 Mechanical properties of NR/2% silica without PDDA

| Sample | 100% Modulus (MPa) | 300% Modulus (MPa) | % Elongation | Tensile strength (MPa) | Tear strength (MPa) |
|---------|--------------------|--------------------|--------------|------------------------|---------------------|
| 1 | 0.52 | 1.05 | 960 | 21.47 | 65.28 |
| 2 | 0.40 | 0.97 | 940 | 18.81 | 65.20 |
| 3 | 0.67 | 1.19 | 920 | 18.52 | 89.15 |
| 4 | 0.47 | 0.85 | 1000 | 22.2 | 97.10 |
| 5 | 0.47 | 1.05 | 960 | 22.14 | 69.22 |
| Average | 0.510 | 1.02 | 956 | 20.63 | 77.20 |
| SD | ±0.100 | ±0.125 | ±29.664 | ±1.818 | ±17.346 |

Table B-11 Mechanical properties of NR/2% silica with 1% I-PDDA

| Sample | 100% Modulus (MPa) | 300% Modulus (MPa) | % Elongation | Tensile strength (MPa) | Tear strength (MPa) |
|---------|--------------------|--------------------|--------------|------------------------|---------------------|
| 1 | 0.47 | 0.99 | 920 | 24.11 | 84.24 |
| 2 | 0.56 | 1.09 | 932 | 25.12 | 86.21 |
| 3 | 0.63 | 1.13 | 932 | 24.64 | 87.27 |
| 4 | 0.62 | 1.12 | 1020 | 25.77 | 78.25 |
| 5 | 0.61 | 1.16 | 920 | 27.19 | 90.29 |
| Average | 0.57 | 1.09 | 944.80 | 25.37 | 85.25 |
| SD | ± 0.064 | ± 0.064 | ± 42.464 | ± 1.189 | ± 4.483 |

Table B-12 Mechanical properties of NR/2% silica with 1% m-PDDA

| Sample | 100% Modulus (MPa) | 300% Modulus (MPa) | % Elongation | Tensile strength (MPa) | Tear strength (MPa) |
|---------|--------------------|--------------------|--------------|------------------------|---------------------|
| 1 | 0.59 | 1.09 | 912 | 25.65 | 77.07 |
| 2 | 0.71 | 1.24 | 948 | 26.87 | 72.49 |
| 3 | 0.60 | 1.18 | 920 | 23.95 | 84.24 |
| 4 | 0.69 | 1.29 | 900 | 23.97 | 81.16 |
| 5 | 0.71 | 1.24 | 980 | 23.69 | 75.47 |
| Average | 0.66 | 1.21 | 932 | 24.83 | 78.09 |
| SD | ± 0.059 | ± 0.079 | ± 32.124 | ± 1.382 | ± 4.650 |

Table B-13 Mechanical properties of NR/2% silica with 1% h-PDDA

| Sample | 100% Modulus (MPa) | 300% Modulus (MPa) | % Elongation | Tensile strength (MPa) | Tear strength (MPa) |
|---------|--------------------|--------------------|--------------|------------------------|---------------------|
| 1 | 0.63 | 1.17 | 980 | 22.76 | 91.89 |
| 2 | 0.66 | 1.22 | 1020 | 24.88 | 70.12 |
| 3 | 0.61 | 1.11 | 960 | 23.39 | 84.39 |
| 4 | 0.63 | 1.15 | 960 | 25.19 | 77.28 |
| 5 | 0.69 | 1.28 | 960 | 23.67 | 96.86 |
| Average | 0.65 | 1.19 | 976 | 23.98 | 84.11 |
| SD | ± 0.034 | ± 0.066 | ± 26.076 | ± 1.025 | ± 10.788 |

Table B-14 Mechanical properties of NR/2% silica with 1% co-PDDA

| Sample | 100% Modulus (MPa) | 300% Modulus (MPa) | % Elongation | Tensile strength (MPa) | Tear strength (MPa) |
|---------|--------------------|--------------------|--------------|------------------------|---------------------|
| 1 | 0.53 | 1.06 | 980 | 21.49 | 74.95 |
| 2 | 0.64 | 1.24 | 1040 | 23.91 | 93.6 |
| 3 | 0.53 | 1.09 | 980 | 21.82 | 67.95 |
| 4 | 0.52 | 1.05 | 980 | 19.49 | 87.98 |
| 5 | 0.55 | 1.16 | 960 | 24.72 | 96.94 |
| Average | 0.56 | 1.12 | 988 | 22.27 | 84.28 |
| SD | ± 0.049 | ± 0.081 | ± 30.332 | ± 2.075 | ± 12.395 |

Table B-15 Mechanical properties of NR/2% silica with 3% I-PDDA

| Sample | 100% Modulus (MPa) | 300% Modulus (MPa) | % Elongation | Tensile strength (MPa) | Tear strength (MPa) |
|---------|--------------------|--------------------|--------------|------------------------|---------------------|
| 1 | 0.71 | 1.38 | 980 | 23.23 | 99.94 |
| 2 | 0.58 | 1.22 | 980 | 24.51 | 94.21 |
| 3 | 0.57 | 1.18 | 960 | 25.96 | 79.74 |
| 4 | 0.59 | 1.23 | 980 | 21.54 | 81.26 |
| 5 | 0.69 | 1.39 | 1000 | 23.32 | 79 |
| Average | 0.63 | 1.28 | 980 | 23.71 | 86.83 |
| SD | ±0.065 | ±0.098 | ±14.142 | ±1.642 | ±9.603 |

Table B-16 Mechanical properties of NR/2% silica with 3% m-PDDA

| Sample | 100% Modulus (MPa) | 300% Modulus (MPa) | % Elongation | Tensile strength (MPa) | Tear strength (MPa) |
|---------|--------------------|--------------------|--------------|------------------------|---------------------|
| 1 | 0.70 | 1.35 | 1000 | 24.01 | 84.81 |
| 2 | 0.68 | 1.41 | 940 | 24.14 | 94.76 |
| 3 | 0.59 | 1.17 | 980 | 22.43 | 94.82 |
| 4 | 0.69 | 1.31 | 980 | 26.15 | 89.03 |
| 5 | 0.65 | 1.35 | 980 | 20.56 | 100.44 |
| Average | 0.67 | 1.32 | 976 | 23.46 | 92.77 |
| SD | ±0.043 | ±0.093 | ±21.908 | ±2.089 | ±6.007 |

Table B-17 Mechanical properties of NR/2% silica with 3% h-PDDA

| Sample | 100% Modulus (MPa) | 300% Modulus (MPa) | % Elongation | Tensile strength (MPa) | Tear strength (MPa) |
|---------|--------------------|--------------------|--------------|------------------------|---------------------|
| 1 | 0.64 | 1.33 | 980 | 24.74 | 74.88 |
| 2 | 0.66 | 1.46 | 960 | 24.48 | 91.65 |
| 3 | 0.63 | 1.33 | 980 | 24.68 | 84.09 |
| 4 | 0.58 | 1.25 | 1000 | 21.71 | 69.56 |
| 5 | 0.57 | 1.09 | 1020 | 24.19 | 78.09 |
| Average | 0.62 | 1.29 | 988 | 23.96 | 79.65 |
| SD | ± 0.039 | ± 0.138 | ± 22.803 | ± 1.275 | ± 8.525 |

Table B-18 Mechanical properties of NR/2% silica with 3% co-PDDA

| Sample | 100% Modulus (MPa) | 300% Modulus (MPa) | % Elongation | Tensile strength (MPa) | Tear strength (MPa) |
|---------|--------------------|--------------------|--------------|------------------------|---------------------|
| 1 | 0.53 | 1.07 | 960 | 19.97 | 82.32 |
| 2 | 0.51 | 0.92 | 1000 | 22.74 | 71.44 |
| 3 | 0.55 | 1.04 | 960 | 20.56 | 81.12 |
| 4 | 0.52 | 0.97 | 1020 | 22.80 | 78.92 |
| 5 | 0.57 | 1.11 | 900 | 20.48 | 69.00 |
| Average | 0.54 | 1.02 | 968 | 21.31 | 76.56 |
| SD | ± 0.024 | ± 0.078 | ± 46.043 | ± 1.352 | ± 5.977 |

Table B-19 Mechanical properties of NR/3% silica without PDDA

| Sample | 100% Modulus (MPa) | 300% Modulus (MPa) | % Elongation | Tensile strength (MPa) | Tear strength (MPa) |
|---------|--------------------|--------------------|--------------|------------------------|---------------------|
| 1 | 0.57 | 1.04 | 920 | 21.59 | 76.61 |
| 2 | 0.59 | 1.06 | 980 | 22.22 | 76.16 |
| 3 | 0.59 | 1.07 | 940 | 24.04 | 70.51 |
| 4 | 0.58 | 1.08 | 960 | 22.70 | 60.19 |
| 5 | 0.55 | 1.03 | 960 | 24.34 | 72.80 |
| Average | 0.57 | 1.05 | 952 | 22.978 | 71.254 |
| SD | ± 0.020 | ± 0.020 | ± 22.803 | ± 1.179 | ± 6.672 |

Table B-20 Mechanical properties of NR/3% silica with 1% I-PDDA

| Sample | 100% Modulus (MPa) | 300% Modulus (MPa) | % Elongation | Tensile strength (MPa) | Tear strength (MPa) |
|---------|--------------------|--------------------|--------------|------------------------|---------------------|
| 1 | 0.65 | 1.19 | 960 | 21.09 | 89.55 |
| 2 | 0.60 | 1.16 | 1000 | 21.62 | 86.17 |
| 3 | 0.67 | 1.19 | 980 | 22.01 | 84.70 |
| 4 | 0.63 | 1.18 | 960 | 19.23 | 96.16 |
| 5 | 0.66 | 1.18 | 920 | 20.67 | 85.26 |
| Average | 0.64 | 1.18 | 964 | 20.92 | 88.37 |
| SD | ± 0.026 | ± 0.012 | ± 29.664 | ± 1.0750 | ± 4.744 |

Table B-21 Mechanical properties of NR/3% silica with 1% m-PDDA

| Sample | 100% Modulus (MPa) | 300% Modulus (MPa) | % Elongation | Tensile strength (MPa) | Tear strength (MPa) |
|---------|--------------------|--------------------|--------------|------------------------|---------------------|
| 1 | 0.65 | 1.18 | 960 | 17.84 | 74.95 |
| 2 | 0.59 | 1.10 | 960 | 18.82 | 84.89 |
| 3 | 0.62 | 1.04 | 980 | 19.21 | 81.64 |
| 4 | 0.57 | 1.18 | 940 | 18.08 | 92.93 |
| 5 | 0.57 | 1.08 | 980 | 21.44 | 90.79 |
| Average | 0.60 | 1.12 | 964 | 19.07 | 85.04 |
| SD | ± 0.033 | ± 0.061 | ± 16.733 | ± 1.431 | ± 7.223 |

Table B-22 Mechanical properties of NR/3% silica with 1% h-PDDA

| Sample | 100% Modulus (MPa) | 300% Modulus (MPa) | % Elongation | Tensile strength (MPa) | Tear strength (MPa) |
|---------|--------------------|--------------------|--------------|------------------------|---------------------|
| 1 | 0.59 | 1.13 | 920 | 18.98 | 74.37 |
| 2 | 0.56 | 1.15 | 900 | 18.5 | 85.58 |
| 3 | 0.57 | 1.07 | 900 | 18.51 | 72.24 |
| 4 | 0.61 | 1.15 | 900 | 18.09 | 76.12 |
| 5 | 0.64 | 1.18 | 960 | 19.15 | 75.41 |
| Average | 0.59 | 1.13 | 916 | 18.65 | 76.74 |
| SD | ± 0.032 | ± 0.041 | ± 26.076 | ± 0.422 | ± 5.151 |

Table B-23 Mechanical properties of NR/3% silica with 1% co-PDDA

| Sample | 100% Modulus (MPa) | 300% Modulus (MPa) | % Elongation | Tensile strength (MPa) | Tear strength (MPa) |
|---------|--------------------|--------------------|--------------|------------------------|---------------------|
| 1 | 0.63 | 1.12 | 988 | 17.97 | 85.83 |
| 2 | 0.54 | 1.03 | 1000 | 18.16 | 72.55 |
| 3 | 0.63 | 1.0 | 1000 | 18.48 | 86.32 |
| 4 | 0.62 | 1.1 | 980 | 19.48 | 84.02 |
| 5 | 0.58 | 1.02 | 980 | 17.74 | 80.43 |
| Average | 0.60 | 1.07 | 989.6 | 18.37 | 81.83 |
| SD | ±0.038 | ±0.047 | ±10.039 | ±0.679 | ±5.679 |

Table B-24 Mechanical properties of NR/3% silica with 3% I-PDDA

| Sample | 100% Modulus (MPa) | 300% Modulus (MPa) | % Elongation | Tensile strength (MPa) | Tear strength (MPa) |
|---------|--------------------|--------------------|--------------|------------------------|---------------------|
| 1 | 0.66 | 1.37 | 1020 | 18.93 | 79.47 |
| 2 | 0.66 | 1.36 | 980 | 20.25 | 79.05 |
| 3 | 0.66 | 1.35 | 1000 | 19.4 | 89.26 |
| 4 | 0.68 | 1.35 | 1020 | 20.07 | 71.99 |
| 5 | 0.66 | 1.34 | 960 | 18.88 | 72.18 |
| Average | 0.67 | 1.35 | 996 | 19.51 | 78.39 |
| SD | ±0.011 | ±0.012 | ±26.076 | ±0.633 | ±7.058 |

Table B-25 Mechanical properties of NR/3% silica with 3% m-PDDA

| Sample | 100% Modulus (MPa) | 300% Modulus (MPa) | % Elongation | Tensile strength (MPa) | Tear strength (MPa) |
|---------|--------------------|--------------------|--------------|------------------------|---------------------|
| 1 | 0.59 | 1.29 | 1020 | 20.52 | 96.76 |
| 2 | 0.62 | 1.32 | 1060 | 21.52 | 100.26 |
| 3 | 0.59 | 1.38 | 1000 | 18.49 | 92.03 |
| 4 | 0.60 | 1.31 | 1020 | 21.58 | 99.51 |
| 5 | 0.65 | 1.27 | 1000 | 18.37 | 98.35 |
| Average | 0.61 | 1.31 | 1020 | 20.09 | 97.38 |
| SD | ± 0.024 | ± 0.041 | ± 24.490 | ± 1.570 | ± 3.270 |

Table B-26 Mechanical properties of NR/3% silica with 3% h-PDDA

| Sample | 100% Modulus (MPa) | 300% Modulus (MPa) | % Elongation | Tensile strength (MPa) | Tear strength (MPa) |
|---------|--------------------|--------------------|--------------|------------------------|---------------------|
| 1 | 0.57 | 1.25 | 980 | 17.63 | 68.05 |
| 2 | 0.59 | 1.29 | 940 | 16.87 | 68.71 |
| 3 | 0.68 | 1.34 | 980 | 15.16 | 83.66 |
| 4 | 0.69 | 1.32 | 1020 | 15.29 | 88.02 |
| 5 | 0.55 | 1.23 | 920 | 18.70 | 77.18 |
| Average | 0.619 | 1.288 | 968 | 16.73 | 77.12 |
| SD | ± 0.064 | ± 0.048 | ± 38.987 | ± 1.520 | ± 8.868 |

Table B-26 Mechanical properties of NR/3% silica with 3% co-PDDA

| Sample | 100% Modulus (MPa) | 300% Modulus (MPa) | % Elongation | Tensile strength (MPa) | Tear strength (MPa) |
|---------|--------------------|--------------------|--------------|------------------------|---------------------|
| 1 | 0.59 | 1.33 | 980 | 17.00 | 61.11 |
| 2 | 0.55 | 1.05 | 980 | 17.48 | 64.85 |
| 3 | 0.59 | 1.07 | 980 | 20.27 | 72.79 |
| 4 | 0.56 | 1.13 | 960 | 16.95 | 81.51 |
| 5 | 0.53 | 0.99 | 980 | 17.27 | 69.47 |
| Average | 0.56 | 1.11 | 976 | 17.79 | 69.95 |
| SD | ± 0.026 | ± 0.130 | ± 8.940 | ± 1.400 | ± 7.840 |

Table B-27 Mechanical properties of NR/4 % silica without PDDA

| Sample | 100% Modulus (MPa) | 300% Modulus (MPa) | % Elongation | Tensile strength (MPa) | Tear strength (MPa) |
|---------|--------------------|--------------------|--------------|------------------------|---------------------|
| 1 | 0.77 | 1.32 | 920 | 16.73 | 83.01 |
| 2 | 0.76 | 1.40 | 860 | 16.82 | 74.70 |
| 3 | 0.67 | 1.18 | 972 | 17.04 | 92.91 |
| 4 | 0.72 | 1.29 | 920 | 17.65 | 88.99 |
| 5 | 0.66 | 1.14 | 948 | 16.72 | 91.47 |
| Average | 0.72 | 1.27 | 924 | 16.99 | 86.22 |
| SD | ± 0.051 | ± 0.106 | ± 41.856 | ± 0.389 | ± 7.466 |

Table B-28 Mechanical properties of NR/4 % silica with 1% I-PDDA

| Sample | 100% Modulus (MPa) | 300% Modulus (MPa) | % Elongation | Tensile strength (MPa) | Tear strength (MPa) |
|---------|--------------------|--------------------|--------------|------------------------|---------------------|
| 1 | 0.76 | 1.33 | 1020 | 18.72 | 59.98 |
| 2 | 0.79 | 1.45 | 980 | 21.92 | 60.59 |
| 3 | 0.84 | 1.47 | 980 | 17.09 | 77.61 |
| 4 | 0.77 | 1.31 | 908 | 19.89 | 59.54 |
| 5 | 0.81 | 1.51 | 920 | 20.32 | 74.7 |
| Average | 0.79 | 1.41 | 961.6 | 19.588 | 66.48 |
| SD | ± 0.033 | ± 0.088 | ± 46.610 | ± 1.807 | ± 8.895 |

Table B-29 Mechanical properties of NR/4 % silica with 1% m-PDDA

| Sample | 100% Modulus (MPa) | 300% Modulus (MPa) | % Elongation | Tensile strength (MPa) | Tear strength (MPa) |
|---------|--------------------|--------------------|--------------|------------------------|---------------------|
| 1 | 0.69 | 1.56 | 940 | 23.05 | 106.15 |
| 2 | 0.61 | 1.44 | 980 | 24.18 | 117.83 |
| 3 | 0.68 | 1.41 | 940 | 23.88 | 96.97 |
| 4 | 0.71 | 1.69 | 960 | 22.62 | 107.61 |
| 5 | 0.70 | 1.56 | 920 | 23.76 | 99.40 |
| Average | 0.68 | 1.5304 | 948 | 23.498 | 105.592 |
| SD | ± 0.039 | ± 0.113 | ± 22.803 | ± 0.642 | ± 8.167 |

Table B-30 Mechanical properties of NR/4 % silica with 1% h-PDDA

| Sample | 100% Modulus (MPa) | 300% Modulus (MPa) | % Elongation | Tensile strength (MPa) | Tear strength (MPa) |
|---------|--------------------------|--------------------------|--------------|------------------------------|---------------------------|
| 1 | 0.60 | 1.31 | 940 | 21.06 | 73.09 |
| 2 | 0.65 | 1.33 | 980 | 19.38 | 88.58 |
| 3 | 0.56 | 1.36 | 940 | 16.05 | 93.14 |
| 4 | 0.60 | 1.29 | 960 | 19.27 | 80.71 |
| 5 | 0.66 | 1.34 | 980 | 22.54 | 73.19 |
| Average | 0.61 | 1.33 | 960 | 19.66 | 81.74 |
| SD | ± 0.039 | ± 0.024 | ± 20 | ± 2.42 | ± 9.020 |

Table B-31 Mechanical properties of NR/4 % silica with 1% co-PDDA

| Sample | 100% Modulus (MPa) | 300% Modulus (MPa) | % Elongation | Tensile strength (MPa) | Tear strength (MPa) |
|---------|--------------------------|--------------------------|--------------|------------------------------|---------------------------|
| 1 | 0.59 | 1.24 | 980 | 21.92 | 71.12 |
| 2 | 0.65 | 1.34 | 1000 | 22.07 | 77.15 |
| 3 | 0.54 | 1.19 | 940 | 17.77 | 80.39 |
| 4 | 0.67 | 1.45 | 1020 | 23.33 | 79.61 |
| 5 | 0.65 | 1.37 | 1020 | 20.39 | 84.77 |
| Average | 0.62 | 1.32 | 992 | 21.096 | 78.608 |
| SD | ± 0.0556 | ± 0.104 | ± 33.46 | ± 2.130 | ± 5.000 |

Table B-31 Mechanical properties of NR/4 % silica with 3 % I-PDDA

| Sample | 100% Modulus (MPa) | 300% Modulus (MPa) | % Elongation | Tensile strength (MPa) | Tear strength (MPa) |
|---------|--------------------|--------------------|--------------|------------------------|---------------------|
| 1 | 0.76 | 1.48 | 980 | 15.04 | 85.63 |
| 2 | 0.71 | 1.51 | 980 | 16.26 | 88.89 |
| 3 | 0.80 | 1.63 | 980 | 22.06 | 104.4 |
| 4 | 0.73 | 1.53 | 1000 | 19.93 | 92.73 |
| 5 | 0.63 | 1.29 | 1020 | 17.48 | 89.05 |
| Average | 0.73 | 1.49 | 992 | 18.15 | 92.14 |
| SD | ± 0.066 | ± 0.123 | ± 16.000 | ± 2.835 | ± 7.29 |

Table B-32 Mechanical properties of NR/4 % silica with 3 % m-PDDA

| Sample | 100% Modulus (MPa) | 300% Modulus (MPa) | % Elongation | Tensile strength (MPa) | Tear strength (MPa) |
|---------|--------------------|--------------------|--------------|------------------------|---------------------|
| 1 | 0.67 | 1.58 | 980 | 21.35 | 101.59 |
| 2 | 0.84 | 1.57 | 980 | 20.23 | 114.27 |
| 3 | 0.81 | 1.71 | 1000 | 21.44 | 101.3 |
| 4 | 0.80 | 1.68 | 1020 | 21.49 | 105.21 |
| 5 | 0.66 | 1.63 | 980 | 21.65 | 96.84 |
| Average | 0.76 | 1.63 | 992 | 21.23 | 103.84 |
| SD | ± 0.085 | ± 0.059 | ± 17.888 | ± 0.57 | ± 6.54 |

Table B-33 Mechanical properties of NR/4 % silica with 3 % h-PDDA

| Sample | 100% Modulus (MPa) | 300% Modulus (MPa) | % Elongation | Tensile strength (MPa) | Tear strength (MPa) |
|---------|--------------------|--------------------|--------------|------------------------|---------------------|
| 1 | 0.71 | 1.55 | 980 | 15.96 | 86.94 |
| 2 | 0.81 | 1.63 | 980 | 21.58 | 107.54 |
| 3 | 0.82 | 1.50 | 1000 | 23.72 | 91.07 |
| 4 | 0.71 | 1.60 | 980 | 25.17 | 85.69 |
| 5 | 0.83 | 1.63 | 1000 | 23.86 | 84.10 |
| Average | 0.77 | 1.58 | 988 | 22.058 | 91.068 |
| SD | ±0.059 | ±0.054 | ±10.954 | ±3.644 | ±9.563 |

Table B-34 Mechanical properties of NR/4 % silica with 3 % co-PDDA

| Sample | 100% Modulus (MPa) | 300% Modulus (MPa) | % Elongation | Tensile strength (MPa) | Tear strength (MPa) |
|---------|--------------------|--------------------|--------------|------------------------|---------------------|
| 1 | 0.74 | 1.36 | 980 | 20.43 | 101.79 |
| 2 | 0.76 | 1.54 | 980 | 22.28 | 102.70 |
| 3 | 0.68 | 1.41 | 980 | 19.61 | 99.15 |
| 4 | 0.62 | 1.19 | 1020 | 19.35 | 98.09 |
| 5 | 0.69 | 1.31 | 1000 | 22.06 | 97.78 |
| Average | 0.69 | 1.36 | 992 | 20.75 | 99.9 |
| SD | ±0.054 | ±0.127 | ±17.889 | ±1.362 | ±2.222 |

BIOGRAPHY

Miss Kittiwat Thongyim was born on September 21, 1986. She graduated with Bachelor's degree of Textile Science & Technology in faculty of Agro-Industry, Kasetsart University from 2005 to 2009. Subsequently, she continued her study in majoring of Applied Polymer and Textile Technology, Department of Material Science, Faculty of Science, Chulalongkorn University. She completely graduated the Master's Degree of Science in Applied Polymer and Textile Technology from 2009 to 2012.